A STUDY OF THE ELECTRICAL AND OPTICAL PROPERTIES OF COBALT-PHOSPHATE GLASSES

BY

MOHAMAD JAMEL BASHA

B.Sc., Drs.

This thesis is submitted in
fulfilment of the requirements for
the degree of Doctor of Philosophy
at Brunel University

1982

To my wife, Norma and my children,
Novia and Hazairi for patiently
accepting the inconveniences during
the course of this work.

ABSTRACT

Binary series $CoO-P_2O_5$ and ternary series $CoO-NiO-P_2O_5$ glasses are prepared. The density, d.c. conductivity, high-field I-V characteristics, memory switching action, a.c. electrical conductivity, infra-red absorption and optical absorption edge of the glasses are presented. The historical background and the formation and theory of the glassy state are reviewed. Previous works on the electrical conductivity of phosphate glasses are reviewed in the framework of Mott's theory.

In the binary glasses, the glass acquires a more compact structure with increased CoO content whereas for the ternary series the results show otherwise. A polaronic model is shown to be generally applicable to explaining the results of electrical conduction measurements. The pre-exponential factor containing the term exp (-2αR) arising from electron tunnelling should not be ignored; thus the theory of the small polaron hopping is in the non-adiabatic regime. The high-field ohmic behaviour is observed up to a field of about 3×10^4 V-cm^{-1}. Apparently, the field dependence is a property of the bulk material. Thin films of glass with 30 Mol % CoO show memory switching phenomena. The results of a.c. measurements characterize hopping conduction as a dominant process in cobalt-phosphate glasses. Results of the infra-red spectra measured in the range 400 cm^{-1} to

4000 cm^{-1} show that the phosphate polyhedra dominate the structure of the glasses. Measurements of the optical gap in the binary series show decreasing values with increased CoO content. It is believed that the fundamental absorption arises from indirect transitions.

AKNOWLEDGEMENTS

The author wish to express his utmost appreciation and gratitude to Professor C.A. Hogarth, Head of Physics Department, Brunel University for his encouragement and guidance while supervising this project.

The author would also like to take advantage of this opportunity of sincerely thanking all who have contributed in any way towards the accomplishment of this work, in particular the following:

Dr. S.M. Elahi, Dr. M.R. Vaschochi, Dr. I.H. Rashed, Mr. N.D. Patel and Mr. M.M. Ahmad for interesting discussions and Mr. A.A. Higazy for co-operation in obtaining some of the results in Section 5.4.2.

Mr. H. Brown, Mr. R. Stevens, Mr. K.R. Schlater, Mr. M. Krasso, Mr. L.E.L. Chandrasekera, Mr. M. Varga, Mr. L. Lightower and the other Physics Department technical staff who have always been available when help and advice were needed.

Mr. C.M. Robinson (Department of Applied Chemistry) and Mr. E.T. Cave (Metallurgy Department) for experimental assistance.

The financial assistance of the University of Science of Malaysia is gratefully aknowledged.

CONTENTS

CHAPTER I

THE NATURE OF THE GLASSY STATE

1.1 INTRODUCTION

The field of glass regarded as amorphous semiconductors has developed immensely in the past twenty years. In recent years much research was directed to deepen the understanding of the structural, electronic, optical, vibrational, magnetic and other properties of these materials and to attempt to approach the present level of understanding of crystalline semiconductors. This effort was stimulated partly by purely scientific interest and partly by the possibility of new applications from which memory devices[1] in the general sense are perhaps the most challenging.

The research met with serious difficulties which are not associated with crystals. The theorists have to learn to live without the Bloch theorem and without the mathematical simplicity introduced by symmetry and long-range order. The experimentalists in turn are plagued with the difficulty of mastering the reproducible preparation of materials, with experimental data curves which are typically less structured and sharp, and with somewhat vague generalities and loosely defined concepts of the present theories. Therefore the progress has been slow and most of the fundamental questions are still open to discussion. The recent book by Mott and

and Davis (1979)[2] represents a substantial attempt to correlate the observed electronic effects in disordered solids on the basis of a few concepts derived from the theoretical considerations and generalized with a sharp physical intuition.

This chapter provides a brief introduction to the general concepts and definitions of the glassy state.

1.2 THE GLASSY STATE

Glass may be described as a transparent substance possessing the properties of hardness, rigidity and brittleness. It is so common a material, so universally known from everyday experience, that its definition may seem superfluous. But already the term Glassy State has a wide meaning in itself. The Glassy State may include elements (Se), oxides (B_2O_3), halides (BeF_2) and organic substances such as resins or plastics.

1.2.1 Definitions

Various definitions of glass have been put forward, varying somewhat with the goal of the writer; but two features are usually mentioned: (i) a glass is formed from an extremely viscous supercooled liquid, and (ii) the liquids which form glasses possess a polymerized network structure with short-range order. A third point is sometimes added, namely the composition is inorganic. This last point is inserted when specific attention is given to the major commercial glasses,

and has led to the ASTM definition of glass as an inorganic product of fusion which has cooled to a rigid condition without crystallizing[3]. It must be aknowledged, however that some organic and semiorganic compounds have vitreous characteristics. This relationship is especially emphasized nowadays, with organic chemists extending their developments toward higher temperature polymers and considering boron-based and aluminium-based polymers as well as silicones.

1.2.2 History In Brief

The word 'glass' is derived from an Indo-European root meaning 'shiny' which could also be related to the words glare, glow and glaze. At times the word 'vitreous' is used, derived from the word for glass in Latin. The basic techniques for working glass are extremely old. Many modern techniques are refinements and mechanizations of these old techniques. The earliest examples of man-made glass have been found among the remains of the ancient Middle Eastern civilizations (about 3000 BC or even earlier). The first important revolution in glass making technique was the invention of the blowing iron (Babylon, about 200 BC). The summary of the history of glass may be obtained from articles in the Encyclopedia Britannica and from the book by Morey (1954)[4].

Faraday (1830)[5] was among the first to study glass in a more basic way. He described glass "rather as a solution of different substances one in another than as a strong chemical compound". Faraday studied the electrolysis and

conductivity of melts of various glasses[6]. In more recent years Goldschmidt (1926)[7] made one of the earliest attempts to discover characteristics common to glass-forming oxides. In the 1930s the understanding of the reasons why certain molecules are glass formers, and of the structure of glass, was enlarged by the papers of Zachariasen (1932)[8] and Warren (1934-1936,1938)[9-12]. Perhaps the 1960s could be described as the "golden age" of glass science because of the profitable application during this period of the basic sciences to understanding glass in terms of its structure and composition.

1.3 GLASS FORMATION

Glasses are usually formed by solidification from the melt. The structure of glasses can be clearly distinguished from that of liquids since the glass structure is effectively independent of temperature. Figure 1.1 shows a plot of the specific volume of the crystal, liquid and glass as a function of temperature. On cooling the liquid, there is a discontinuous change in volume at the melting point if the liquid crystallizes. However, if no crystallization occurs, the volume of the liquid decreases at about the same rate as above the melting point until there is a decrease in the expansion coefficient at a range of temperature called the glass transformation range. Below this temperature the glass structure does not relax at the cooling rate used. The expansion coefficient for the glassy state is usually about the same as that for

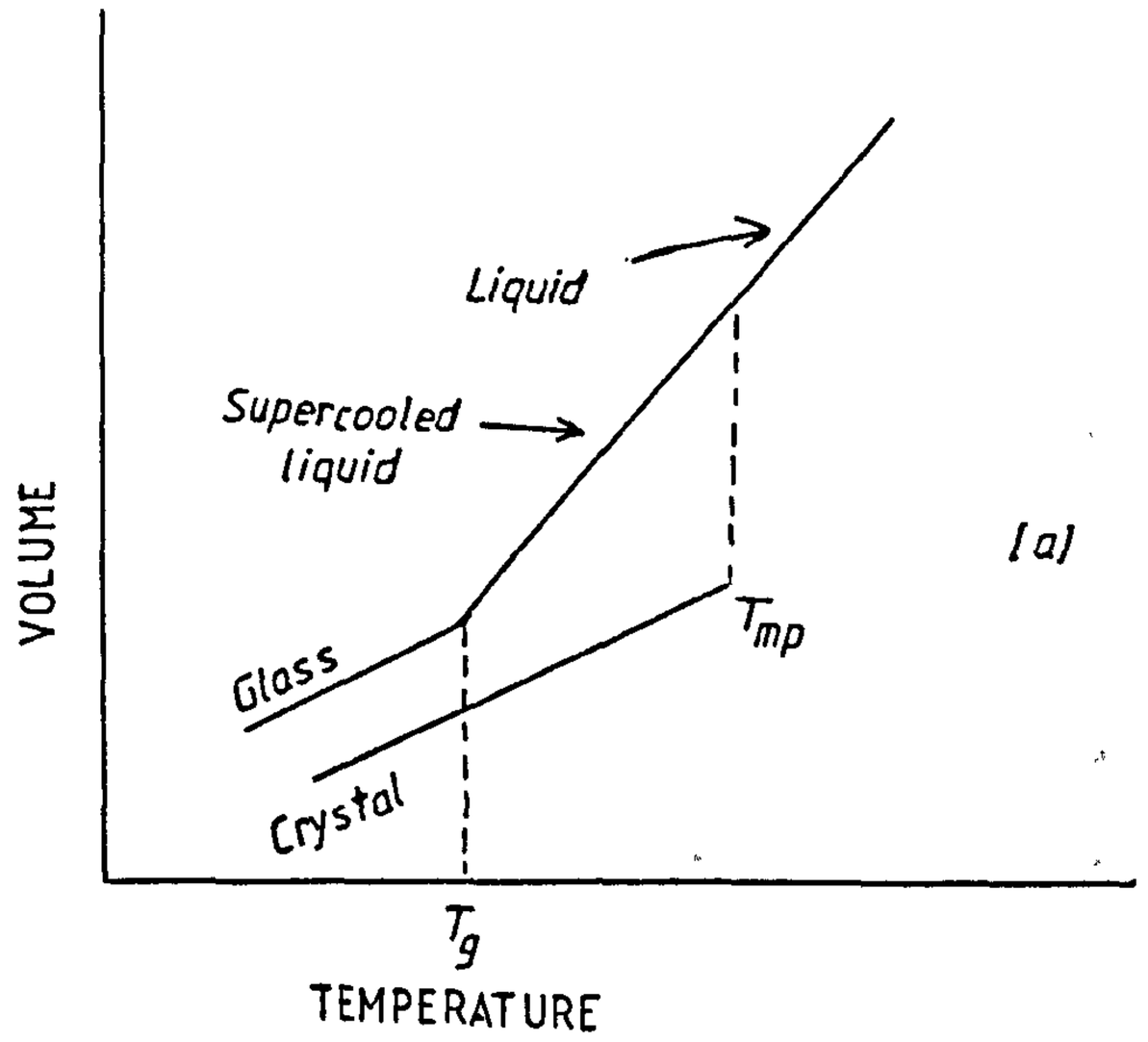

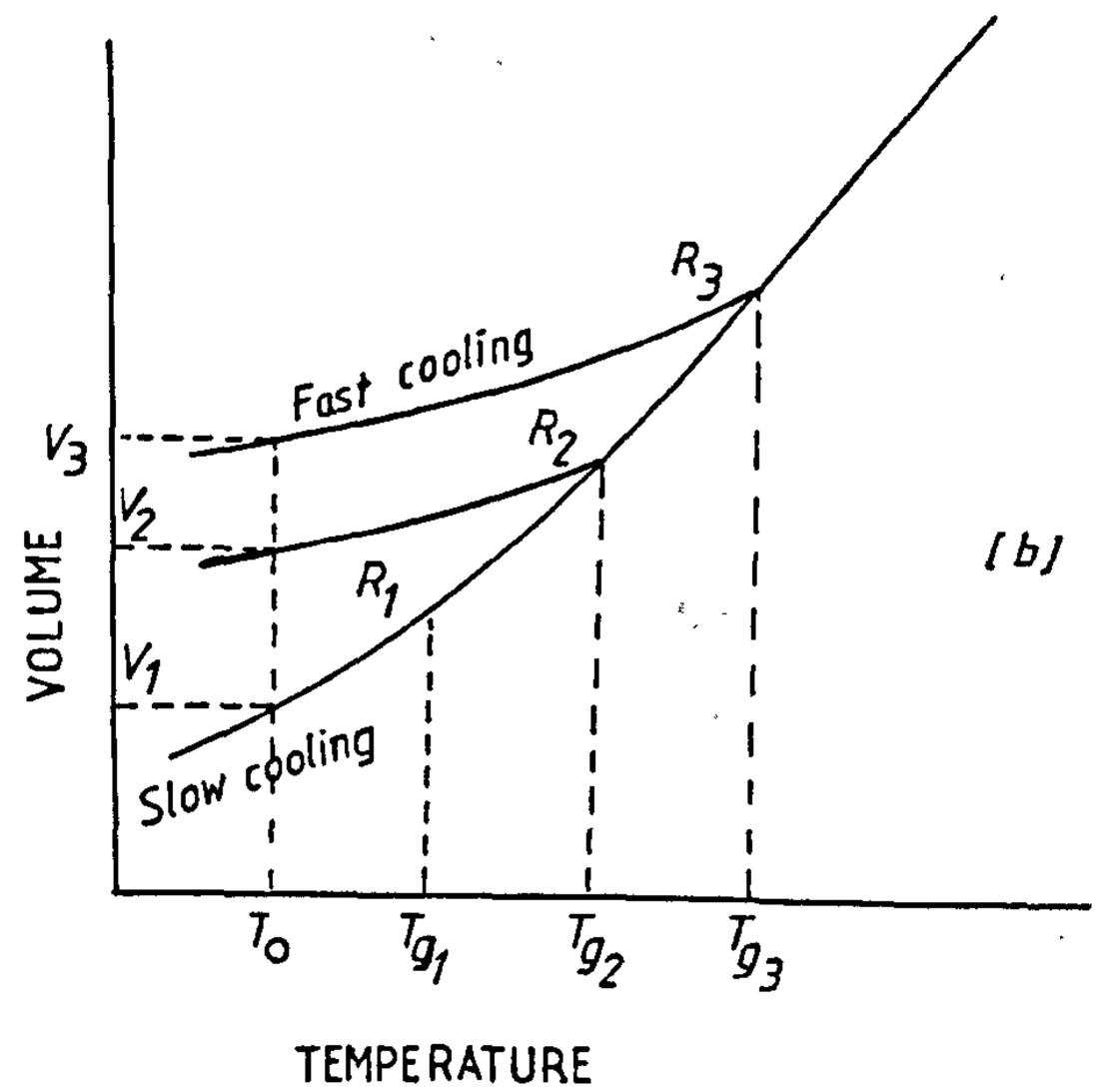

Fig. 1.1 Volume-temperature relations. (a) Relations for liquid, glass, and crystal; (b) glasses formed at different cooling rates $R_1 < R_2 < R_3$.

the crystalline solid. If slower cooling rates are used so that the time available for the structure to relax is increased, the supercooled liquid persists to a lower temperature, and a higher density glass results. Similarly, by heating the glassy material in the annealing range, in which slow relaxation can occur, the glass structure in time approaches an equilibrium density corresponding to the supercooled liquid at this temperature. A concept useful in discussing the properties of glasses is the glass transition temperature T_g, which corresponds to the temperature of the intersection between the curve for the glassy state and that for the supercooled liquid (Figure 1.1). Different cooling rates, corresponding to different relaxation times, give rise to a different configuration in the glassy state equivalent to different points along the curve for the supercooled liquid. In the transition range the time for structural rearrangements is similar in magnitude to that of experimental observations. Consequently the configuration of the glass in this temperature range changes slowly with time toward the equilibrium structure. At somewhat higher temperatures the structure corresponding to equilibrium at any temperature is achieved very rapidly. At substantially lower temperatures the configuration of the glass remains sensibly stable over long periods of time.

In discussing the structural characteristics of glasses, reference is often made to the structure of a particular glassy material. It should be noted, however, that any determination of glass structure is only meaningful within

limits seen from the volume-temperature relations shown in Figure 1.1b. As the liquid is cooled from a high temperature without crystallizing, a region of temperature is reached in which a bend appears in the volume-temperature relation. In this region, the viscosity of the material has increased to a sufficiently high value, typically about 10^{12} to 10^{13} P, so that the sample exhibits solidlike behaviour. As shown in Figure 1.1b, the glass transition temperature increases with increasing cooling rate, as do the specific volumes of the glasses which are formed. In the case shown, the specific volume of the glass at temperature T_0 can be V_1 or V_2 or V_3, depending on which of the three cooling rates was used in forming the glass. The maximum difference in specific volume obtainable with variations in the cooling rate is typically in the range of a few percent; only within this range can one speak of the structure of a glass without carefully specifying its mode of formation.

1.4 METHODS OF PREPARATION

Non-crystalline solids can be formed in other ways besides cooling from the liquid state, and their structure may differ significantly from glasses formed by the cooling of liquids. Among these alternative methods are :

1.4.1 Condensation From The Vapour

This method is most widely used and most effective for materials which are difficult to form as non-crystalline solids.

When a vapour stream formed by electron-beam evaporation impinges on the cold substrate, thermal energy is extracted from the atoms before they can migrate to their lowest free-energy configuration (the crystalline state).

1.4.2 Electrodeposition

Ta_2O_5, Ge and certain Ni-P alloys are among the materials which have been prepared in this way.

1.4.3 Chemical Reactions

Silica gel, for example, can be prepared from ethyl silicate by the reaction

$$Si(O\ Eth)_4 \xrightarrow[catalyst]{H_2O} Si(OH)_4 \xrightarrow{H_2O} SiO_2$$

In this reaction the SiO_2 resulting from the condensation of the silicic acid is non-crystalline. A similar silica gel can be formed by the reaction of sodium silicate with acid. These reactions are particularly effective in the case of hydrogen-bonded structures in aqueous media. For example, the reaction

$$Al_2O_3 + 6H_3PO_4 \rightleftharpoons 2Al(H_2PO_4)_3 + 3H_2O$$

forms a non-crystalline gel in which hydrogen bonding predominates.

1.5 MODELS OF GLASS STRUCTURE

A number of models have been suggested to describe the structure of glasses. The models which have been most widely

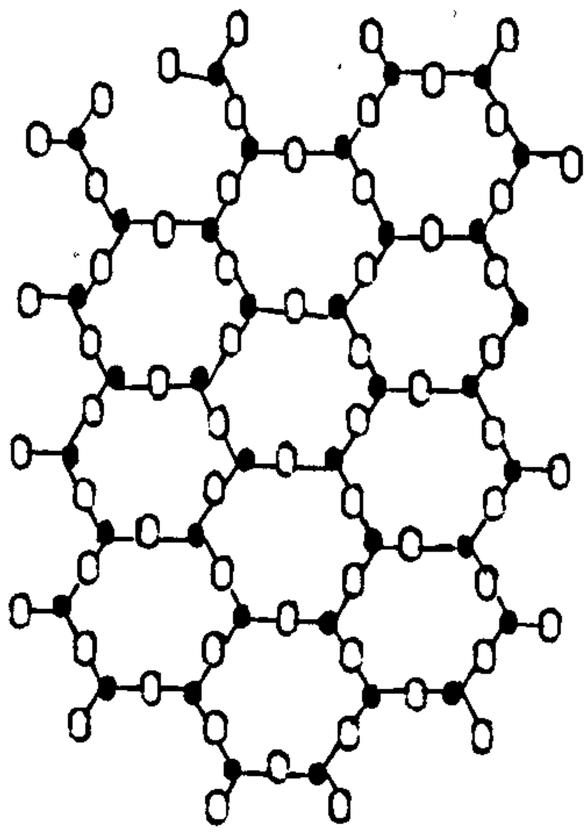

[a]

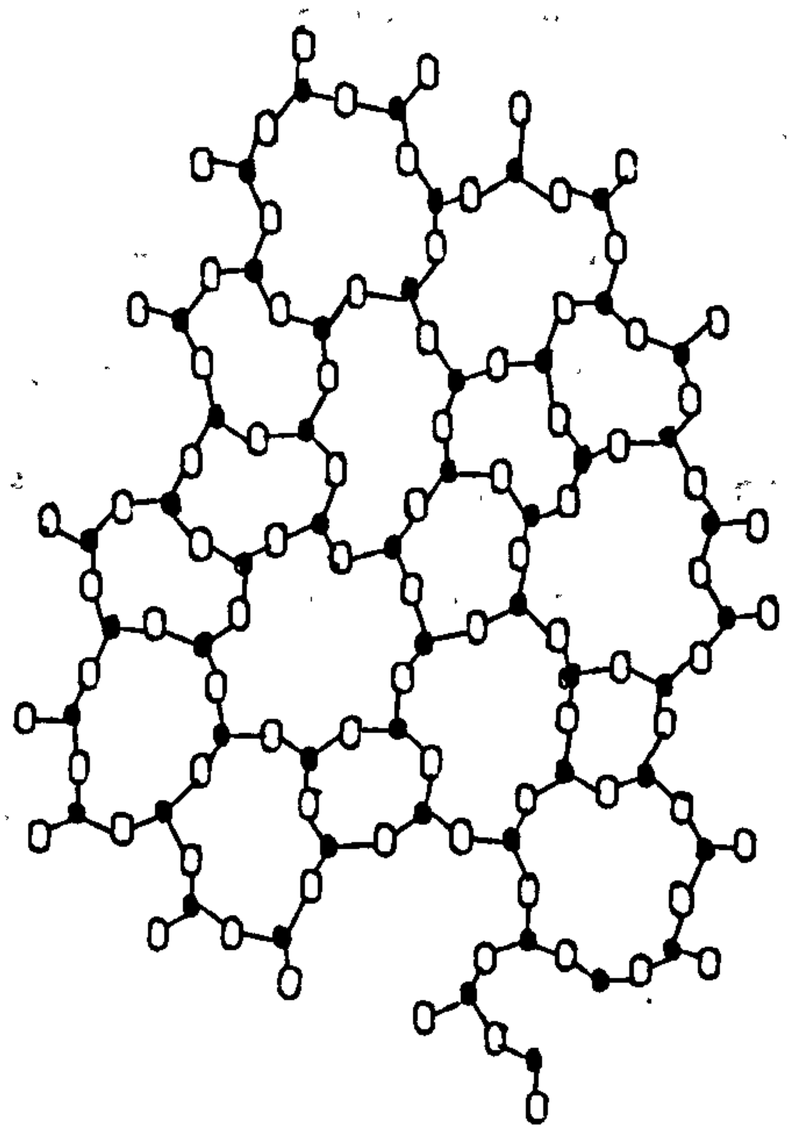

[b]

Fig. 1.2 Schematic representation of (a) ordered crystalline form and (b) random-network glassy form of the same composition.

applied are the microcrystallite[13] and the random-network models[8]. There are several other models such as the amorphous cluster type models[14] which are assemblies of small and tightly bound, but non-crystalline clusters of atoms.

1.5.1 The Random-Network Model

According to this model, glasses are viewed as three-dimensional networks or arrays, lacking symmetry and periodicity, in which no unit of the structure is repeated at regular intervals. In the case of oxide glasses, these networks are composed of oxygen polyhedra. Adopting the hypothesis that a glass should have an energy content similar to that of the corresponding crystal, Zachariasen (1932)[18] considered the conditions for constructing a random network such as shown in Figure 1.2 and suggested four rules for the formation of an oxide glass :

1. Each oxygen ion should be linked to not more than two cations.
2. The coordination number of oxygen ions about the central cation must be small, four or less.
3. Oxygen polyhedra share corners, not edges or faces.
4. At least three corners of each polyhedron should be shared.

In practice, the glass-forming oxygen polyhedra are triangles and tetrahedra, and cations forming such coordination polyhedra have been termed network formers. Alkali silicates form glasses easily, and the alkali ions are supposed to occupy random positions distributed through the structure, located

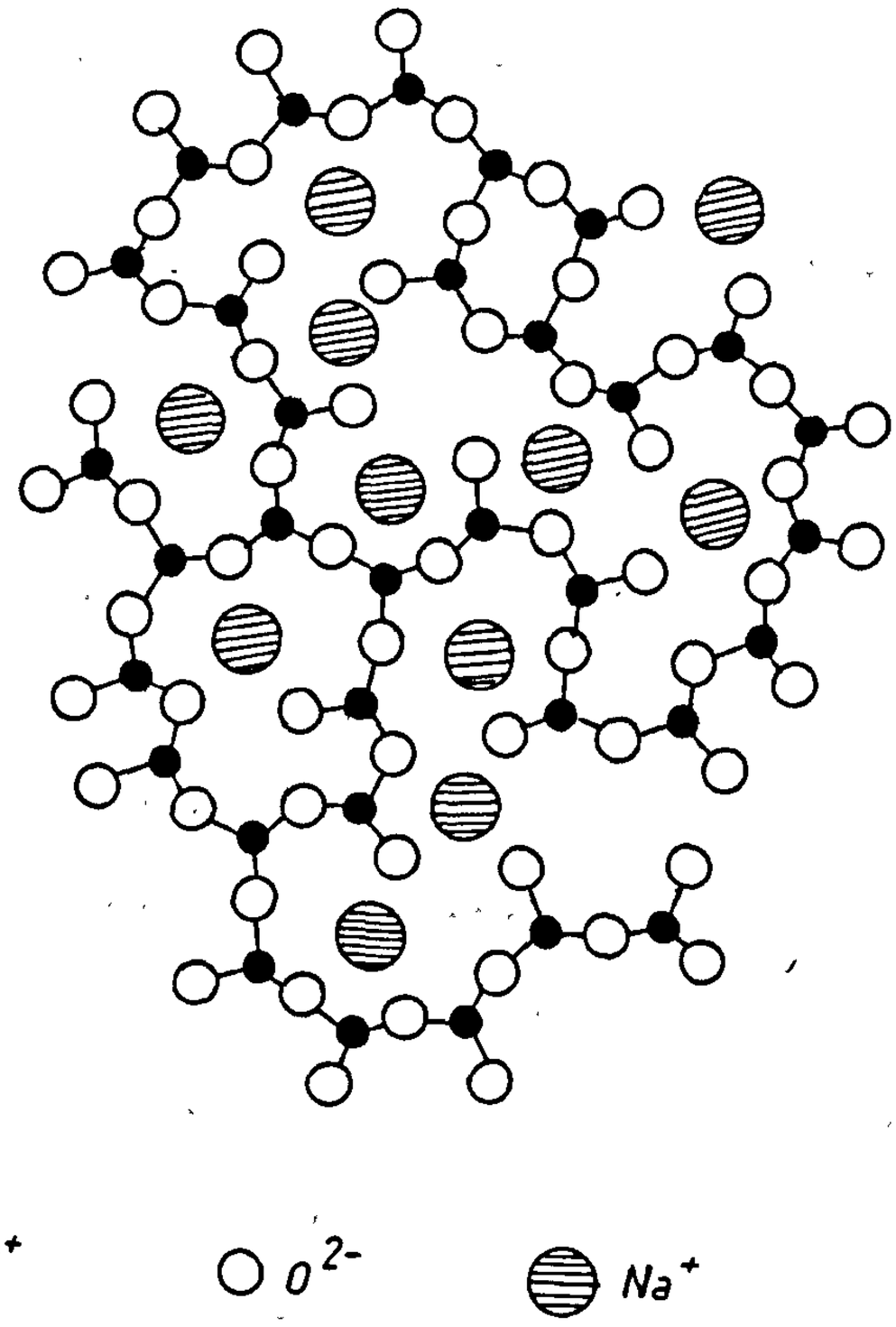

Figure 1.3 Schematic representation of the structure of a sodium silicate glass.

to provide local charge neutrality (Figure 1.3). Since their major function is viewed as providing additional oxygen ions which modify the network structure, they are called network modifiers. Cations of higher valence and lower co-ordination number than the alkalis and alkaline earths may contribute in part to the network structure and are referred to as intermediates. In a general way the role of the cations depends on valency and co-ordination number and the related value of single-bond strength.

The random-network model was originally proposed to account for glass formation as resulting from the similarity of structure and internal energy between crystalline and glassy oxides. Although this remains one factor to be considered, it is believed that kinetic considerations preventing crystallization during cooling are more important. The model remains, however, as the best general picture of many silicate glasses and may readily be generalized as a random-array model in which no unit of the structure is repeated at regular intervals in three dimensions. In this form, the model is used to describe a variety of liquid and glass structures, both oxide and non-oxide, in which three-dimensional networks are not possible

1.6 GLASS CLASSIFICATION

Several writers have suggested various schemes for the classification of non-crystalline materials. Grigorovici

(1969)[15] tried to classify such materials using the idea that the first co-ordination number is preserved in going from the crystalline to the non-crystalline phase[16]. However, this scheme could not accommodate materials like glasses containing transition-metal ions, silicate, borate and multicomponent glasses different in stochiometric percentages. A similar approach of classification has been adopted by Stevels (1971)[17] and by Bell and Dean (1972)[18] by introducing certain parameters. This has proved to be difficult since many physical parameters were required. Mott and Davis (1971)[19] presented another scheme, characterized by the nature of the chemical bonds. This scheme seems to include most of the reported amorphous materials. Mott and Davis (1979)[2] further discussed the classification of non-crystalline materials on the basis of co-ordination numbers. They have also stated that another scheme of classification might be to group materials according to whether their amorphous structure is best described by continuous random networks, by assemblies of distorted layers, molecules, or polymeric units or by close packing of atoms, etc. The difficulty of this scheme is that there are insufficient data to classify many materials properly.

Fritzsche (1973)[20] reported another scheme based on the idea of isolating those materials whose uppermost valence band is made up of non-bonding (lone pair) orbitals, example those containing a large proportion of a two-fold co-ordinated chalcogenide elements S, Se, Te or O.

Five general categories of glasses are presented as follows.

1.6.1 Elemental Glasses

A glass of this category contains only one kind of atom. Elements of group VI of the periodic table, S, Se and Te can form glasses. These elements are known to form a vitreous network when mixed or chemically bonded to each other and are known to be very viscous in the liquid state and to undercool very easily.

1.6.2 Oxide Glasses

They form the main glasses available on a commercial basis. Oxide glasses can be divided into two groups.

(a) Glass Formers.

Oxides which form glasses when cooled from the melt are termed glass-forming oxides or glass formers (Table 1.1). Each glass-forming oxide can be mixed with a second oxide or mixture of these oxides and still form a glass. But, in general, there are usually limits to the percentage of the oxides involved.

(b) Conditional Glass Formers.

This group of oxides TeO_2, WO_3, MoO_3, V_2O_5 etc cannot form glasses on their own, but they can do so when melted with a suitable quantity of a second or a mixture of oxides.

Table 1.1

Glass Formers :	B_2O_3	SiO_2	GeO_2	P_2O_5	As_2O_3	Sb_2O_3
	In_2O_3	SnO_2	PbO_2	As_2O_5		
Conditional Glass Formers :	TeO_2	SeO_2	MoO_2	WO_3	Bi_2O_3	Al_2O_3
	BaO	V_2O_5	SO_3			

The most important of the oxide glasses are silica glass (SiO_2), borate glasses (B_2O_3), transitional-metal oxide glasses and phosphate glasses (P_2O_5).

(i) Silica Glasses

There are many types of silicate glasses example soda lime-silicate glasses (Na_2O-CaO-SiO_2), lead alkali silicate glasses, borosilicate glasses and alumina silicate glasses.

(ii) Borate Glasses

Boric oxide (B_2O_3) is the second most important glass forming oxide and is used for special and technical purposes.

(iii) Transition-Metal Oxide Glasses

These glasses consist of inorganic oxides containing an appreciable amount of transition-metal ions (Fe, Cu, V, Co, W, Mo, Mn) which can enter the glass in two or more valence states

(iv) Phosphate Glasses

These glasses are based on P_2O_5 as a glass forming oxide. Of the three known oxides of phosphate, P_2O_3, P_2O_4 and P_2O_5, only the pentoxide forms glasses.

1.6.3 Halide Glasses

In the halogen group, F and Cl form glasses when reacted with metals. The only halides generally accepted as glass formers are BeF_2 and $ZnCl_2$.

1.6.4 Hydrogen-Bond Glasses

The presence of the hydrogen bond in certain oxides leads to the formation of glasses. The chemical bonds linking the atoms in the oxides are known to be partly ionic and partly covalent. Water itself will form glass if the vapour is cooled very rapidly. A number of aqueous solutions form glasses far more readily, e.g. solutions of H_2O, HCl, $HClO_4$, NH_4OH, KOH and LiCl.

1.6.5 Chalcogenide Glasses

The chalcogenide glasses are those containing the group VI (chalcogenide) elements, sulphur, selenium and tellurium, form glasses over a fairly wide regions of composition when mixed with the group V elements, phosphorus, arsenic, antimony and bismuth. Examples are As-S, As-Se, Ge-Se, etc. This category of electronically conducting glasses has been

intensely studied because of their potential application in active electronic devices.

CHAPTER II

THEORY OF AMORPHOUS SEMICONDUCTORS

2.1 INTRODUCTION

Since the work of Bloch (1928)[21] it has been known that there are universal features in the electronic structures of crystals. The most important are energy bands separated by gaps, crystal momentum as a good quantum number and the form of the wave function. All these provide the conceptual foundations of much of solid-state physics. The existence of such universal features is a result of the regularity of arrangement of atoms in the crystals. But in non-crystalline materials there is no such regularity. In the circumstances theorists have tried to develop an alternative approach to introduce new ideas which go some way towards explaining the basic properties of non-crystalline materials. A great deal of progress has been made but we have to admit that there are still many theoretical uncertainties and alternatives which have not yet been resolved.

In this chapter we introduce some of the theoretical concepts appropriate to the discussion of electronic processes in non-crystalline materials. These theoretical concepts have only emerged long after the theory of electronic processes in crystals was well understood (Frohlich (1947)[22], Anderson (1958)[23]).

2.2 THE UNIVERSAL FEATURES OF THE STRUCTURES OF PERFECT AND IMPERFECT CRYSTALS.

In a perfect crystal each electron is described by a Bloch wave function.

$$\Psi = U(x,y,z)\exp(i\underline{k}.\underline{r}) \qquad (2.1)$$

where U(x,y,z) has the periodicity of the lattice, $\underline{k}$ is the quantum number for the electron. As in the free electron case, an electron described by Equation 2.1 goes everywhere in the crystal with equal probability. Figure 2.1a shows the density of states N(E) as a function of energy E for a perfect crystal. For the case of an imperfect crystal, due to the presence of phonons or impurities, scattering takes place. The perfect phase coherence, i.e., long-range order in the phase, is lost. A mean free path L is introduced such that

$$\frac{1}{L} = N\int_0^{\pi} I(\theta)(1-\cos\theta)2\pi\sin\theta\, d\theta \qquad (2.2)$$

where N are the impurities or phonons per unit volume and I(θ) is the differential scattering cross-section. Equation 2.2 is based on the assumptions that the Fermi surface is spherical; in such case I(θ) is independent of the initial direction of motion of the electrons. The characteristic of the conduction and valence bands of many crystalline solids is such that the energy E(k) is dependent on the direction of $\underline{k}$. The density of states N(E) as a function of energy E for an imperfect crystal is shown in Figure 2.1b. In these

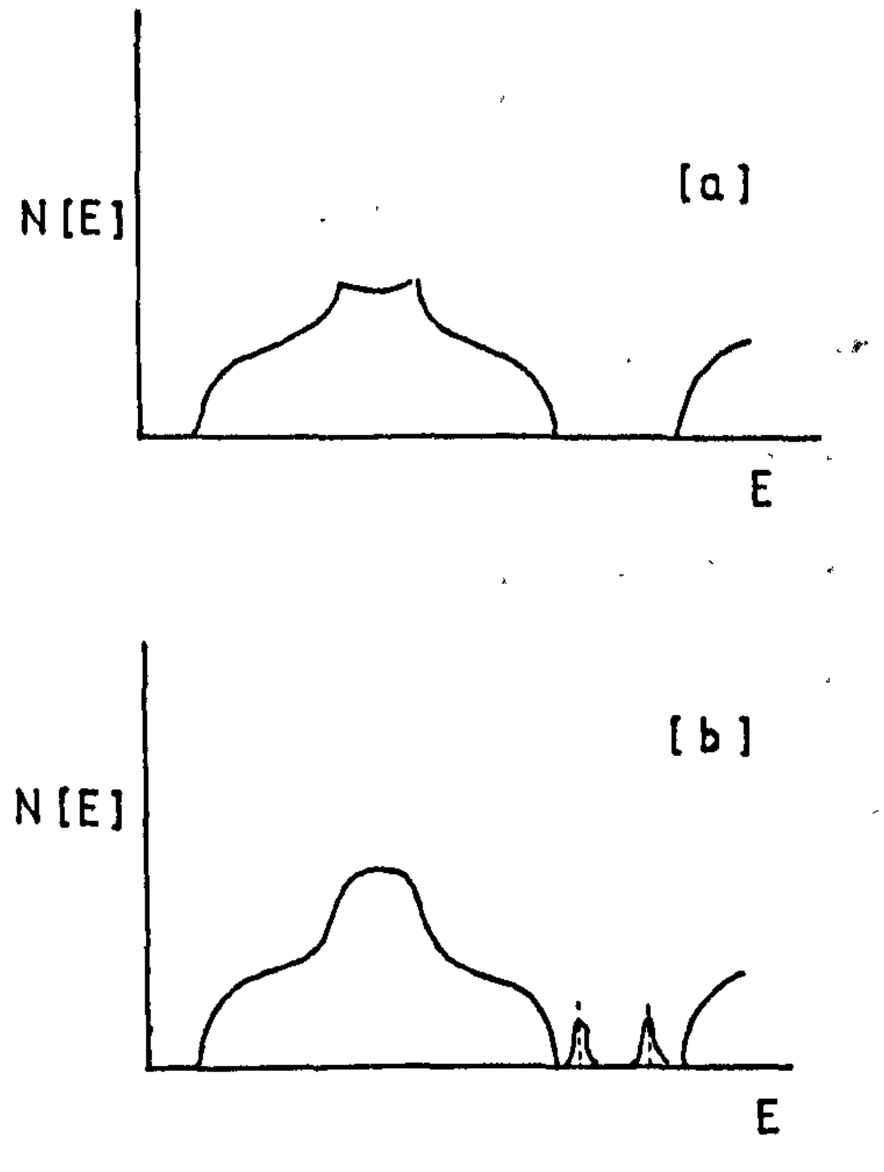

Figure 2.1 Density of states N(E) as a function of energy E for (a) a perfect crystal (b) an imperfect crystal.

two cases, Figure 2.1a and Figure 2.1b, there are continuous bands of energy levels separated by gaps with square root singularities at the band edges. The square root singularities associated with saddle points within the band in Figure 2.1a are eliminated by scattering in Figure 2.1b.

Before we could proceed to presenting the simplest possible model of electronic structure containing the essential features common to all disordered materials, it is necessary to present first of all a brief account of a quantitative criterion for state localization by Anderson (1958)[23].

2.3 ANDERSON LOCALIZATION

Sufficient disorder can produce characteristic solutions to the Schrodinger equation which are localized in space. Anderson (1958)[23] proved this and gave a quantitative criterion for localization, by using a tight-binding approx-mation, in which a crystalline array of potential wells produces a narrow band of levels (Figure 2.2).

A non-periodic potential can be formed in two ways.

a) By displacement of each centre by a random amount such that the long-range order does not exist.

b) A random potential is added to each well such that an electron encounters potential wells of unequal depths (Figure 2.3).

Anderson (1958)[23] found that if the disorder exceeds a critical limit, all the states will be localized. Taking V_0

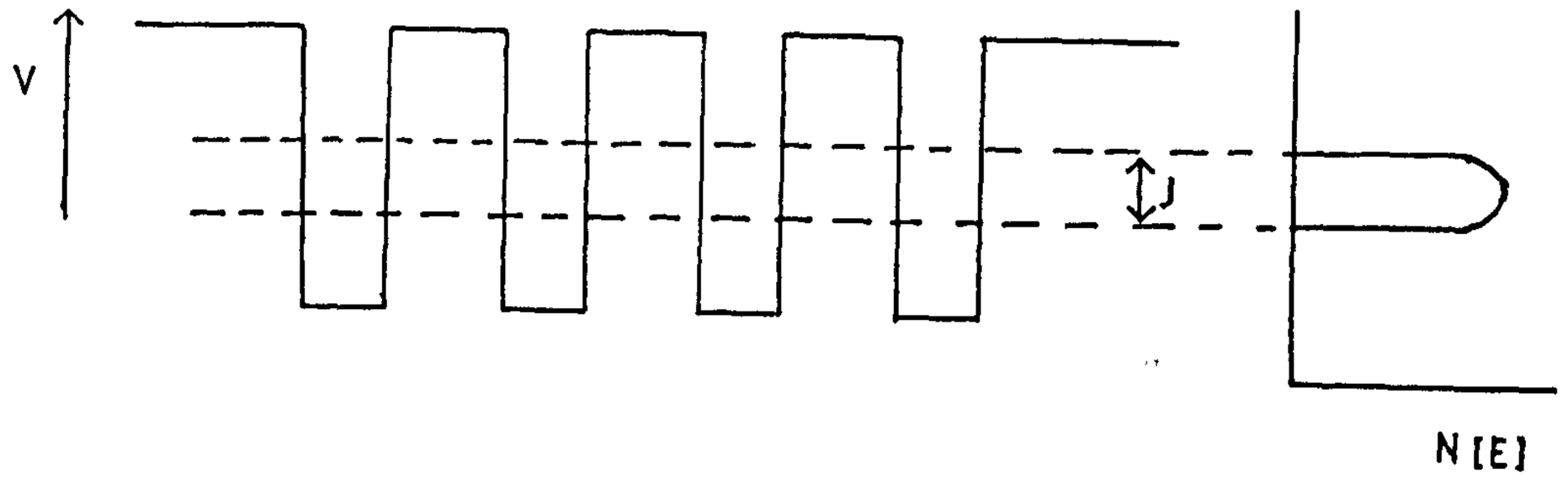

Figure 2.2 Potential well for a crystalline lattice. The density of states N(E) is also shown.

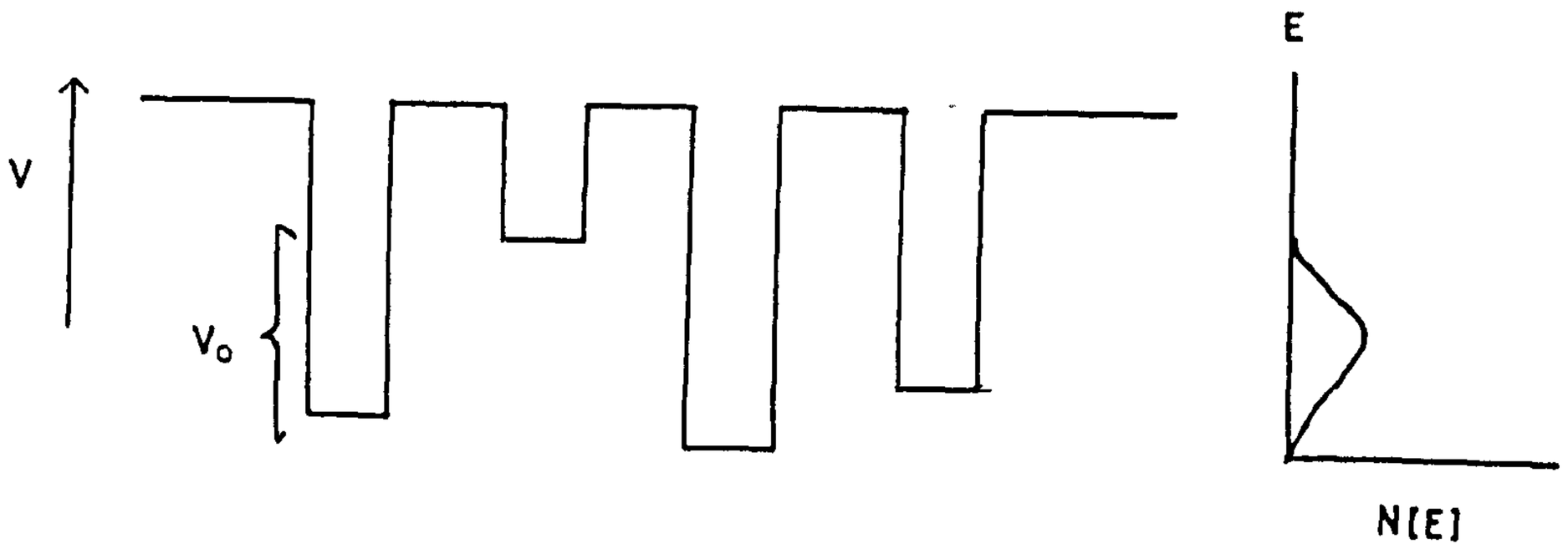

Figure 2.3 Potential wells for the Anderson Lattice.

as the root mean square (r.m.s.) variation of the potential, according to Anderson, no charge diffusion takes place if

$$(V_0/J) > 2$$

where $$J \text{ (the bandwidth)} = 2zI \qquad (2.3)$$

z is the co-ordination number and I is the transfer integral, in which case

$$I = \int \Phi^*(\underline{r}-\underline{R}_n) H \Phi(\underline{r}-\underline{R}_{n+1}) d^3x \qquad (2.4)$$

where H is the Hamiltonian function.

2.4 THE BASIC MODEL

The model, Mott (1967)[24] can be considered as a natural extrapolation of results based on perfect and imperfect crystals and is shown as in Figure 2.4.

Taking a perfect crystal with a single isolated band as a starting point, randomness is introduced continuously through some disordering process. As the randomness increases, the band becomes broader and the nature of the wave-functions changes. For $E_C < E < E_C'$ the states remain extended. At the energies E_C, E_C' the states are localized, so that for $E < E_C$ and $E_C' < E$ there are tails of localized states.

For the states in the middle of the band, the long-range phase order is lost but the states remain extended. On the

other hand, for the states in the tails of the band, the effect of the randomness forced the amplitude of the wave function to be different from zero only in a finite region, changing the character of the states from extended to localized. Localized and extended states cannot belong to the same energy except accidentally; any infinitesimally small perturbation would mix the two states, transforming both of them to extended. As a consequence, there are two characteristic energies E_C, E_C' separating the regions of localized states from that of extended states. The energies E_C',E_C are termed the mobility edges. As the randomness increases, more and more localized states are created, and the mobility edges E_C', E_C move inward into the band. The mean free paths of the extended states are reduced. When the randomness reaches a certain critical value all the states in the band are localized. This is the Anderson (1958)[23] transition.

2.5 BAND MODELS

Any single model cannot describe the essential features of all amorphous materials. This is due to the fact of the large differences in the nature of the various groups of amorphous semiconductors. Here we present a few models which are presently in use.

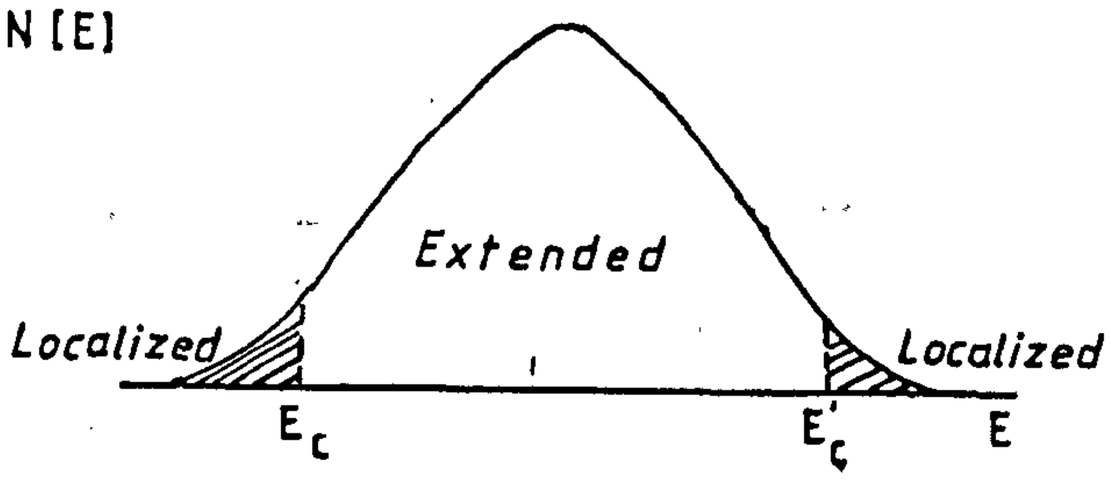

Figure 2.4 The simplest model for the density of states of a single isolated energy band in a disordered material. Localized states are shown shaded. E_C, E_C' separate the ranges of energy where states are localized and non-localized.

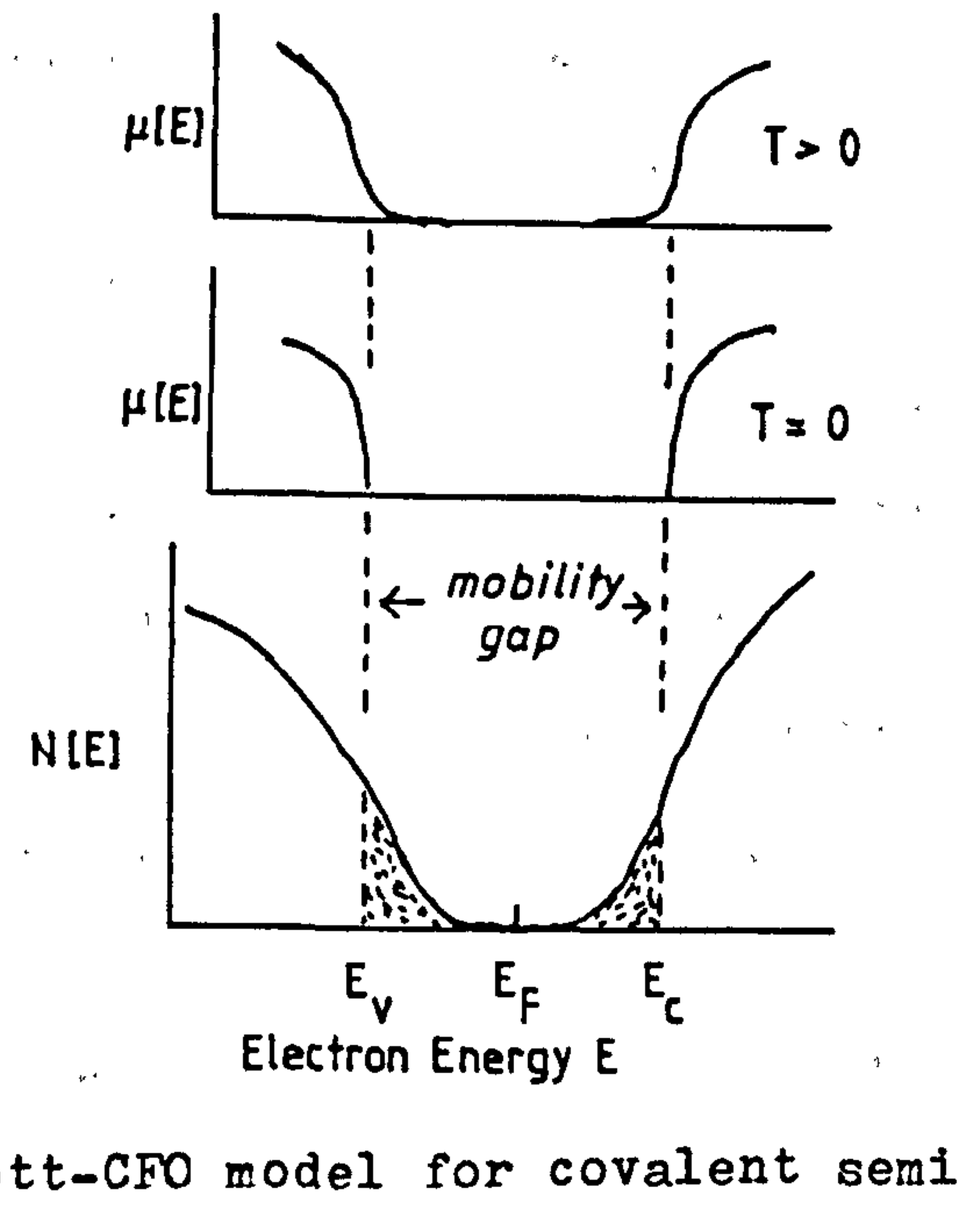

Figure 2.5 Mott-CFO model for covalent semiconductors having three dimensional cross-linked network structure. The critical energies E_C and E_V define the mobility gap. For $T > 0$ the mobility $\mu(E)$ may be finite in the gap because of thermally assisted tunnelling. E_F= Fermi energy. The distribution of localized gap states may be non-monotonic when defect states of a certain energy are prevalent.

2.5.1 Mott-CFO Model

This model is derived from the concept of an ideal covalent random network structure. The observation that amorphous semiconductors are transparent in the infra-red and exhibit a thermally-activated conductivity suggest that the valence and conduction bands are separated by a gap. Translational and compositional disorder are assumed to cause fluctuations of the potential of sufficient magnitude that they give rise to localized states extending from the conduction and valence bands into the gap. These localized states are not associated with definite imperfections but are the result of the randomness of the potential. Their number and energy spread increases with the degree of the randomness and the strength of the scattering. It is important to note that the valence band tail states are assumed to be neutral when occupied and the conduction band tail states are neutral when empty. This places the Fermi energy somewhere near the gap centre. In addition one expects that deviations from the ideal covalent random network, such as vacancies,dangling bonds, and chain ends, contribute localized states in certain energy ranges. These then give rise to a non-monotonic density of localized states curve.

Mott (1967,1969a,1969b,1969c,1970a)[25-29] shows the character of the wavefunction changes at critical energies E_C and E_V which separate the extended and the localized states.

Here the electron and hole mobilities drop sharply from a low-mobility band transport with finite mobility at T = 0 to a thermally activated tunnelling between localized gap states which disappears at T = 0. These mobility edges (Cohen, Fritzsche, and Ovshinsky (1969)[30]) define a mobility gap E_C- E_V which contains only localized states. This model is believed to apply to alloy glasses which contain compositional and positional disorder.

2.5.2 Davis -Mott Model

This band model was proposed by Davis and Mott (1970)[31]. The mobility edges for electrons and holes lie again at E_C and E_V (Figure 2.7). A stronger distinction is made between localized states which originate from lack of long-range order and others which are due to defects in the structure. The first kind of localized states extends only to E_A and E_B in the mobility gap. The defect states form longer tails but of insufficient density to pin the Fermi level. Moreover, the authors propose a band of compensated levels near the gap centre in order to pin the Fermi level and to account for the behaviour of the a.c. conductivity. The centre band may be split into two bands (Mott (1971)[32]).

2.5.3 Marshall-Owen Model

In this model (Marshall and Owen (1971)[33]), the position of the Fermi level is determined by bands of donors

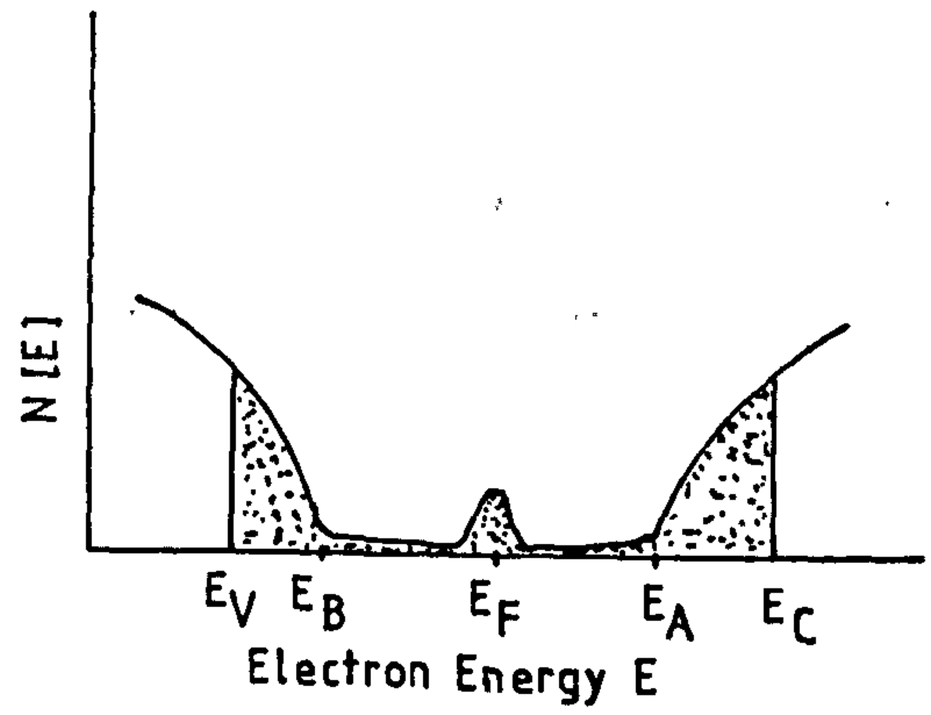

Figure 2.6 Model suggested by Davis and Mott (1970)[31] E_C-E_V is the mobility gap. The ranges E_C-E_A and E_B-E_V contain localized states originating from lack of long-range order. Thermally assisted hopping may take place in these ranges. A band of compensated levels is proposed to lie near the gap.

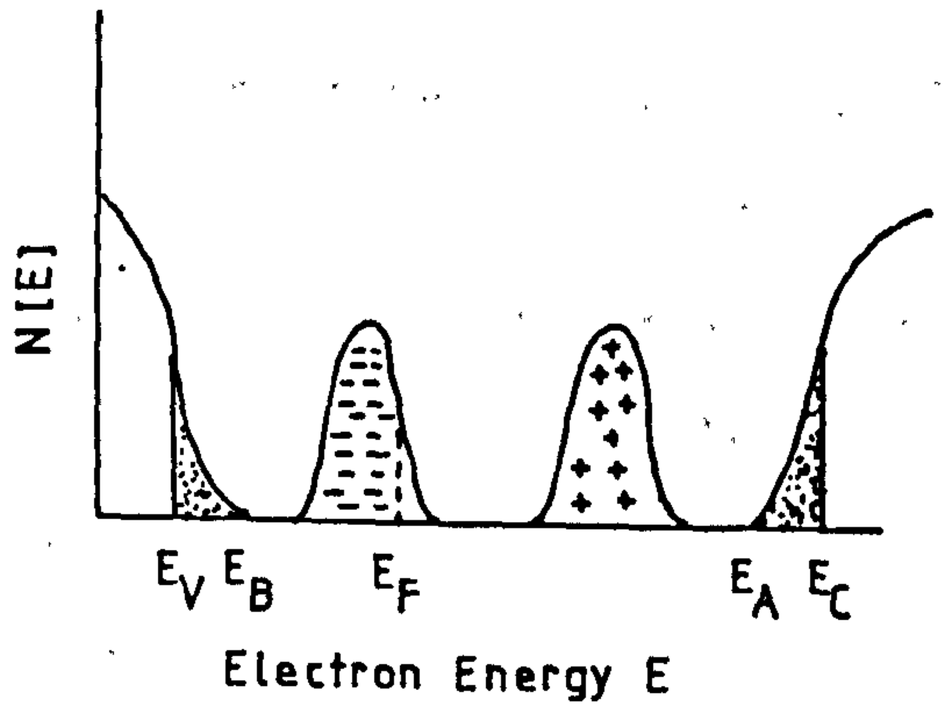

Figure 2.7 Density of states N(E) suggested by Marshall and Owen (1971)[33] for As_2Se_3. A band of localized acceptor states lies below and a band of donor states above the gap centre. As T is increased E_F moves toward the gap centre.

and acceptors in the upper and lower halves of the mobility gap, respectively. The concentrations of donors and acceptors adjust themselves by self-compensation to be nearly equal so that the Fermi level remains near the gap centre. At low temperature it moves to one of the impurity bands because self compensation is not likely to be complete. This model is based mainly on the observation that the high field drift mobility in As_2Se_3 is of the Poole-Frenkel form, presumably because of the field-stimulated emission of carriers from charged trapping centres (acceptors).

2.5.4 Sharp Band Edge Model

Molecular solids and tight binding, semi-insulating materials with large band gaps have electronic structures which are relatively insensitive to disorder. In these materials tail states are negligible and a band model not significantly different from that of crystals with sharp band edges is appropriate. Since the molecular units are well defined entities, one expects that the energies of localized defect states fall into rather narrow energy ranges deep in the gap. Because the energy to create a defect state is of the order of the band gap, their number will be small and self compensation, as well as association of donor and acceptor type defects are energetically favoured. This model is useful for describing oxide films, oxide glasses, a-Se and molecular semi-insulating materials.

2.6 ELECTRICAL PROPERTIES OF NON-CRYSTALLINE SEMICONDUCTORS

The purpose of the models described above is to provide the density of extended and localized states N(E) and the mobility $\mu(E)$ as a function of energy such that one can proceed to calculate the conductivity, using the Kubo-Greenwood formula[34,35].

The formula for conductivity was based on a degenerate electron gas at zero temperature, states being occupied up to an energy E_F. Taking the case for a non-periodic field, the eigenfunctions for an electron will be in the form $\psi_E(x,y,z)$ and these are normalized to give one electron in a volume Ω If an electron makes a transition from a state with energy E to any of the states with energy $E + \hbar\omega$, then the matrix element $x_{E',E}$ is defined as

$$x_{E',E} = \int \psi^*_{E'} x \psi_E \, d^3x$$

Further defining

$$D_{E',E} = \int \psi^*_{E'} \frac{\delta}{\delta x}(\psi_E) \, d^3x$$

then the conductivity for frequency ω, written as $\sigma_E(\omega)$ is

$$\sigma_E(\omega) = \left[(2\pi e^2\hbar^2\Omega)/(m^2\omega)\right] \int \left[f(E)\,|1 - f(E+\hbar\omega)| - f(E+\hbar\omega)\,|1-f(E)|\right] |D|^2_{av} N(E)N(E+\hbar\omega) \, dE \quad (2.5)$$

the suffix av represents an average over all states having energy values near $E' = E + \hbar\omega$. To obtain the d.c. conductivity we take the limit $\sigma(\omega)$ when ω approaches zero. At T = 0 this depends only on the values of the quantities

in the integral $E = E_F$. $\sigma_E(0)$ is defined as

$$\sigma_E(0) = [(2\pi e^2\hbar^3\Omega)/m^2]|D_E|^2_{av}\,[N(E)]^2 \qquad (2.6)$$

where

$$D_E = \int \psi^*_{E'}\,\frac{\delta}{\delta x}\psi_E\,d^3x \quad (E=E')$$

The av represents an average over all states E and all states E' such that $E = E'$, so that at $T = 0$ the conductivity $\sigma(0)$ is given by

$$\sigma(0) = [\sigma_E(0)]_{E=E_F}$$

where E_F is the Fermi energy. Equation 2.6 is the Kubo-Greenwood formula. If the states with energy E are localized, all the functions D_E vanish, because $\int \psi_E \frac{\delta}{\delta x} \psi_E\,d^3x$ is zero, and overlap between two localized functions ψ_1, ψ_2 with the same energy is impossible.

2.6.1 d.c. Conductivity

Adopting the notation of Davis and Mott (1970)[31], we may expect to find three principal contributions to the conductivity.

a) Band conduction of electrons excited above E_c or holes below E_v. The conductivity is (for electrons)

$$\sigma = \sigma_o \exp\left(-\frac{E_c - E_F}{kT}\right) \qquad (2.7)$$

where σ_o is the minimum metallic conductivity. A plot of $\ln\sigma$ versus $1/T$ will yield a straight line if $E_c - E_F$ is a linear function of T over the temperature range measured.

b) Transport by carriers excited into localized gap states near the mobility edges, near E_A and E_B (Figure 2.6) or the donor acceptor bands of Figure 2.7. The conductivity will thus be of the form

$$\sigma = \sigma_1 \exp(- \frac{E - E_F + W_1}{kT}) \qquad (2.8)$$

where W_1 is the activation energy for hopping. σ_1 is expected to be several decades smaller than σ_o. For the Davis -Mott Model $E = E_A$ (or E_B). As the principal temperature dependence is through the carrier activation term, an approximately linear dependence of $\ln \sigma$ versus $1/T$ is again expected.

c) Conduction near E_F should be of the form

$$\sigma = \sigma_2 \exp(- W_2/kT) \qquad (2.9)$$

where W_2 is the hopping energy. Since the density of states near E_F and the range of their wave functions is probably smaller near E_F than near E_A or E_B one expects $\sigma_2 \ll \sigma_1$
At temperatures such that kT is less than the bandwidth or if N(E) is as shown in Figure 2.5, hopping will not be between nearest neighbours. For this so-called variable range hopping process Mott (1969a,1972)[26,36] derived the relation

$$\sigma = A \exp(- B/T^{\frac{1}{4}}) \qquad (2.10)$$

where A and B are constants and B is given by

$$B = 2(a^3/kN(E_F))^{\frac{1}{4}}$$

a is the decay constant and $N(E_F)$ is the density of states near the Fermi level.

2.6.2 a.c. Conductivity

From the previous section we find that there are three mechanisms of charge transport that can contribute to a direct current in amorphous semiconductors. They can also contribute to the a.c. conductivity as follows.

i) Transport by carriers excited to the extended states near E_c or E_v. For these case we expect $\sigma(\omega)$ of the Drude (1902)[37] type,

$$\sigma(\omega) = \sigma(0)/(1 + \omega^2\tau^2) \qquad (2.11)$$

where τ is the relaxation time, ω is the angular frequency and $\sigma(0)$ is the d.c. conductivity. The Drude formula is hardly applicable for small values of τ. Even when τ is large, deviations from the Drude formula are expected if the density of states varies with energy over a range $\hbar/\tau$.

ii) Transport by carriers excited into the localized states at the edges of the valence or conduction band. There are no complete theoretical treatments of $\sigma(\omega)$ for hopping under conditions of non-degenerate statistics. But the result would expected to be of the kind derived under degenerate conditions (see (iii)). Thus

$$\sigma(\omega) \propto \omega[\ln\ (\nu_{ph}/\omega)]^4 \qquad (2.12)$$

where ν_{ph} is the phonon frequency. This varies as ω^s, where $s<1$ when $\omega < \nu_{ph}$. The conductivity of many chalcogenide glasses and oxide films (Argall and Jonscher (1968)[38], Linsley, Owen, Hayatee (1970)[39], Sayer et al (1971)[40]) exhibits over a large frequency range a dependence on frequency as

$$\sigma(\omega) = \text{const.}\ \omega^s \qquad (2.13)$$

with $0.7 < s < 1$.

iii) Hopping transport by electrons with energies near the Fermi level for a finite $N(E_F)$. Austin and Mott (1969)[41] adapted the theory of Pollack and Geballe (1961)[42] and obtained

$$\sigma(\omega) = [(\pi e^2 kT)/3][N(E_F)]^2 \alpha^{-5} \omega[\ln\ (\nu_{ph}/\omega)]^4 \qquad (2.14)$$

The frequency dependence predicted by Equation 2.14 can be written as $\sigma(\omega) \propto \omega^s$ where s is a weak function of frequency if $\omega << \nu_{ph}$. A plot of $\ln\sigma(\omega)$ verses $\ln\omega$ is approximately linear with slope s given by

$$s = d[\ln\{\ln^4(\nu_{ph}/\omega)\}]/[d(\ln\omega)]$$
$$= 1 - 4/[\ln\ (\nu_{ph}/\omega)]$$

2.7 OPTICAL ABSORPTION

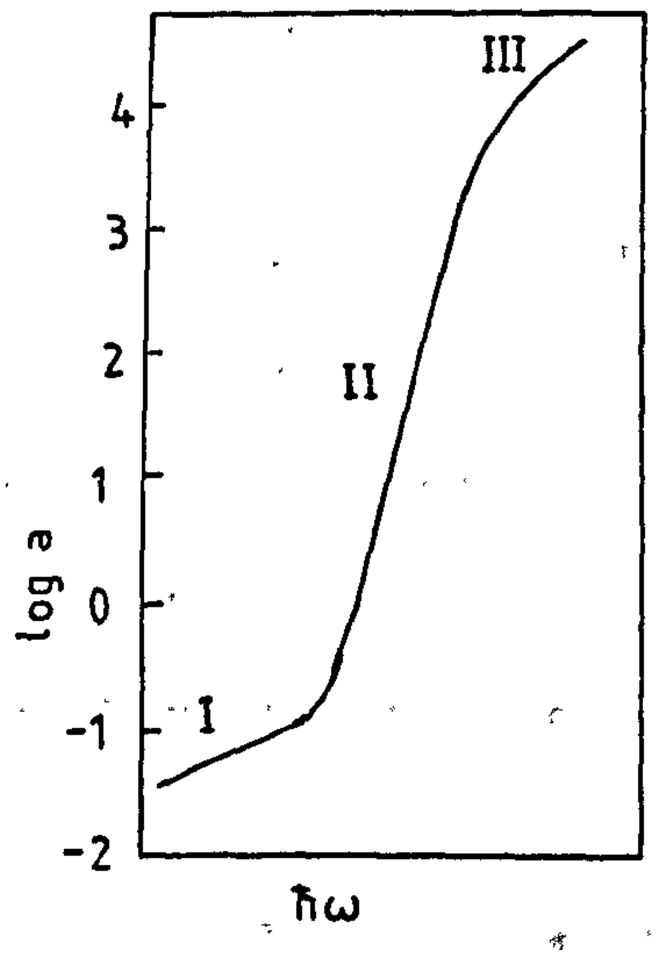

Fig. 2.8 Parts I, II, III of the absorption edge.

In many armorphous compound semiconductors the absorption coefficient a as a function of photon energy has the shape shown in Figure 2.8. The absorption curve may be divided into three regions: (I) which sometimes obeys Urbach's rule, (II) another exponential region which may extend over 4 orders of magnitude and for which the slope is largely independent of temperature (except at high temperatures) and (III) a region of high absorption ($a \geq 10^4 cm^{-1}$) which obeys the relationship

$$\hbar\omega\alpha(\omega) \backsim (\hbar\omega - E_g^{opt})^r \qquad (2.15)$$

where r is a constant normally in the range 1 to 3.

Equation 2.15 has been used to define the optical gap E_g^{opt}.

Basically there are two types of optical transition that can occur at the fundamental edge of crystalline semiconductor, direct and indirect. Both involve the interaction of an electromagnetic wave with an electron in the valence band region. However, indirect transitions also involve simultaneous interaction with lattice vibrations. Thus the wave-vector of the electron can change in the optical transition, the momentum change being taken or given up by phonons. The fundamental absorption edge in most amorphous semiconductors follows an exponential law, i.e. $\ln\alpha$ is proportional to $\hbar\omega$. There are several explanations for the existence of an exponential absorption edge. Tauc (1970a)[43] suggested that it arises from electronic transitions between states in the band-edge tails, the density of which is assumed to fall off exponentially with energy. However, Davis and Mott (1970)[31] felt that this explanation is unlikely. The exponential tail is more likely to be due to the effect of internal electric fields (due to charged impurity states, dangling bonds, voids, bent bonds and also to the vibrating atoms in the materials).

Mott (1970)[29] discussed the form of the optical absorption edge in amorphous semiconductors by neglecting

the presence of any electric field or exciton effect. He made other assumptions as well,

a) The matrix elements for the electronic transitions are constant over the range of photon energies of interest.

b) The k-conservation selection rule is relaxed.

If $\sigma(\omega)$ is the conductivity at frequency ω, the corresponding absorption coefficient is given by

$$a = [(4\pi)/(n_o c)]\,\sigma(\omega) \qquad (2.16)$$

where n_o is the refractive index. The conductivity is given by

$$(\omega) = [(2\pi e^2 \hbar^3 \Omega)/m] \int [N(E)N(E+\hbar\omega)\ |D|^2]/(\hbar\omega) \qquad (2.17)$$

where Ω is the volume of the specimen and D the matrix element of $\frac{\delta}{\delta x}$. The integration is over all pairs of states in the valence and conduction bands separated by energy $\hbar\omega$. From the assumption that E_o corresponds to h, the transition $\hbar\omega = E_A - E_B$ (using the notation of Figure 2.6) and $N(E) \backsim E^{\frac{1}{2}}$ at the bottom of each band, Tauc (1969)[43] derived a formula for absorption near the edge as

$$a(\omega) \backsim (\hbar\omega - E_o)^2/\hbar\omega \qquad (2.18)$$

Combining the above equation with Equation 2.16 we get

$$a(\omega) = \frac{B(\hbar\omega - E_o)^2}{\hbar\omega} \qquad (2.19)$$

where B is a constant.

The absorption of many amorphous materials is observed to obey this relation above the exponential tails. The constant E_o can be used to define an optical gap E_g^{opt}. The relation between $a(\omega)$ and $\hbar\omega$ has also been derived by Davis and Mott (1970)[31] using different assumptions. Assuming that the density of states at the band edges are linear functions of the energy, such that $N(E_c) = N(E_v)$, $E_c - E_A = E_B - E_v = \Delta E$ and that transitions in which both the initial and final states are localized can be deglected, then from Equation 2.18

$$a(\omega) = \frac{(\frac{4\pi}{n_o c})\ \sigma_o(\hbar\omega - E_o)^2}{\hbar\omega\Delta E} \qquad (2.20)$$

Here E_o is $E_A - E_v$ or $E_c - E_B$, whichever is the smaller.

CHAPTER III

ELECTRICAL PROPERTIES OF TRANSITION-METAL OXIDE PHOSPHATE GLASSES

3.1 INTRODUCTION

Oxide glasses containing transition-metal ions were first reported to have semiconducting properties in 1954[44]. Since then most studies have been on systems based on phosphates, although semiconducting oxide glasses based on other glass formers have also been made. Early work up to 1964 has been reviewed by Mackenzie (1964)[45], while more recent reviews by Mott (1968)[46], Austin and Mott (1969)[41] and Owen (1970)[47] have treated semiconducting glasses as a part of the general problem of electrical properties of non-crystalline materials. Sayer and Mansingh (1972)[48] and Kinser and Wilson (1974)[49] on the other hand were mostly concerned only with the phosphates.

Transition-metal oxides can form homogeneous glasses when mixed with P_2O_5, but the P_2O_5 (glass former) does not play a major role in the electrical conduction. The general condition for the semiconducting behaviour is that the transition-metal ion should be capable of existing in more than one valence state, such that conduction occurs by movement of carriers from the lower valency state to the higher valency state.

In this chapter we shall discuss the theoretical aspects of the conductivity in term of polaron theory and then review briefly the experimental results with respect to the theory.

3.2 POLARON THEORY

Many authors have suggested thermally activated hopping as the mechanism of charge transport in glasses containing transition-metal oxides[45,50,51] . A careful study of the conductivity as a function of temperature on such glasses strongly suggests that the charge carrier is well described by a small-polaron. The theory of conduction by a small polaron has been chiefly developed by Holstein (1959)[52] and by Friedman (1964)[53].

One striking feature of small-polaron conduction is a transition between conduction in a polaron band, characterized by exact conservation of the lattice energy, and conduction by hopping which is characterized by an alteration in the phonon occupation numbers. Above the critical temperature, the dominant conduction mechanism is thermally-activated hopping in which the electron-site change is accompanied by the emission and absorption of many phonons and hence, a change in the phonon occupation numbers. Below the critical temperature, the conduction is in a polaron band characterized by site transfers in which the phonon occupation numbers are unchanged. The temperature dependence of conductivity in transition-metal oxide glasses can be explained on the

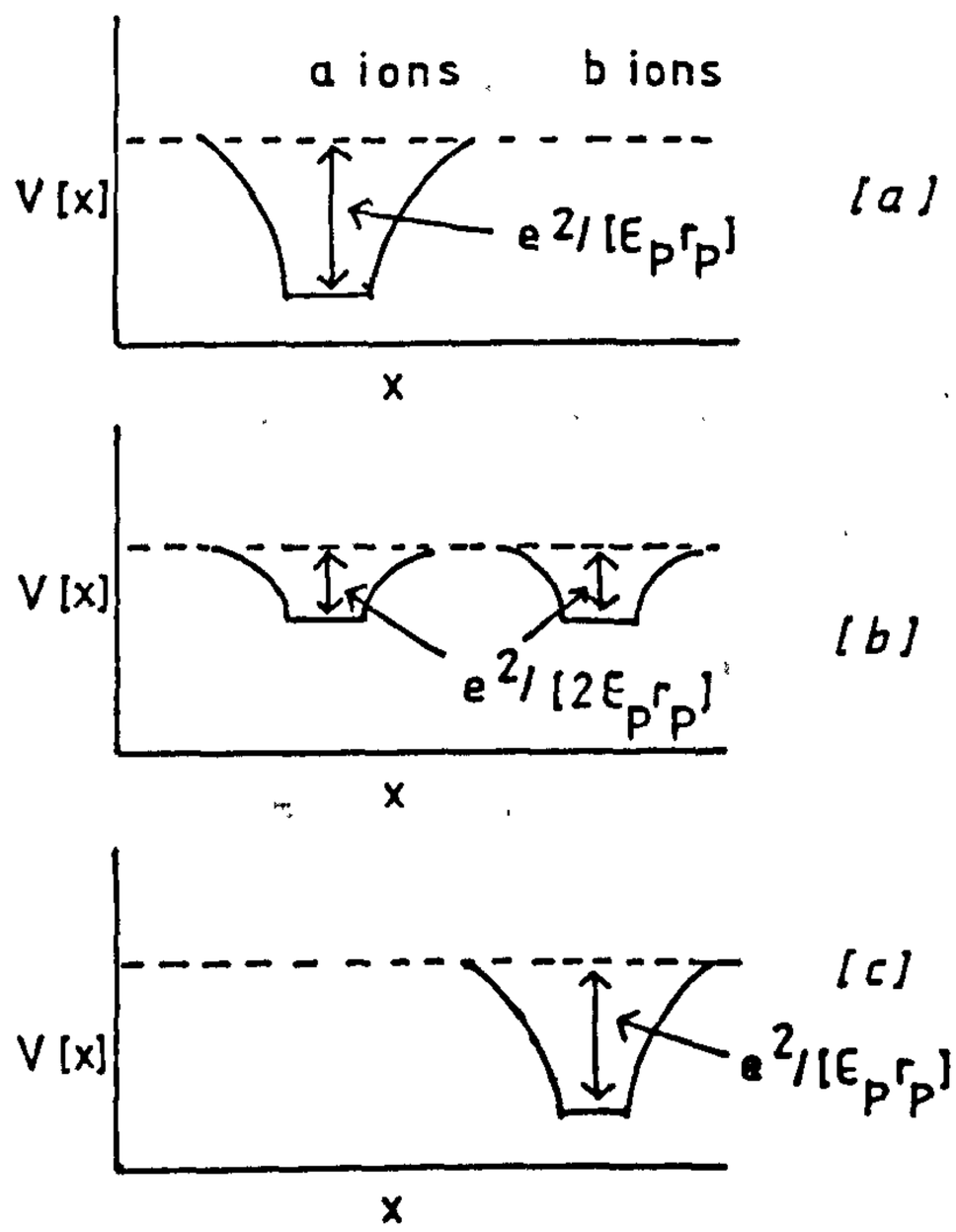

Figure 3.1 The polarization wells for two transition-metal ions in glass during the hopping process: (a) before hopping (b) thermally activated state when electron can move, (c) after hopping (Mott (1968)[46]).

basis of such a change in the transport mechanism.

Figure 3.1 presents Mott's[46] picture of an electron-hopping process between a and b ions in a lattice. Initially, as in Figure 3.1a, the electron is trapped in a potential well. The smallest activation energy corresponds to the state as shown in Figure 3.1b when thermal fluctuation ensures that the wells have the same depths. The energy necessary to produce this configuration is given by

$$W_H = \tfrac{1}{2}W_P \qquad (3.1)$$

W_P the polaron binding energy is given by[46]

$$W_P = e^2/2\epsilon_P r_P \qquad (3.2)$$

where ϵ_P the effective dielectric constant as defined by

$$1/\epsilon_P = 1/\epsilon_\infty - 1/\epsilon_S$$

ϵ_S and ϵ_∞ are the static and high-frequency dielectric constants of the material and r_p is the polaron radius. Equation 3.1 is only correct when R, the distance between centres, is large[54]. When the concentration of sites is large and therefore the two polarization clouds overlap, W_H must be dependent on the jumping distance. Mott (1968)[46] modified Equation 3.1 to obtain

$$W_H = \tfrac{1}{4}(e^2/\epsilon_P)(1/r_P - 1/R) \qquad (3.3)$$

In order that the polaron should be small, the polaron radius r_P should be greater than the radius of the ion on which the electron is localized, but less than the distance R separating these sites. Bogomolov et al (1967)[55]

calculated the value of r_p for crystalline solids

$$r_p = \tfrac{1}{2}(\pi/6N)^{1/3} \qquad (3.4)$$

where N is the number of sites per unit volume. Hence the polaron should decrease in size as the number of sites increases. In disordered systems an additional term, W_D, that is the energy difference arising from the differences of neighbours between a and b sites, may appear in the activation energy for the hopping process. Austin and Mott (1969)[41] show that the activation energy for the hopping process in the high temperature region is

$$W = W_H + \tfrac{1}{2}W_D + W_D^2/16W_H \qquad (3.5)$$

In the case where $W_H > W_D$ the last term in Equation 3.5 can be neglected. In a generalized polaron model, the activation energy $W = W_H - J$ where J is a polaron bandwidth related to the electron wave function overlap on adjacent sites[48]. Theories have been proposed to cover both adiabatic and non-adiabatic hopping process. In the adiabatic regime, Emin and Holstein (1969)[57] show that the mobility

$$\mu = \frac{4eR^2\omega_o}{3kT}\exp(-(W_H - J)/kT) \qquad (3.6)$$

where R is the interatomic spacing and ω_o the mean phonon frequency. For the case of non-adiabatic hopping, Friedman and Holstein (1963)[58] derive an expression for the mobility as

$$\mu = \frac{3eR^2J^2}{2kT}(\pi/kTW_H)^{\frac{1}{2}}\exp(-W_H/kT) \qquad (3.7)$$

Holstein (1969)[58] shows the condition that for adiabatic

hopping

$$J > (2kTW_H/\pi)^{\frac{1}{4}}(\hbar\omega_o/\pi)^{\frac{1}{2}} \qquad (3.8a)$$

and

$$J < (2kTW_H/\pi)^{\frac{1}{4}}(\hbar\omega_o/\pi)^{\frac{1}{2}} \qquad (3.8b)$$

for non-adiabatic hopping. An estimate of the polaron bandwidth J can be made using the relation[19]

$$J \backsim (e^3 N(E_F)^{\frac{1}{2}}/\varepsilon_p^{3/2}) \qquad (3.9)$$

$N(E_F)$ being the density of states near the Fermi level. Mott (1968)[46] has postulated the following equation for the conductivity in transition-metal oxide glasses.

$$\sigma = (\nu_{ph} N e^2 R^2/kT)C(1 - C)e^{-2\alpha R_e - W/kT} \qquad (3.10)$$

where R is the site spacing, N is the number of sites per unit volume, C is the fraction of sites occupied by an electron in the low valence state, α is the tunnelling probability, ν_{ph} the jump frequency and W is the activation energy for conduction. Austin and Mott (1969)[41] show that

$$W = W_H + \tfrac{1}{2}W_D \quad \text{for} \quad T > \tfrac{1}{2}\theta_D \qquad (3.11)$$

$$W = W_D \quad \text{for} \quad T < \tfrac{1}{4}\theta_D \qquad (3.12)$$

where θ_D, the Debye temperature, defined by $\hbar\omega = k\theta_D$. Equation 3.10 can be compared to the common Arrhenius equation

$$\sigma = \sigma_o \exp(-W/kT) \qquad (3.13)$$

Mott (1968)[46] has pointed out that at very low temperatures the observed value for W_D should approach zero because the most probable jump will not be to nearest neighbours but to more distant sites where the energy difference is small.

The temperature dependence of conductivity under this condition is given by

$$\ln \sigma = A - B/T^{\frac{1}{4}} \qquad (3.14)$$

where A and B are constant and B is given by

$$B = 2.1((\alpha^3)/kN(E_F))^{\frac{1}{4}}$$

$$= 2.4(W_D(\alpha R)^3/k)^{\frac{1}{4}}$$

where $N(E_F)$ is a density of state at the Fermi level.

3.3 ELECTRICAL PROPERTIES

In almost all published work on transition-metal oxide glasses the electrical conductivity is discussed in terms of the Mott theory[41,46]. The analysis of d.c. conductivity is frequently based on Equation 3.10. The variation of conductivity with glass composition is difficult to interpret since the parameters C, W, N and R vary with the proportion and nature of the transition metal ion.

In this section the experimental data of various workers will be discussed in term of the pre-exponential term σ_o of Equation 3.13 and the activation energy.

3.3.1 The Pre-exponential Factor

Iron phosphate glasses show a maximum in conductivity for a reduced transition-metal ion ratio $C = \frac{1}{2}$ as predicted by Equation 3.10[59] but in the vanadate system the maximum

occurs for the value of C between 0.1 and 0.2[60,61]. A similar result was observed in V_2O_5 - TeO_2 glasses[62]. Various explanations have been proposed for this deviation from C = 0.5. Linsley et al (1970)[60] suggest that a fraction of V^{4+} ions are firmly trapped in complexes. Sayer and Mansingh (1972)[48] have proposed that the correlation effect due to short-range Coulomb repulsion will modify C in Equation 3.10 to $C(1 - C)^{n+1}$ where n is the number of sites surrounding the polaron at which strong interaction occurs. In the CuO - P_2O_5 glasses the conductivity increases with ratio $C = Cu^+/Cu_{total}$ and with no observed maximum. Tsuchiya and Moriya (1975)[63] suggest that this is a consequence of ionic conduction of Cu^+ ions; in other words, the glass exhibits a mixed conduction phenomenon in which both ionic and electronic conduction occur in the glass.

The importance of the tunnelling term, $\exp(-2\alpha R)$, to the conductivity is not as obvious as that of the C term and the activation energy. Sayer and Mansingh (1972)[48] have shown that for a series of phosphate glasses containing different transition-metal ions, a semilogarithmic plot of the conductivity measured at a temperature of 500 K versus the high temperature activation energy gives a straight line with a slope corresponding to a measurement temperature of 530 K. They concluded that the pre-exponential term of Equation 3.10 inclusive of $\exp(-2\alpha R)$ is virtually constant for all phosphate glasses containing different 3d transition metal ions. As a consequence, the hopping of a small polaron

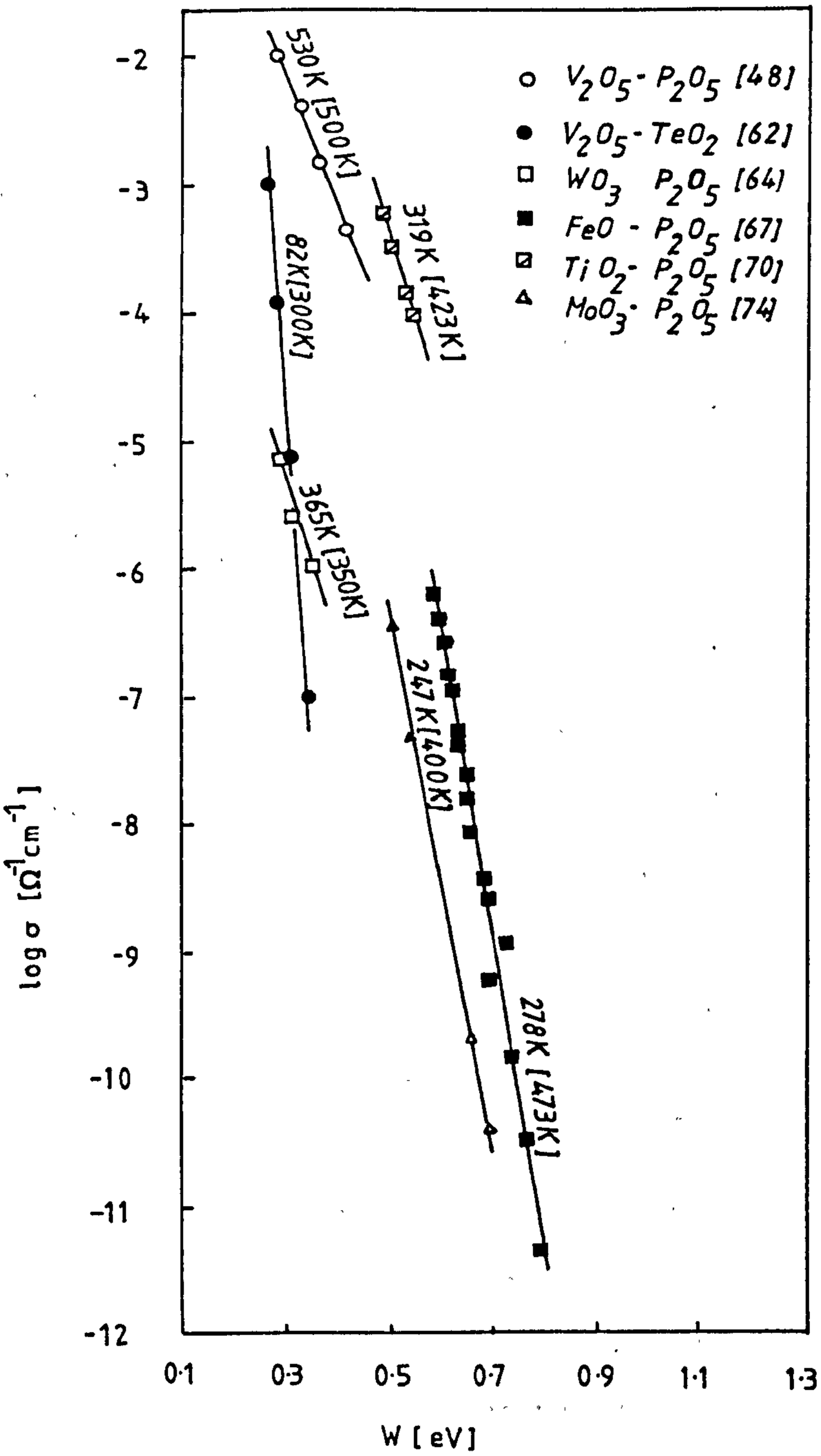

Figure 3.2 The relationship between a logarithm of conductivity and activation energy in various glasses. Experimental temperatures are indicated in parentheses. The open value corresponds to the slope.

in these systems should exhibit an adiabatic character. The Mansingh et al (1978)[64] work on WO_3-P_2O_5 glasses agrees with the results of Sayer and Mansingh (1972)[48]. Murawski et al (1979)[65] compile the results of other authors (Figure 3.2)[59,60,66,67,68] and, using the approach of Sayer and Mansingh (1972)[48], they showed that for the glass systems of V_2O_5-TeO_2, FeO-P_2O_5, MoO_3-P_2O_5, TiO_2-P_2O_5 and V_2O_5-B_2O_3-BaO, the $(kT)^{-1}$ values are 1.6 - 3.5 times higher than the experimental values. As such, the tunnelling term should not be a constant, therefore the hopping polaron for these systems should be in the non-adiabatic regime. For the determination of α, most authors applied Equation 3.10 by calculating R and C values from the composition, based on the assumption that the site distribution is random and assuming the value of ν_{ph} of 10^{11} - 10^{13} s^{-1}. Greaves (1973)[66] showed the possibility of calculating α from the small polaron theory. Experimentally, α values can be obtained from $\log \sigma_o = f(R)$. Murawski and Gzowski (1973)[67] have shown that in iron-phosphate glasses $\log \sigma_o$ is a linear function of R. This is consistent with the result of Hirashima and Yoshida (1977)[68]. The α-value can also be estimated from the low temperature dependence of conductivity, if the variable hopping is observable.

3.3.2 Activation Energy

The separation of the observed activation energy W into a polaron term W_H and a disorder term W_D is a rather difficult

problem. One such estimate is shown by the Miller-Abrahams theory[69] for impurity conduction in doped and compensated semiconductors. The value of W_D was calculated as a thermal activation energy for a random distribution of impurities in a broad-band semiconductor, and

$$W_D = (e^2/\epsilon_s R)K \qquad (3.15)$$

where R is the average distance between transition-metal ions, and K is a constant of order ~ 0.3 which depends on the compensation and is tabulated by Miller and Abrahams (1969)[69]. The value of W_D obtained from Equation 3.15[70] is consistent with the low-temperature (< 100 K) activation energy in V_2O_5-P_2O_5[70], WO_3-P_2O_5[64] and TiO_2-P_2O_5[70] glasses. W_D can also be calculated from the low temperature dependence equation (Equation 3.14), but the value of disorder energy calculated by this method is higher than the low-temperature activation energy in vanadate[71] and tungstate glasses[64]. In iron-containing glasses the observed activation energy is very large. The disorder energy obtained from $\frac{1}{2}W_D = W - W_H = 0.22 - 0.4$ eV[72] (W_H from Equation 3.3) is much higher than the estimated Miller-Abraham disorder term. This discrepancy has been pointed out by Austin (1970)[71] who suggested that an additional term ΔU describing the structural difference between transition-metal ions should appear in the activation energy equation.

$$W = W_H + \tfrac{1}{2}W_D + \Delta U \qquad (3.16)$$

Table 3.1 shows some of the parameters discussed in this chapter.

A careful study of the conduction processes in semiconducting oxide glasses suggests that the polaron model is generally applicable. In many cases Equation 3.10 agrees with experimental data.

Table 3.1

Composition (Mol %)	W^a (eV)	W_D (eV)	r_p (Å)	α ($Å^{-1}$)	Reference
$V_2O_5 - P_2O_5$ (88-49 % V_2O_5)	0.29-0.42	0.1 [b,c]	2.1	-	40,48
$V_2O_5 - P_2O_5$ (80-60 % V_2O_5)	0.31-0.36	0.36-0.43	2.6 - 2.9	2.9-4.0	66
$WO_3 - P_2O_5$ (78-65 % WO_3)	0.29-0.35	0.1 [b]	1.2 - 1.16	2.8-2.4	64
$MoO_3 - P_2O_5$ (85-60 % MoO_3)	0.5 -0.69	-	1 - 2	0.45-0.8	74
$TiO_2 - P_2O_5$ (71-66 % TiO_2)	0.48-0.54	0.05 [b]	1.7	-	70
$FeO - P_2O_5$ (55-15 % FeO)	0.58-0.76	0.44-0.8	1.9 - 3.1	1.5	67,72

a - High temperature experimental value.

b - Low temperature W.

c - Calculated from Miller-Abraham (1969)[69].

CHAPTER IV

GLASS PREPARATION

4.1 INTRODUCTION

Most of the semiconducting oxide glasses described in the literature are based on the V_2O_5-P_2O_5 system[39,45,48]. Relatively less information is obtainable about the cobalt-phosphate glasses. In this chapter we report the results of our measurement (structural) on the binary series (CoO-P_2O_5 glasses) and the ternary series (CoO-NiO-P_2O_5 glasses). The following two chapters will cover the electrical and optical properties.

4.2 GLASS PREPARATION

The glasses were prepared using the oxides CoO, NiO and P_2O_5 (all oxides were supplied by BDH Chemicals Ltd, Poole, England). Two series of glasses were prepared, the binary, CoO-P_2O_5 glasses and the ternary, CoO-NiO-P_2O_5 glasses.

The appropriate weights of oxides were carefully mixed in an alumina crucible and placed in a furnace maintained at 300 °C for one hour. This helps to minimize material volatilization. The crucible was then transferred to a melting furnace maintained between 1200 - 1300 °C (depending on composition - refer Table 4.I) for two hours with frequent

stirring. The homogenized melts were then cast onto a steel-plate mould (preheated at 400 °C). The glasses formed were transferred to an annealing furnace maintained at 400 °C for one hour, and then subsequently allowing slow cooling. The glasses prepared were in a disc-form about 3 cm in diameter and 3 mm thickness. The glasses were chemically stable and relatively insoluble in water. To safeguard against contamination, all the glasses were stored in a vacuum. Table 4.1 shows the range of glass composition examined in this work. Figure 4.1 is a block-diagram showing the stages of preparation.

It should be noted that besides the alumina crucibles, platinum and silica crucibles were also tried. It was found that the surface of the silica crucible dissolved in the molten glass and thus should not be used in the preparation of these series of glasses.

4.3 X-RAY EXAMINATION.

Amorphous materials are often defined operationally by their diffraction patterns, that is, the diffraction patterns consist of a few broad haloes rather than sharp Bragg reflections. All the glass samples were tested using the x-ray Debye-Scherrer powder camera and results showed the absence of crystalline characteristics. Figure 4.2 shows a typical x-ray diffraction photograph of cobalt-phosphate glass.

4.4 DENSITY MEASUREMENT

The densities of the glasses were measured using the displacement method with toluene ($C_6H_5CH_3$, weight per ml at 20 °C = 0.860 - 0.865 gm) as the immersion liquid. Equation 4.1 shows the formula used in the calculation.

$$\rho_g = \rho_l m_1/(m_1 - m_2) \qquad (4.1)$$

where m_1 and m_2 are weights of glass in air and in liquid respectively and ρ_l is the weight per ml of the immersion liquid. Table 4.1 shows the densities of the glasses prepared together with the calculated values of molar volume. The molar volume was calculated from the sum of the molecular weights of each constituent of the glass composition divided by the glass density[75]. Figure 4.3 and Figure 4.4 show the density variation with CoO content in the binary and ternary systems respectively. The results show increases in density as the CoO content increases in the binary system whereas the density decreases with increasing CoO content in the ternary system.

The density of glass 5050 is found to be higher than the value measured by Sayer and Mansingh (1972)[48]. This difference is probably due to the differences of conditions under which the glasses were made.

The variation in molar volume with respect to CoO content is shown in Figure 4.5 for the binary system and Figure 4.6 for the ternary system. The graphs show linear relations

for both systems with decreasing molar volume for an increasing CoO content for the $CoO-P_2O_5$ glasses, and a increasing molar volume with increasing CoO content for the $CoO-NiO-P_2O_5$ glasses. The changes in the molar volume are not considerable in both glass systems. This tends to suggest that the structure of these glasses is considered to be constant with composition[76].

Table 4.1 Preparation Conditions And Analysis

Glass No.	Mol % CoO	Mol % NiO	Mol % P_2O_5	Melting Temperature (C)	Density ($g-cm^{-3}$)	Molar Volume (cm^3)
2575	25		75	1200	2.79	44.8
3070	30		70	1200	2.82	43.0
4060	40		60	1250	2.89	39.8
4555	45		55	1250	2.94	38.0
5050	50		50	1250	3.00	36.1
5545	55		45	1300	3.11	32.9
6040	60		40	1300	3.30	30.8
400555	40	5	55	1250	2.99	37.3
351055	35	10	55	1250	3.04	36.7
301555	30	15	55	1250	3.08	36.2
252055	25	20	55	1250	3.12	35.8

CHAPTER V

D.C. AND A.C. PROPERTIES OF COBALT-PHOSPHATE GLASSES

5.1 INTRODUCTION

In this chapter we present the results of the d.c. and a.c. measurement. The electrical conductivity of the glass is reviewed in the framework of Mott's theory[46].

5.2 SAMPLE PREPARATION

The disc-shaped samples (as described in the previous chapter) were ground mechanically with a flexibox grinding machine using different grades of SiC powder. On achieving a thickness of about 2 mm the samples were then cleansed with acetone and polished with a polishing machine using a diamond paste of grade 6μm.

A three terminal electrode configuration (Figure 5.1) were prepared by vacuum evaporation technique using gold as the electrode material. The prepared samples were then kept at 200°C for two hours to ensure good contacts of the electrodes.

5.3 ELECTRICAL CIRCUIT AND MEASURING TECHNIQUE.

For both the d.c. and a.c. measurement a common sample holder was used, as shown in Figure 5.2. The sample was

kept in position with a pressure contact maintained by a spring. The heater was in the form of a cylindrical wire-wound furnace. The temperature of each side of the sample was separately measured with Cu-constantan and chromel-alumel thermocouples. In the equilibrium conditions, the temperature was maintained to within $\pm$ 3 °C before measurements were made.

For the d.c. measurement, the current was measured using a keithley 610B electrometer with a keithley 240A high voltage supplier. Figure 5.3 shows a diagram of the circuit used.

In the a.c. case, the frequency range covered was from 100 Hz to 20 kHz. A voltage signal of up to 30 V was supplied across the sample using a Wayne Kerr audio frequency generator S121. A Wayne Kerr waveform analyser A321 was used as the detector along with the universal bridge B221. Figure 5.4 shows the circuit used for a.c. measurement.

Figure 5.5 and Figure 5.6 are photographs of the vacuum system and some of the instruments used.

5.4 D.C. MEASUREMENTS

5.4.1 Results

The procedure of sample preparation as quoted above yielded ohmic contacts and linear V - I characteristics were noted up to 6×10^3 Vcm^{-1}. Figure 5.7 shows the V - I characteristics for glass containing 50 Mol % CoO. Other glass samples both in the binary and ternary systems show similar characteristics. The d.c. conductivity of $CoO-P_2O_5$ and $CoO-NiO-P_2O_5$ glasses was measured in the temperature range from room temperature to 553 K. All measurements were made under a vacuum of about 10^{-5} torr. Plots of log. conductivity versus 1000/T of the transition-metal oxide glasses of various compositions are shown in Figures 5.8 and 5.9. The convention used in the graphs is as shown in Table 1.1 : for the binary glasses, glass 3070 represents glass containing 30 Mol % CoO and 70 Mol % P_2O_5 and for the ternary system, glass 351055 represents glass containing 35 Mol % CoO, 10 Mol % NiO and 55 Mol % P_2O_5. The activation energy (W), is determined from the slope of the curves of $\log \sigma$ versus 1000/T. Figures 5.10 and 5.11 show the variation of activation energy with CoO content for the binary and ternary systems respectively. As can be seen in the binary system, the activation energy increases with increasing CoO content whereas in the case of the ternary system the activation energy decreases with CoO content with the exception of

glass 400555.

All glasses show the following characteristics. Above 450 K the conductivity of the sample is well described by a single activation energy, whereas below that temperature the conductivity varies very slowly with temperature and displays no single activation energy. From room temperature to about 400 K the conductivity seems to be quite constant. Figure 5.12 shows the above characteristics for glass 5050.

A general trend observed in Figure 5.8 and Figure 5.9 is that the magnitude of the conductivity at any temperature tends to be smallest in those glasses having the highest thermal activation energy. This is consistent with the general formula proposed by Mott (1968)[46] and in good agreement with the result of Sayer and Mansingh (1972)[48].

It is found that the resistivity of all the glasses understudy is quite constant and time independent. This characteristic can be taken as evidence that the conduction is electronic[77].

5.4.2 Discussion

The general behaviour of the curve (Figure 5.8 and Figure 5.9) is very similar to that reported for vanadium phosphate glasses[40,66] and other transition-metal oxide glasses at high temperature ($T > \theta_D/2$)[64,78,79]. The d.c. conductivity at any fixed temperature increases with decreasing concentration

of CoO for the binary glasses whereas the conductivity increases with increasing concentration of CoO for the ternary glasses (with the exception of glass 400555). Figures 5.13 and 5.14 show the above characteristic at T = 500 K. The activation energy above 450 K is almost independent of temperature. Sayer and Mansingh (1972)[48] have shown that for a series of phosphate glasses containing different transition-metal ions, a semilogarithmic plot of the conductivity measured at a temperature of 500 K versus the high-temperature activation energy gives a straight line with a slope corresponding to a measurement temperature of 530 K. They concluded that the pre-exponential term of Equation 3.10 inclusive of exp (-2 α R) is virtually constant for all phosphate glasses containing 3d transition-metal ions. As a consequence the hopping of a small polaron in the system should exhibit an adiabatic character. Figure 5.15 shows the conductivity of the glasses under study with respect to the activation energy at a temperature of T = 500 K plotted together with the result of Sayer and Mansingh (1972)[48]. As shown, the results are quite comparable. The conductivity of the 50 Mol % CoO glass is higher than the value obtained by Sayer and Mansingh (1972)[48]. This discrepancy may be due to the difference in the number of reduced transition-metal ions in the two samples.

Apparently based on the approached of Sayer and Mansingh (1972)[48] the slope of Figure 5.16 (CoO-NiO-P_2O_5 system)

corresponds to a measured temperature of 529 K. However for the binary system (Figure 5.17) the $(kT)^{-1}$ value is 1.3 times higher than the experimental values. Thus as suggested by Murawski et al (1979)[65], the exp (-2aR) term should not be ignored. Hence for the $CoO-P_2O_5$ system it may be reasonable to assume that the hopping of a small polaron in this system should exhibit a non-adiabatic character[65].

The temperature dependence of conductivity shown in Figures 5.8 & 5.9 is consistent with a polaron model for conduction in all the glasses. The polaron model predicts that an appreciable departure from a linear $\log\sigma$ versus $1/T$ plot should occur below a temperature of $\frac{1}{2}\theta_D$, where θ_D is given by $\hbar\omega_o = k\theta_D$. Figure 5.12 shows that the departure from linearity is at a temperature of about 450 K which suggests that $\frac{1}{2}\theta_D$ may be of the order of 450 K for these series of glasses. Taking the vibration band at 530 cm^{-1} to be the same as the optical phonon frequency[48] ω_o the value obtained for $\frac{1}{2}\theta_D$ is about 382 K.

Many authors[48,65,66,41] made the assumption that the small polaron radius (r_p) can be calculated from Equation 3.4 postulated by Bogomolov et al (1967)[55]. The total cobalt-ion concentration was calculated using equation[50]

$$N = (\rho_g CoN_o)/(A.W. \times 100) \qquad (5.1)$$

where N = concentration of cobalt ion (cm^{-3}), ρ_g = the density of glass (gcm^{-3}), N_o = Avogadro's number, A.W. = atomic

weight of cobalt in grams and Co = weight percent of cobalt in the glass matrix. Using the relationship $R = (1/N)^{1/3}$, the mean distance between cobalt ion can be calculated. The values of r_p calculated were recorded in Table 5.1. As shown the polaron radius is a function of CoO content and decreases as the cobalt content increases. r_p in each composition is less than the corresponding Co - Co distance, and is much greater than the cobalt ion, Co^{2+}, radius (0.82 Å)[80]. Thus a critical condition for the formation of small polarons holds for cobalt-phosphate glasses. An estimate of the polaron radius can also be made by using Equation 3.2. In this case it is assumed that the polaron binding energy W_p is twice the activation energy at high temperature[41]. Using the value of $\epsilon_p = 2.5$[48], the value Of r_p for glass 5050 was obtained as r_p = 1.1 Å. This discrepancy between the value calculated using Equation 3.4 may arise due to the difficulty of defining the lattice spacing R in a non-cubic system.

The small polaron coupling constant γ can be obtained from the equation $\gamma = (W_p)/(h\omega_o)$. Substituting the high temperature activation energy of glass 5050, leads to a value of 37 for the coupling constant. This indicates that a strong coupling requirement for the application of small polaron theory to cobalt glasses is satisfied[40,52]. Several other authors have reported coupling values, $\gamma > 10$, for transition-metal oxide glasses[40,66,79,72].

As can be seen from Figure 5.8, at any fixed temperature the conductivity of $CoO-P_2O_5$ glasses seems to decrease with increased content of CoO (Figure 5.13 shows the above characteristic at T = 500 K). Most authors show that conductivity generally increases with higher concentrations of transition-metal ions. Assuming that an increase of CoO content would increase the concentrations of transition-metal ions, the conductivity of $CoO-P_2O_5$ glasses should increase with increasing CoO content, but results of this work show otherwise. As suggested by Murawski et al (1979)[65], Co ions in glasses exhibit a different behaviour. When present in large concentrations, almost all these ions exist in the Co^{2+} valence state rather than the higher valence state. Consequently $CoO-P_2O_5$ glass show very low conductivity. Higazy (1982)[81] prepared $Co_3O_4-P_2O_5$ glasses of range from 4 % to 60 % content of cobalt oxide and found that the ratio Co^{2+}/Co_{total} increases with increasing cobalt oxide content. He obtained a value of $Co^{2+}/Co_{total} = 0.34$ for glass with 4 % cobalt oxide content and $Co^{2+}/Co_{total} = 0.52$ for glass with 7 % cobalt oxide content. For glass with 25 % to 60 % cobalt oxide content the value of Co^{2+}/Co_{total} increases from 0.88 to 0.99. Sarver (1966)[80] show that cobalt oxide will decompose to CoO when fired at 1000 °C. As the melting point of the glasses prepared by Higazy (1982)[81] is over 1200 °C it is reasonable to assume that the glasses have similar structure with the glasses prepared in the present work. From a straightforward hopping model, it is

expected that the conductivity goes through a maximum at a value of the ratio Co^{2+}/Co_{total} = 0.5, in which all sites contribute equally. It is assume that the glasses prepared in the present work have values of Co^{2+}/Co_{total} exceeding 0.5; thus the result as shown in Figure 5.13 is quite justified.

5.5 HIGH-FIELD EFFECT

5.5.1 Introduction

The low conductivity of many non-crystalline semiconductors makes it possible to apply large electric fields and to explore the conduction properties beyond the ohmic regime without danger of excessive heating. At high enough fields, whether conduction is by electrons or ions, in practically all cases, deviations from Ohm's law are observed.

In general two kinds of field-enhanced conductivity can be distinguished; (a) the free carrier density is increased by field emission from traps and charged centres as in the case of the Poole-Frenkel effect[32], (b) the mobility becomes field dependent.

In transition-metal oxide glasses ohmic behaviour can be observed up to fields of about 10^5 V-cm^{-1}. At higher fields the conductivity, for simple hopping between near neighbour sites, varies as

$$\sigma(E) = \sigma(0)[\sinh(eRE/2kT)]/(eRE/2kT) \qquad (5.2)$$

where $\sigma(0)$ is the conductivity in the ohmic region and R is the jump parameter. Equation 5.2 implies a departure from ohmic behaviour at a field of $E = (kT)/(eR)$. At this particular field an estimate of the value of R could be obtained. In the low field limit, Equation 5.2 leads to the appropriate ohmic behaviour $\sigma(E) \longrightarrow \sigma(0)$.

5.5.2 Experimental Technique.

Samples were prepared from blown films of the molten glass. Two terminal silver paint electrodes were applied on the sample. The thickness of the glass films was measured using a "Sigma Comparator". Figure 5.18 shows the diagram of the device holder and heating system.

5.5.3 Results And Discussion.

Figure 5.19 shows the I-V characteristics for glass 3070 of thickness 55 μm. As can be seen there is a well-defined ohmic conduction up to a field of about 3×10^4 V-cm^{-1} at room temperature. The field at which the glass deviates from linearity increases with increasing temperature. The value of R (the jump parameter) at room temperature is estimated as 92 Å decreasing to 63 Å at 533 K. R seems to decrease linearly with temperature above 453 K (Figure 5.20). This result seems to be consistent with the d.c. conductivity measurement (Section 5.4.1) in which above 453 K the

conductivity of the glass is well described by a single activation energy, whereas below that temperature the conductivity varies very slowly with temperature. The estimated value of R is over ten times larger than the average ion spacing for the same glass. Austin and Sayer (1974)[82] and Moridi (1975)[83] reported values of four to ten times the average ion spacing. Austin and Sayer (1974)[82] conclude that polaron hopping does in fact occur across distances comparable with nearest-neighbour distances but that the discrepancy is caused by an enhancement of the field. They suggest that the effect is caused largely by internal microscopic barriers which present a higher than average impedance to carrier migration, the applied field will be dropped mainly across the high-impedance barriers and hence appear to be effectively enhanced.

Jonscher (1967)[84] stated that there is much experimental evidence suggesting that for fields above some 10^4 V-cm^{-1}, many dielectric films exhibit I-V characteristics of the form

$$I \propto \exp[(e\beta E^{\frac{1}{2}})]/(kT) \qquad (5.3)$$

where in the case of Schottky effect

$$\beta = \beta_S = [\, e/(4\pi\epsilon_o \epsilon)]^{\frac{1}{2}} \qquad (5.4)$$

and in the case of Poole-Frenkel effect

$$\beta = \beta_{PF} = [\, e/(\pi\epsilon_o \epsilon)]^{\frac{1}{2}} \qquad (5.5)$$

ϵ_o is the permittivity of free space and ϵ the relative

dielectric constant. Figure 5.21 shows a plot of log I versus $V^{\frac{1}{2}}$ for glass 3070. The value of β obtained is about 1.83×10^{-4} $eV(cm/V)^{\frac{1}{2}}$. Using Equation 5.4 (Schottky effect) the calculated value of the relative dielectric constant $\epsilon = 4.4$ and using Equation 5.5 the calculation yields $\epsilon = 17.7$. It should be noted that the author obtained a value of ϵ for glass 3070 as 29.0 measured at room temperature with a frequency of 20 kHz. Furthermore from the fact that the conductivity of the sample is independent of the specimen thickness, it is suggested that Schottky emission did not determine the high-field electrical conductivity of cobalt-phosphate glasses[85]. The field dependence was a property of the bulk material. The Poole-Frenkel formula seems to provide a good fit to the experimental data. More theoretical and experimental data will be required before the field dependence can be positively associated with an appropriate mechanism.

5.6 SWITCHING PHENOMENA

5.6.1 Introduction

The discovery of non-destructive switching in thin films of certain chalcogenide alloys (Ovshinsky(1959,1963,1967, 1968))[1,86,87,88] provoked an explosive increase of interest in the physics of non-crystalline semiconductors. Numerous papers have been published since then in an attempt to

understand the process of switching (threshold and memory) of these materials. Fritzsche (1974)[89] has given quite an extensive review concerning switching and memory in amorphous semiconductors.

Basically there are two main types of switching, threshold and memory. In both cases before operation the samples are in the high resistance "OFF" state and the switching process occurs when the voltage exceeds a threshold voltage (V_{th}). In the case of memory switching the resultant state after operation is stable, but can be returned to the initial state by passing a sustained pulse of high current. However, in the case of threshold switching as the current in the "ON" state is reduced, the threshold switch reverts to the original state at holding current. Figure 5.22 shows the I-V characteristics of a threshold switching device and Figure 5.23 for the case of a memory switching device.

Various models proposed to explain the switching process may be categorized into[89]:

(a) Homogenous Model: The semiconducting film is assumed to remain essentially homogeneous and amorphous during switching. Switching is either explained as a thermal process with electronic corrections or as an electronic process with thermal corrections applied to the relevant parameters.

(b) Heterogeneous Model: A heterogeneous structure change in the region of the current filament plays a dominant role.

5.6.2 Experimental Methods, Results and Discussion.

Sample preparation and device holder and heating system are as mentioned in Section 5.5.2. The switching characteristics were measured using the circuit as shown in Figure 5.2.4. The series resistance $R_1 = 1 \times 10^5 \Omega$ limits the current in the "ON" state.

Figure 5.25 shows the I-V characteristic of glass 3070, thickness 34 μm. As shown the current gradually increases with increasing voltage. At the threshold voltage of 80 V the sample switched to the "ON" state and the current increased from 4.5×10^{-10} amp to 3.0×10^{-6} amp. The voltage drop across the sample was 1.2 volt. The low resistance "ON" state was retained after removal of the applied voltage. On applying a high current pulse, the device returned to the "OFF" state. The value of the threshold voltage is not reproducible. Drake et al (1969)[90] reported that it is dependent on the external switching conditions. Moridi and Hogarth (1978)[91] obtained similar results in copper-calcium-phosphate glass devices. The threshold voltage in this work varies from 80 volts - 30 volts. Figure 5.26 shows the I-V characteristic of glass 3070 at a temperature of 453 K. The device under study switched at all temperatures from room temperature to 513 K. It was noticed that switching to the "OFF" state was more difficult at higher temperature.

From the result, it is reasonable to suggest that thermal effects are involved in the switching process in cobalt-phosphate glasses. During the memory switching a crystalline channel is believed to form at the threshold voltage leading to the low-resistance "ON" state. The high current pulse applied to the device to return it back to the "OFF" state suggests that revitrification of the material is occurring.

5.7 A.C. MEASUREMENTS

5.7.1 Results

The total a.c. conductivity and dielectric constant, ϵ, were measured over a frequency range of 0.1 - 20 kHz and a temperature range of 293 - 533 K. The a.c. conductivity is given by the following relation

$$\sigma(\omega) = \sigma_{total} - \sigma_{dc} \qquad (5.6)$$

where σ_{dc} is the d.c. conductivity. The measured values of dielectric constant ϵ at various temperatures and frequencies are reported in Table 5.2. Figure 5.27 shows the real part of the a.c. conductivity of glass 5050 as a function of 1000/T. The a.c. conductivity (glass 5050) as a function of 1000/T is as shown in Figure 5.28. There is an increase in conductivity with respect to frequency but in a fixed frequency the change in conductivity within the measured range of temperature is very slight. Figure 5.29 shows the

variation of log conductivity with log frequency for glass 5050 at room temperature. All glasses show similar behaviour as glass 5050.

5.7.2 Discussion

In the context of semiconducting glasses the a.c. conductivity Equation 5.6 is normally used and the results expressed in the form [92]

$$\sigma(\omega) = A\omega^{s} \qquad (5.7)$$

where A is a constant which increases slightly with temperature, ω the angular frequency, $\sigma(\omega)$ the a.c. conductivity and $0.5 < s < 1$. The values of s (Table 5.2) obtained for various composition of glass fall within the range 0.90 - 1.0.

Mott and Davis (1971)[19] interpret the power-law a.c. conductivity (Equation 5.7) in terms of hopping between pairs of isolated sites close to the Fermi-level and with a random distribution of separation distances R. Thus

$$\sigma(\omega) \propto (\epsilon_s - \epsilon_\infty)\int(\omega^2\tau)/(1 + \omega^2\tau^2)\ dN \qquad (5.8)$$

where $dN = 4\pi R^2 N(E_F)dR$ and $N(E_F)$ is the density of states at the Fermi-level. The factor $(\epsilon_s - \epsilon_\infty)$ is given by the equation

$$(\epsilon_s - \epsilon_\infty) = [(4\pi Ne^2R^2)/(3kT)]\exp[-W/(kT)] \qquad (5.9)$$

with $N = N(E_F)$. For phonon-assisted quantum mechanical tunnelling the result is

$$\sigma(\omega) \approx (e^2/a^5)(N(E_F))^2 kT\omega(\ln\ \nu_{ph}/\omega)^4 \qquad (5.10)$$

The frequency factor ($\ln\ \nu_{ph}/\omega$) varies as $\omega^{-0.2}$ over a wide frequency range so that

$$\sigma(\omega) \propto T\omega^{0.8} \qquad (5.11)$$

For thermally-assisted hopping over a barrier

$$\sigma(\omega) \propto T\omega^{1.0} \qquad (5.12)$$

Pollack (1976)[93] has developed the analysis more rigorously by transforming the microscopic random variables of the physical problem into a random impedance network of capacitors and resistors. He finds,

$\sigma(\omega) \propto T\omega^{0.8}$ for tunnelling

$\sigma(\omega) \propto T^2\omega^{1.0}$ for hopping over a barrier

$\sigma(\omega) \propto T^2\omega^{0.75}$ for a mixture of tunnelling and hopping

The experimentally derived values of s (as shown in Table 5.2) characterized the process of hopping conduction as a dominant process at a temperature range from room-temperature to 533 K. The dielectric constant, ϵ, changes little over the measured range of frequency. This result is in common with many non-crystalline materials[94].

Table 5.1

Glass	N(x 10^{21})	R (Å)	r_p (Å)	W (eV)	$\sigma_{T=500\ K}$ ($\Omega^{-1}.cm^{-1}$)	σ_0(x 10) ($\Omega^{-1}.cm^{-1}$)
2575	3.3	6.6	2.6	1.11	2.3×10^{-10}	2.8
3070	4.1	6.2	2.5	1.13	1.1×10^{-10}	2.7
4060	6.1	5.4	2.2	1.18	6.1×10^{-11}	4.8
5050	8.3	4.9	2.0	1.22	3.1×10^{-11}	6.1
6040	11.7	4.4	1.7	1.30	6.6×10^{-12}	8.4
252055	4.2	6.2	2.5	1.33	2.6×10^{-12}	7.0
301555	4.9	5.8	2.3	1.26	7.9×10^{-12}	4.0
351055	5.7	5.5	2.2	1.20	4.7×10^{-11}	5.8
400555	6.4	5.3	2.1	1.24	2.1×10^{-11}	6.7

Table 5.2

Glass	$S_{T=RT}$	$S_{T=453\ K}$	$S_{T=553\ K}$	G at 1 kHz		G at 20 kHz	
				T = RT	T = 533 K	T = RT	T = 533 K
2575	0.99	0.98	0.97	28.3	30.1	27.2	27.7
3070	0.99	0.99	0.98	30.0	31.4	29.0	29.7
4060	0.99	0.99	0.98	29.5	31.7	28.5	29.6
5050	0.99	0.99	0.98	30.1	31.3	29.1	29.9
6040	0.99	0.99	-	25.3	-	24.3	-
252055	0.99	0.98	0.98	31.8	32.7	30.6	31.3
301555	0.98	0.98	0.98	28.8	29.5	27.5	28.2
351055	0.98	0.98	0.98	28.7	29.9	27.5	28.2
400555	0.98	0.98	0.98	34.5	35.8	33.3	34.1

RT = Room temperature.

CHAPTER VI

THE OPTICAL PROPERTIES OF COBALT-PHOSPHATE GLASSES

6.1 INFRA-RED SPECTRA OF COBALT-PHOSPHATE GLASSES

6.1.1 Introduction

The infra-red spectra of binary phosphate glasses have been investigated by numerous workers[78,79,83,95,96,97]. Reviews of numerous infra-red works have been compiled by Wong and Angell (1971)[98] and Donald and Mc Millan (1978)[99]. Corbridge and Lowe (1954)[95] have done extensive work on numerous inorganic phosphorus compounds. Their work has been used as a basis of interpretation by succeeding authors. Shih and Su (1965)[100] carried out an extensive study on the infra-red spectra of alkali (Li, Na, K and Rb) and alkaline-earth (Cd, Sr and B) metaphosphate glasses and concluded that the infra-red spectra of the vitreous metaphosphates observed are essentially the same, except for some diffuseness in the alkaline-earth series.

Using the approach of Corbridge and Lowe (1954)[95], Muller (1969)[101] concluded that the principal absorption of the P=O group lies at 1282 cm^{-1} to 1205 cm^{-1} in polymeric phosphate chains. The $P-O^{(-)}$ group is characterized by a frequency at 1110 cm^{-1}. The P-O-P ring frequency in the

cyclic phosphate occurs between 805 cm^{-1} and 740 cm^{-1}. Sayer and Mansingh (1972)[48] studied various transition-metal oxide phosphate glasses and qualitatively suggested that phosphate tetrahedra dominate the structure of Mn, Ni, Co and Cu glasses, while the structure of the form MO_n, where M is the transition-metal ion, dominate glasses formed with Ti, V, Mo and W.

6.1.2 Experimental Technique

Measurements of the infra-red spectra were recorded using a Unicam SP 2000 double beam infra-red spectrometer, in the range 400 cm^{-1} to 4000 cm^{-1} at room temperature. Glass samples were ground into fine powder and then a small amount of the glass powder was mixed and ground with KBr. The KBr pellets were made by pressing the mixture at 10 - 15 tons for a few minutes under vacuum.

6.1.3 Results And Discussion

Figure 6.1 shows the infra-red spectra of $CoO-P_2O_5$ glasses and Figure 6.2 the infra-red spectra of the ternary series (for the case of the ternary series CsCl pellets were used). As can be seen both the binary and ternary series show similar spectra. Comparison with the infra-red spectrum of P_2O_5 shows that some of the absorption bands of the glasses

are similar to P_2O_5. There is a sharp spectral line at about 500 cm^{-1} in all the glasses. This is known to be a fundamental frequency of the $(PO_4)^{3-}$ group[102]. The absorption band at 760-780, 930, 1080 and 1280 cm^{-1} possibly are due to the P-O-P ring frequency, P-O stretching frequency and the stretching vibration of the P=O double bond. Two absorption bands were observed at about 1670 cm^{-1} and 3440 cm^{-1} for all the glasses. These are believed to be caused by small amount of water in the glass[78,83,103,104].

The infra-red spectra of the binary and ternary glasses appeared to be similar, a result which indicates that the infra-red spectra in this region arise primarily from the vibrations of phosphate groups in the glass. This behaviour may be qualitatively summarized by suggesting that phosphate polyhedra dominate the structure of cobalt glasses.

6.2 ABSORPTION EDGE OF $CoO-P_2O_5$ GLASSES

6.2.1 Introduction

The optical absorption constant α of most amorphous semiconductors increases exponentially with photon energy in the range $1<\alpha<10^4$ cm^{-1} (Figure 2.8). Below a value of α smaller than 1 cm^{-1} the absorption curves change less rapidly with photon energy. It is uncertain whether this part of the absorption curve truly represents absorption or whether

light scattering accounts for the loss of light intensity[104].

In Part III of Figure 2.8, $\alpha > 10^4$ cm^{-1}, the absorption curve begins to level off. The absorption coefficient can be written as (Equation 2.15)

$$\alpha(\omega) = [B(\hbar\omega - E_g^{opt})^2]/(\hbar\omega) \qquad (6.1)$$

where B is a constant and E_g^{opt} is the so-called optical gap.

Below $\alpha \approx 10^4$ cm^{-1} the absorption constant is larger than the value obtained from Equation 6.1 and the edge is broadened (Figure 2.8). For α between 1 and 10^4 cm^{-1} (Part II)

$$\alpha(\omega) \backsim \exp(\hbar\omega)/E_e \qquad (6.2)$$

where E_e is a measure of the steepness of the exponential tail. This exponential dependence is called the Urbach law[105]. E_e is in the range of 0.05 to 0.08 eV[106] below and at room temperature: above room temperature E_e increases with temperature.

6.2.2 Experimental Technique

The samples were prepared in the form of thin blown films with thickness of about 3 - 10 μm. The film thickness was measured using a 'Sigma Comparator' which is sensitive to changes in thickness of 1 x 10^{-4} cm. *It is found that the thickness of the films formed by the above method is not quite uniform and thus the absolute values of the absorption coefficient may have considerable error. Measurements were

made in the wavelength range of 200 - 750 nm using a Perkin-Elmer model 137 UV Spectrometer at room temperature. The optical absorption coefficients $\alpha(\omega)$ were calculated from the optical transmission spectra by using the equation

$$\alpha(\omega) = (1/d)\ln I_o/I_t$$

where d is the thickness of the sample, I_o and I_t are the intensities of incident and transmitted beam respectively.

6.2.3 Results

Figure 6.3 shows the optical absorption spectra for cobalt-phosphate glasses as a function of wavelength in the range 200 - 390 nm. The fundamental absorption edge moves to higher wavelengths as the CoO content is increased, or the thickness of the glass specimen is increased. Figure 6.4 illustrates the plot of $(\alpha\hbar\omega)^{\frac{1}{2}}$ versus $(\hbar\omega)$ in accordance with Equation 6.1. As can be seen there is a well-defined linear relation region in the curves. The extrapolation of the linear part intersects the abscissa at photon energy E_g^{opt}, the so-called optical gap. The values of E_g^{opt} for all the glasses are recorded in Table 6.2. Figure 6.5 shows the variation of E_g^{opt} as a function of CoO content. The E_g^{opt} increases with increasing P_2O_5 content. Figure 6.6 shows the variation of E_{th} versus CoO content. E_{th} is defined as the onset of the energy at which the plot of $(\alpha\hbar\omega)^{\frac{1}{2}}$ versus $(\hbar\omega)$ becomes non-linear. As shown a linear graph is obtained.

Paul and Douglas (1968)[107] studied the optical absorption of divalent cobalt in binary alkali borate glasses and found that the Co^{2+} in octahedral symmetry absorbs almost throughout the visible region, having absorption maxima at approximately 500 and 550 nm. Co^{2+} in tetrahedral symmetry has absorption maxima around 540, 600 and 635 nm. The overall absorptions in both cases are broad. Figure 6.7 shows the optical absorption spectra for glass 5050 as a function of wavelength in the range 350 -750 nm. All the other binary glasses show similar characteristics. As shown, the result is quite similar to the result of Paul and Douglas (1968)[107].

6.2.4 Discussion

Stevels (1953)[108] suggests that the movement of the ultraviolet absorption band to longer wavelengths corresponds to transitions from the non-bridging oxygens which bind an excited electron less tightly than a bridging oxygen. Successive workers[109,97,110] have used this idea in explaining their result. As can be seen from Figure 6.3 the shift of the ultraviolet absorption band to longer wavelengths with increasing CoO content could be explained in the same context. Thus the result of Figure 6.5 showing the variation of E_g^{opt} with composition can be explained by suggesting that the non-bridging oxygen ion content increases with increasing CoO content, shifting the band edge to lower energies and

thus consequently leads to a decrease in E_g^{opt}.

Over a range of energies near the absorption edge, the absorption coefficients fit Equation 6.1. This can be taken as evidence of indirect transitions. The estimate values of B are recorded in Table 6.2.

The exponential behaviour of the absorption edge (Urbach law) can be demonstrated in the cobalt-phosphate glass (Figure 6.8). Several explanations have been put forward for the existence of an exponential edge. Tauc (1969)[43] suggests that it arises from electronic transitions between states in the band-edge tails, the density of which is assumed to fall off exponentially with energy. However, Davis and Mott (1970)[31] considered this explanation unlikely because the slope of the observed exponential absorption edge does not differ greatly for a variety of materials. Dow and Redfield (1970)[111] propose that the Urbach rule arises from an electric field broadening of an exciton. Although the values of E_e obtained in this work are much larger than the values observed in some amorphous semiconductor materials[31,106], E_e does vary slightly with variation of composition. Thus a model based on electronic transitions between localized states is unfavourable.

The so-called optical gap is 4 - 5 times larger than the high temperature activation energy (measured above 453 K). This is consistent with the results of many workers on oxide and chalcogenide glasses which show that the

electrical energy gap is less than the value of the optical gap on the same glass. The results suggest that the electronic activation is not across the whole mobility gap but is possibly from one or more trapping levels to the conduction band or from bonding states to a trapping level.

Table 6.1 Infra-red Absorption Band Position (cm^{-1})

Glass						
2575	480	760-780	930	1060	1290	3440
3070	490	760-780	930	1080	1280	3440
4060	490	760-780	930	1080	1270	3440
5050	500	760-780	930	1080	1270	3440
252055	520	760-780	930	1080	1270	3400
301555	520	760-780	930	1080	1270	3400
351055	500	760-780	930	1080	1280	3400
400555	500	760-780	930	1080	1280	3400
CoO (oxide)	590	680				
P_2O_5 (crystalline)[79]	380	480	560	760	1000	1200	
P_2O_5 (vitreous)[79]		475	650	780	950	1150	1285

Table 6.2

glass	Thickness ($x10^{-4}$ cm)	E_g^{opt} (eV)	W (eV)	B ($x10^5$ $cm^{-1}.eV^{-1}$)	E_{th} (eV)	E_e (eV)
2575	4	5.50	1.11	1.0	6.0	0.44
3070	3	5.41	1.13	0.8	5.9	0.40
4060	7	4.91	1.18	0.6	5.6	0.44
5050	5	4.70	1.22	0.4	5.3	0.43

CHAPTER VII

CONCLUSIONS AND SUMMARY

In the study of a glass system about which very little is already known, it is necessary to measure a variety of physical properties so that some conclusions may be drawn about the structure, the ordering, if any, the mode of electrical conduction and the way in which light is absorbed or transmitted by the glass. In this thesis some inferences about structure and molar volume have been drawn from simple density measurements but in the absence of a full structural investigation, the conclusions drawn in this thesis are as far as one can go on the available evidence, i.e. the increased density of glass suggests that a more compact structure is acquired as one adds CoO. Discussions with colleagues have suggested a programme of future work on the determination of the radial distribution function using an X-ray diffractometer specially built for these studies. In the thesis the analysis of the optical data and of the electrical conduction each enable characteristic energies to be determined and it is in the interpretation of some of these that assumptions need to be made if the analysis is to be other than very much simplified.

In the case of a number of transition-metal ion phosphate glasses it is helpful to make measurements, using

powdered glass samples, of electron spin resonance. Unfortunately in cobalt-phosphate glasses the fact that the Co^{2+} ion is very strongly magnetic in its own right causes the normal electron spin resonance spectrum to be suppressed and consequently it was not possible to estimate the concentration of paramagnetic cobalt ions as it is in the case of copper-phosphate glasses and also of vanadate and molybdate glasses. The experiment was tried using a Varian E-3EPR instrument but it was not possible to obtain an analysable clean resonance curve. This was unfortunate since one likely prediction of the proposed conduction process in these glasses is that the number of free charge carriers, which is determined by the concentration of reduced valency Co centres would remain constant with temperature from say 77 - 400 K and the variation in electrical conductivity with temperature would be due to an activated mobility. As a further aid in this general direction, some thought was given to the measurement of Hall effect from which in conjunction with the conductivity, the Hall mobility could be inferred, at least to a first approximation. Unfortunately, the very high resistivity of cobalt phosphate glass samples meant that their impedance was too high to make reliable measurements. In this laboratory construction and testing of a Van der Pauw apparatus has just been completed and it is hoped that some attempts to study the Hall coefficient by means of this technique may be successful, although

since a very small Hall angle is predicted, it may be that the system will not be sufficiently sensitive to distinguish between a real Hall voltage and background noise. Previous work on phosphate glasses, in contrast to vanadate and molybdate glasses, suggests that the Seebeck coefficient in these materials is small and incapable of yielding much in the way of useful information. Measurements of Seebeck coefficient could in principle, along with measurements of electrical conductivity, give useful information about charge carrier effective mass or possibly the Fermi energy but the rather dubious nature of such measurements in phosphate glasses makes this a poor prospect for further analysis. Thus in our attempts to examine the origins of electron motion in our glasses we have been limited to measurements of d.c. conductivity, high-field effects and a.c. conductivity.

As will be discussed below, the a.c. measurements are indicative of a hopping process of some kind. The results of the d.c. conductivity measurements of cobalt-phosphate glass seem to comply with a polaronic conduction process. Small polarons have been suggested previously as the mode of conduction in oxide glasses containing transition-metal ions[2,48,71,78,79,83] and indeed one would expect to find this mode of conduction in materials where the bonding is predominantly polar rather than in chalcogenide glasses where the bonding is largely covalent.

The variation of conductivity with glass composition is difficult to interpret since the parameters C, W, N and R^{**} vary with the proportion and nature of the transition-metal ion. Most authors have shown that conductivity generally increases for higher concentrations of transition-metal ions. The results of this work show that the conductivity decreases with increasing CoO content. It is suspected that within the range of glasses prepared, the valuesof C have exceeded 0.5. The knowledge of the value of C for these series of glass would be very helpful to confirm this expectation but unfortunately the inability to measure a clean electron spin resonance spectrum makes this very difficult indeed. Evidently polaron theory places no restriction against electron hopping between transition-metal ions of different chemical elements such as we should find in glasses containing both cobalt and nickel. As shown in Table 5.1 the addition of NiO into the glass system lowers the conductivity compared to the binary glass with similar CoO content. A knowledge of the concentration of both types of transition-metal ion is necessary to explain this phenomenon. Sayer and Mansingh (1972)[48] have suggested that the pre-exponential term of

---

**C is the fraction of sites occupied by an electron in the low valence state, W is the activation energy for conduction, N is the number of sites per unit volume and R is the site spacing.

Equation 3.10 inclusive of exp (-2αR) term is virtually constant for all series of phosphate glasses and suggested that the conduction mode is polaronic hopping in the adiabatic regime. We believe this is not so for cobalt-phosphate glass, and consider that the polaronic hopping is in the non-adiabatic regime as suggested in Chapter V. Calculating the value of α (the decay constant) would help to forecast the regime of polaronic hopping, but controversies exist over the approach to be used. For small values of R the adiabatic condition may arise in which the term exp (-2αR) approximates to unity, but for R>5 Å, as is the case for these glasses (Table 5.1) the non-adiabatic condition is expected. *

The a.c. measurement was expressed in term of the power law $\sigma(\omega) \propto \omega^s$. The values of s (Table 5.2) obtained for various composition fall within the range 0.97 - 1.00. The experimentally derived values of s are indicative of a hopping process of some kind. As can be seen from Table 5.2 the variation of dielectric constant against frequency within the range of frequency used is very slight.

In the high-field region there is a well defined ohmic conduction up to a field of about 3×10^4 V-cm^{-1}. The field dependence was found to be a property of the bulk material. The non-ohmic behaviour was analysed in terms of the polaron hopping mechanism but the value of R was found to be about 14.8 times greater than the Co - Co

spacing in the glass of similar composition. This sort of lack of agreement is well known in oxide glasses and has been discussed by various authors[82,83]. The high-field data was fitted according to the Poole-Frenkel formula. The experimental value of ϵ, the relative dielectric constant, seems to match with the result obtained in the a.c. measurement. This problem has recently been discussed by Hogarth and Ghauri (1982)[112] who used the low frequency values of ϵ in their analysis of the high-field data on cadmium-zinc-phosphate glasses and got better agreement to the Poole-Frenkel formula. The justification for this assumption was the slower time for the ions to re-arrange themselves in the alternating polarising field and the association of this factor in the choice of ϵ. Further experimental data on cobalt-phosphate glasses with different CoO content would be useful to study details of the high field conduction mechanism.

A sample of cobalt-phosphate glass shows a memory switching characteristic. The high current pulse applied to the device to return it back to the 'OFF' state suggests the possibility of revitrification of the material. It is believed that a crystalline channel is formed at the switching voltage leading to the low-resistance 'ON' state. An electron transmission-diffraction micrograph of the switching device could be useful to study and analyse the supposed crystalline conductive channel formed during switching. Thus the nature of the channel could be indicated

to discuss the memory phenomena on a more quantitative basis. Although similar experiments have been reported for a number of phosphate glasses, the somewhat brittle nature of the thin blown films made the experiment virtually impossible with the cobalt-phosphate glasses.

The infra-red absorption spectra are not very informative, since the main absorption peaks seem to be mainly characteristic of phosphate tetrahedra. The absorption band at about 500 cm^{-1} shifts to lower wave numbers as the amount of P_2O_5 is increased. This band is known to be related to the fundamental frequency of the $(PO_4)^{3-}$ group[102]. All the glasses show distinct absorption bands at 760-780, 930, 1080 and 1280 cm^{-1} which are quite independent of glass composition. By comparison with published data on many other phosphate glasses[95] it is possible that they are due to the P-O-P ring frequency, P-O stretching frequency and the stretching vibration of the P=O double bond.

The analysis of the optical absorption edge can be made in a number of ways and the method used in this work is to analyse in accordance with indirect transitions and such plots give reasonable values of optical activation energy. Only the binary series were studied and the values of the so-called optical gap found to decrease with increased CoO content (Figure 6.5). The optical data could also be fitted to an exponential Urbach formula. The value of the E_e, a measure of the steepness of the exponential tail, is

about 0.44 eV and substantially constant for varying CoO content.

It is tempting to try and draw some sort of energy band diagram for cobalt-phosphate glasses but any such diagram can only be drawn very tentatively since much of the background information is not yet available. Nevertheless an attempt at suggesting some form of density of states curve will be made. The information used will be the optical gap, activation energies, Urbach tails and the data are at least consistent with a sketch shown in Figure 7.1. As the

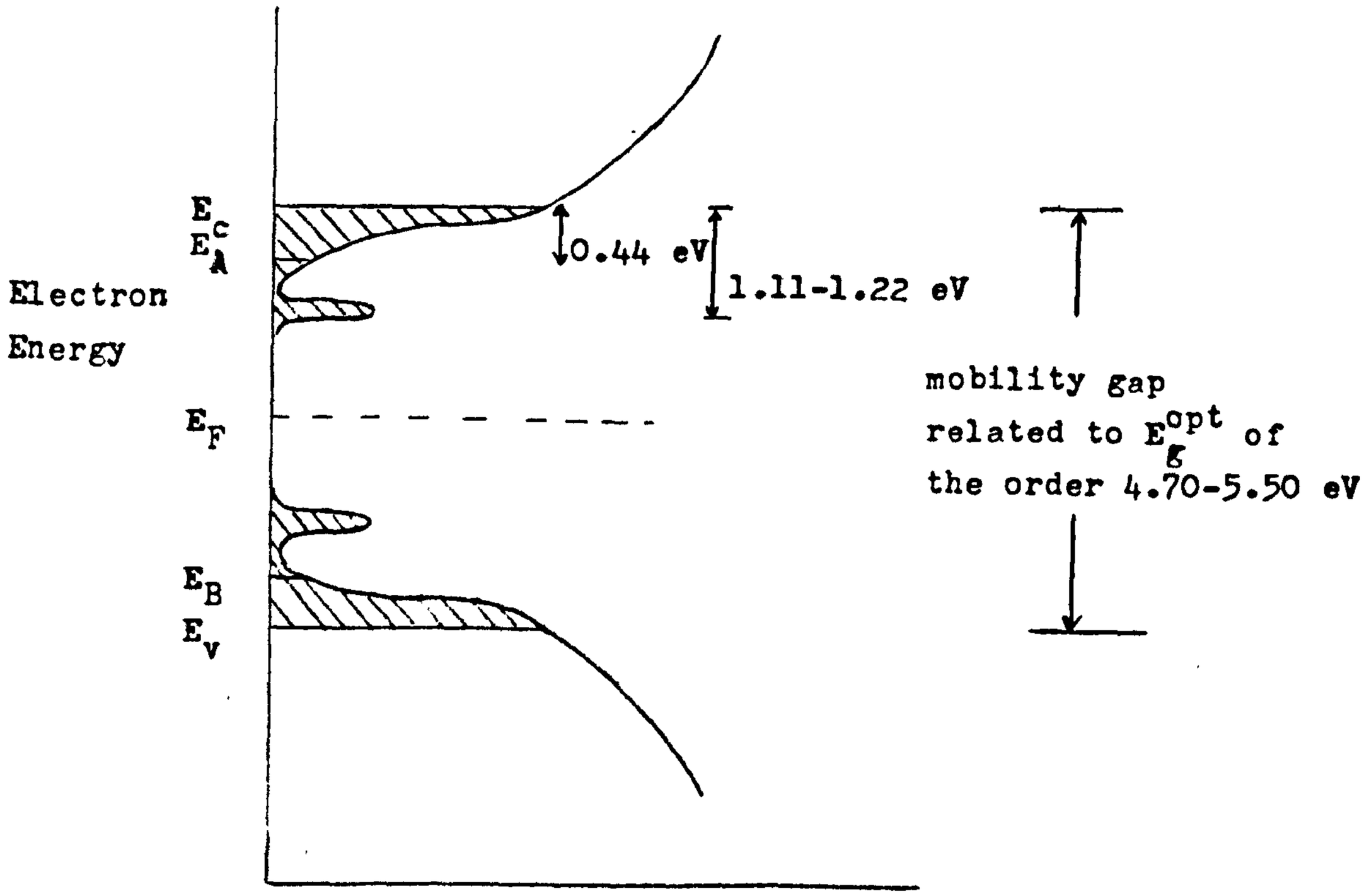

Figure 7.1 Density of states diagram for $CoO-P_2O_5$ glass

CoO content increases the optical gap decreases from 5.50 eV to 4.70 eV (Table 6.2) and the activation energy increases from 1.11 eV to 1.22 eV. The so-called optical gap is 4-5 times larger than the activation energy for glass of similar composition. The result agrees with the supposition that the electronic activation is not across the whole mobility gap but is possibly from one or more trapping level to the conduction band. In the simplest model we may assume that the Urbach tail gives a measure of the band tails[106]. The data seem to suggest that in the energy band diagram (Figure 7.1), the mobility edges E_c and E_v shift inward with increasing CoO content thus resulting to a smaller mobility gap. The band tails (E_c-E_A and E_B-E_v) and trapping centre bands also shift inward with virtually the same magnitude as the shifting of the mobility edges.

REFERENCES

(1) Ovshinsky, S.R.,(1968), Phy. Rev. Letters., 21, 1450

(2) Mott, N.F. and Davis, E.A., (1979), Electronic Processes in Non-Crystalline Materials, 2nd Ed., Oxford Univ. Press.

(3) ASTM Standards on glass and glass products prepared by ASTM Committee C14, American Society For Testing Materials, April 1955.

(4) Morey, G.W., (1954), The Properties of Glass, 2nd Ed., Reinhold, New York.

(5) Faraday, M., (1830), Phil. Trans. Roy. Soc., 49.

(6) Faraday, M., (1914), Experimental Researches in Electricity, repr. by J.M. Dent, London, p. 38 & 115.

(7) Goldschmidt, V.M., (1926), Geochemische Verteilungsgesetze der Elemnte, vii, vid. Akad.

(8) Zachariasen, W.H., (1932), J. Am. Chem. Soc., 54,3841.

(9) Warren, B.E. and co-workers., (1934), J. Am. Ceram. Soc., 17, 249.

(10) —— (1935), J. Am. Ceram. Soc., 18, 239.

(11) —— (1936), J. Am. Ceram. Soc., 19, 202.

(12) —— (1938), J. Am. Ceram. Soc., 21, 287.

(13) Huckel, W., (1951), Structural Chemistry of Inorganic Compounds, Elsevier Publishing Company, Vol II p. 776.

(14) Grigorovici, R., (1971), Electrical and Structural Properties of Amorphous Semiconductors, Edit, P.G. Le Comber and J. Mort, Academic Press, London and New York, p. 91

(15) Grigorovoci, R. (1969), J. Non-Cryst. Solids., 1, 603

(16) Ioffe, A.F. and Regel, A.R., (1960), Prog. Semicond., 4, 239

(17) Stevels, J.M., (1971), J. Non-Cryst. Solids., 6, 307

(18) Bell, R.J. and Dean, P., (1972), Phil. Mag., 25, 1381

(19) Mott, N.F. and Davis, E.A., (1971), Electronic Processes in Non-Crystalline Materials, 1st Ed., Oxford Univ. Press.

(20) Fritzsche, H., (1973), Proc. 13th Session of Scottish Univ. Summer School in Physics, Academic Press, London p.55.

(21) Bloch, F., (1928), Z. Physik, 52, 555

(22) Frohlich, H., (1947), Proc. Roy. Soc. (London), A188, 521.

(23) Anderson, P.W., (1958), Phys. Rev., 109, 1492.

(24) Mott, N.F., (1967a), Adv. Phys., 16, 49.

(25) ——— (1967), Adv. Phys., 16, 49.

(26) ——— (1969a), Phil. Mag., 19, 839.

(27) ——— (1969b), Contemp. Phys., 10, 125.

(28) ——— (1969c), Festkorperprobleme, 9, 22.

(29) ——— (1970a), Phil. Mag., 22, 7.

(30) Cohen, M.H., Fritzsche, H. and Ovshinsky, S.R., (1969), Phys. Rev. Letters, 22, 1065.

(31) Davis, E.A. and Mott, N.F., (1970), Phil. Mag., 22, 903.

(32) Mott, N.F., (1971), Phil Mag., 24, 911.

(33) Marshall, J.M. and Owen, A.E., (1971), Phil. Mag., 24,1281.

(34) Kubo, R., (1956), Can. J. Phys., 34, 1274.

(35) Greenwood, D.A., (1958), Proc. Phys. Soc., 71, 585.

(36) Mott, N.F., (1972), J. Non-Cryst. Solids, 8-10, 1.

(37) Drude, P., (1902), Ann. d. Physik., 7, 687.

(38) Argall, F. and Jonscher, A.K., (1968), Thin Solid Films, 2, 185.

(39) Linsley, G.S., Owen, A.E., Hayatee, F.N., (1970), J. Non-Cryst. Solids, 4, 208.

(40) Sayer, M., Mansingh, A., Reyes, J.M. and Rosenblatt, G., (1971), J. Appl. Phys., 42, 2857

(41) Austin, I.G. and Mott, N.F., (1969), Adv. in Phys., 18,41.

(42) Pollack, M. and Geballe, T.H., (1961), Phys. Rev., 122,1742.

(43) Tauc, J., (1969), The Optical Properties of Solids, ed. F. Abeles, North-Holland, Amsterdam.

(44) Denton, E.P., Rawson, H. and Stanworth, J.E., (1954), Nature, 173, 1030.

(45) Mackenzie, J.D., (1964), Modern Aspects of the Vitreous State, Vol. 3, ed. J.D. Mackenzie, Butterworths, London.

(46) Mott, N.F., (1968), J. Non-Cryst. Solids, 1, 1.

(47) Owen, A.E., (1970), Contemp. Phys., 11, 257.

(48) Sayer, M. and Mansingh, A., (1972), Phys. Rev. B, 6, 4629.

(49) Kinser, D.L. and Wilson, L.K., (1974), Recent Advances in Science and Technology of Materials, ed. A. Bishay,

(50) Nester, H.H., and Kingery, W.D., (1965), Proc. Intern. Cong. Glass, 7th Brussels, p. 106.

(51) Hansen, K.W. and Splan, M.T., (1966), J. Electrochem. Soc., 113, 895.

(52) Holstein, T., (1959), Ann. Phys., 8, 325.

(53) Friedman, L., (1964), Phys. Rev., 135, A233.

(54) Killias, H.R., (1966), Phys. Letters, 20, 5.

(55) Bogomolov, V.N., Kudinov, E.K. and Frisov, Y.a., (1967), Fiz. Tverd. Tela, 9, 3175.

(56) Emin, D. and Holstein, T., (1969), Ann. Phys. (N.Y.), 53, 439.

(57) Friedman, L. and Holstein, T., (1963), Ann. Phys. (N.Y.), 21, 494.

(58) Holstein, T., (1969), Ann. Phys., 8, 343.

(59) Hansen, K.W., (1965), J. Electrochem. Soc., 112, 10.

(60) Linsley, G.S., Owen, A.E., and Hayatee, F.M., (1970), J. Non-Cryst. Solids, 4, 208.

(61) Kitaigorodskii, I.I., Frolov, V.K., and Kuo-Cheng, (1960), Glass Ceram., 17, 1613.

(62) Flynn, B.W., Owen, A.E. and Robertson, J.M., (1977), Proc. 7th Int. Conf. on Amorphous and Liquid Semiconductors, ed. W.E. Spear, CICL, Edinburgh, pg 678.

(63) Tsuchiya, T. and Moriya, T., (1975), Glass and Ceram. Bull., 22, 55.

(64) Mansingh, A., Dhawan, A., Tandon, R.P. and Vaid, J.K., (1978), J. Non-Cryst. Solids, 27, 309.

(65) Murawski, L., Chung, C.H. and Mackenzie, J.D., (1979), J. Non-Cryst. Solids, 32, 91.

(66) Greaves, G.N., (1973), J. Non-Cryst. Solids, 11, 427.

(67) Murawski, L. and Gzowski, O., (1973), Phys. Stat. Sol. (a), 19, K 125.

(68) Hirashima, H. and Yoshida, T., (1977), Proc. 11th Int. Cong. on Glass, Prague, Vol. II, ed. J. Gotz, North-Holland, Amsterdam, p. 365.

(69) Miller, A. and Abrahams, E., (1969), Phys. Rev., 120, 745.

(70) Vaughan, J.G., Perry, L.H. and Kinser, D.L., (1977), Phys. Chem. Glasses, 18, 87.

(71) Austin, I.G. and Garbett, E.S., (1973), Electronic and Structural Properties of Amorphous Semiconductors, ed. P.G. Le Comber and J. Mort, Academic Press, New York, p261.

(72) Murawski, L. and Gzowski, O., (1976), Acta Phys. Pol., A50, 463.

(73) Austin, I.G., (1970), J. Non-Cryst. Solids, 2, 474.

(74) Mansingh, A., Vaid, J.K. and Tandon R.P., (1977), J. Phys., C10, 4061.

(75) Rashed, I., (1980), PhD Thesis, Brunel University, England.

(76) Drake, C.F., Stephan, J.A. and Yates, B., (1978), J. Non-Cryst. Solids, 28, 61.

(77) Mackenzie, J.D., (1964), J. of Amer. Ceram. Soc., 47, 211.

(78) Hekmat-Shoar, M.H., (1979), PhD Thesis, Brunel University, England.

(79) Mohammad Elahi, S., (1979), PhD Thesis, Brunel University, England.

(80) Sarver, J.F., (1966), Trans. Brit. Ceram. Soc., 65, 191.

(81) Higazy, A.A., (1982), results to be published.

(82) Austin, I.G. and Sayer, M., (1974), J. Phys. C, Solid State Physics., 7, 905.

(83) Moridi, G.R., (1975), PhD Thesis, Brunel University, England.

(84) Joncher, A.K., (1967), Thin Solid Films, 1, 213.

(85) Marshall, J.M. and Miller, G.R., (1973), Phil. Mag., 27, 1151.

(86) Ovshinsky, S.R., (1959), Electronics, 32, 76.

(87) _____ (1966), U.S. Patent 3, 271, 591.

(88) Ovshinsky, S.R., (1967), Bull. Sci. USSR, Edited by B.T. Kolomiets, 9, 91.

(89) Fritzsche, H., (1974), Amorphous and Liquid Semiconductors, Edited by J. Tauc, Plenum Press, London and New York p. 313.

(90) Drake, C.F., Scanlan, I.F. and Engel, A.,(1969), Phys. Stat. Sol., 32, 193.

(91) Moridi, G.R. and Hogarth, C.A., (1978), Int. J. Elect., Vol 44, 3, 297.

(92) Pollack, M. and Geballe, T.H., (1961), Phys. Rev., 122, 1742.

(93) Pollack, M., (1976), Electronic Phenomena in Non-Crystalline Semiconductors, Proc. 6th Int. Conf. on Amorphous and Liquid Semiconductors , Leningrad, p. 79, Edited by B.T. Kolomiets (Acad. Sci. USSR).

(94) Gevers, M.,(1946), Phillips. Res. Repts., 1, 279.

(95) Corbridge, D.E.C. and Lowe, E.J., (1954), J. Chem. Soc. Part 1, p. 493, Part IV, p. 4555.

(96) Bishay, A.M. and Makar, L., (1969), J. Am. Ceram. Soc., 52, 605.

(97) Bartholomew, R.F., (1972), J. Non-Cryst. Solids, 7, 221.

(98) Wong, J. and Angell, C.A., (1971), Appl. Spect. Rev., 4, 155.

(99) Donald, I.W. and Mc Millan, P.W., (1968), J. Mater. Sci., 13, 2301.

(100) Shih, C.K. and Su, G.J., (1965), &th Inter. Congress on Glass, Brussels, Belgium, p. 1.3.3, 48.

(101) Muller, K.P., (1969), Glastechn. Ber., 42, 83.

(102) Nakamoto, K., (1963), Infra-red Spectra of Inorganic and Co-ordination Compounds, Wiley, New York.

(103) Anvari, S.F., (1976), PhD Thesis, Brunel University, England.

(104) Tauc, J., Menth, A. and Wood, D.L., (1970), Phys. Rev. Letters, 25, 749.

(105) Urbach, F., (1953), Phys. Rev., 92, 1324.

(106) Tauc, J. and Menth, A., (1972), J. Non-Cryst. Solid, 8-10, 569.

(107) Paul, A. and Douglas R.W., (1968), Phys. and Chem. Glasses, Vol. 9, No 1, 21.

(108) Stevels, J.M., (1953), Proc. 11th Inter. Congr. Pure Appl. Chem., 5, 519.

(109) Anderson, G.W. and Compton, W.D., (1970), J. Chem. Phys. 52, 6166.

(110) Sigel, G.H., (1972), J. Phys. Chem. Solids, 32, 2373.

(111) Dow, J.D. and Redfield D., (1970), Phys. Rev. B1, 3358.

(112) Hogarth, C.A. and Ghauri, M.A., (1982), Int. J. Electronics, Vol. 52, 3, 201-207.

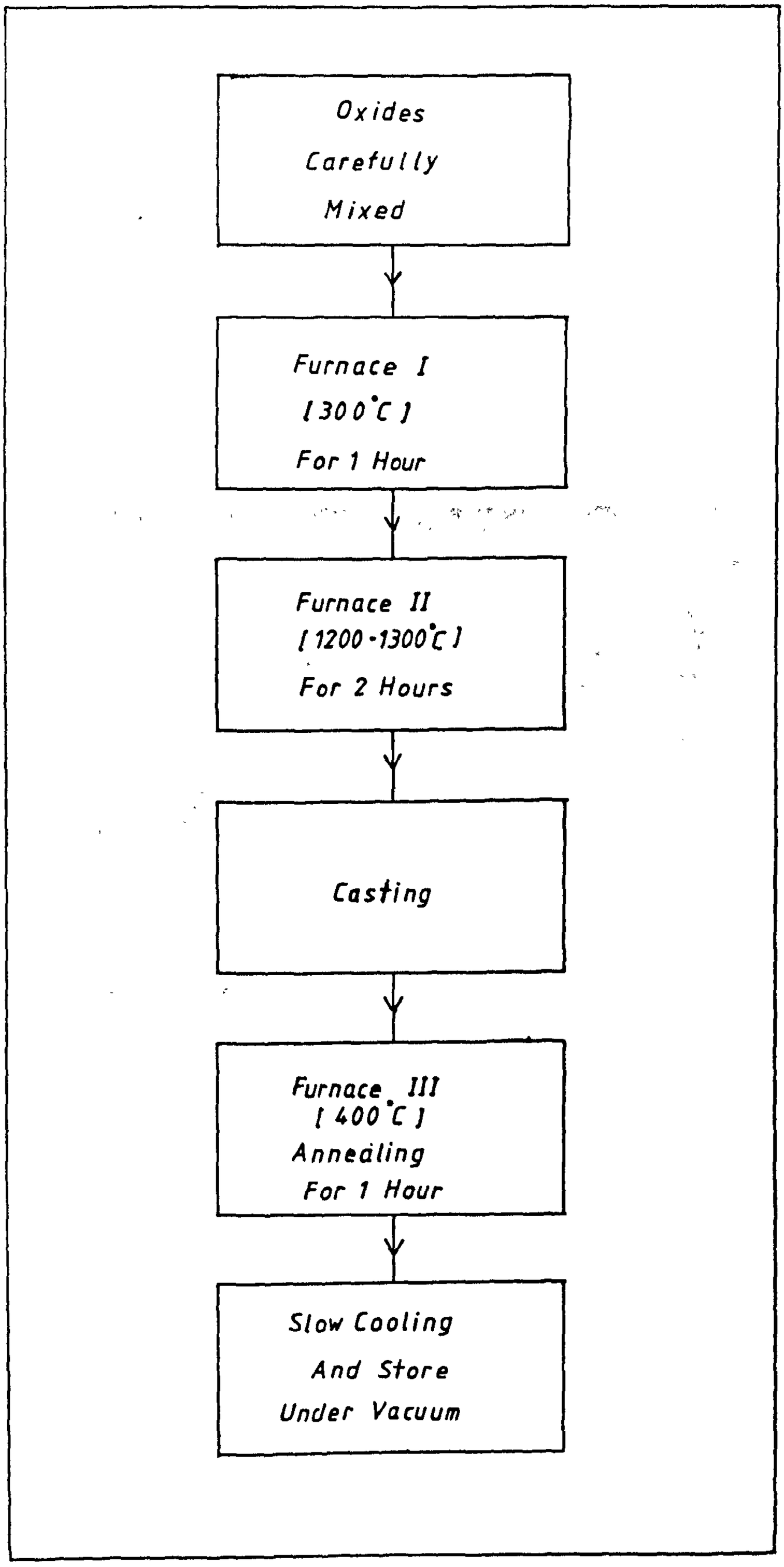

Figure 4.1 Stages of preparation.

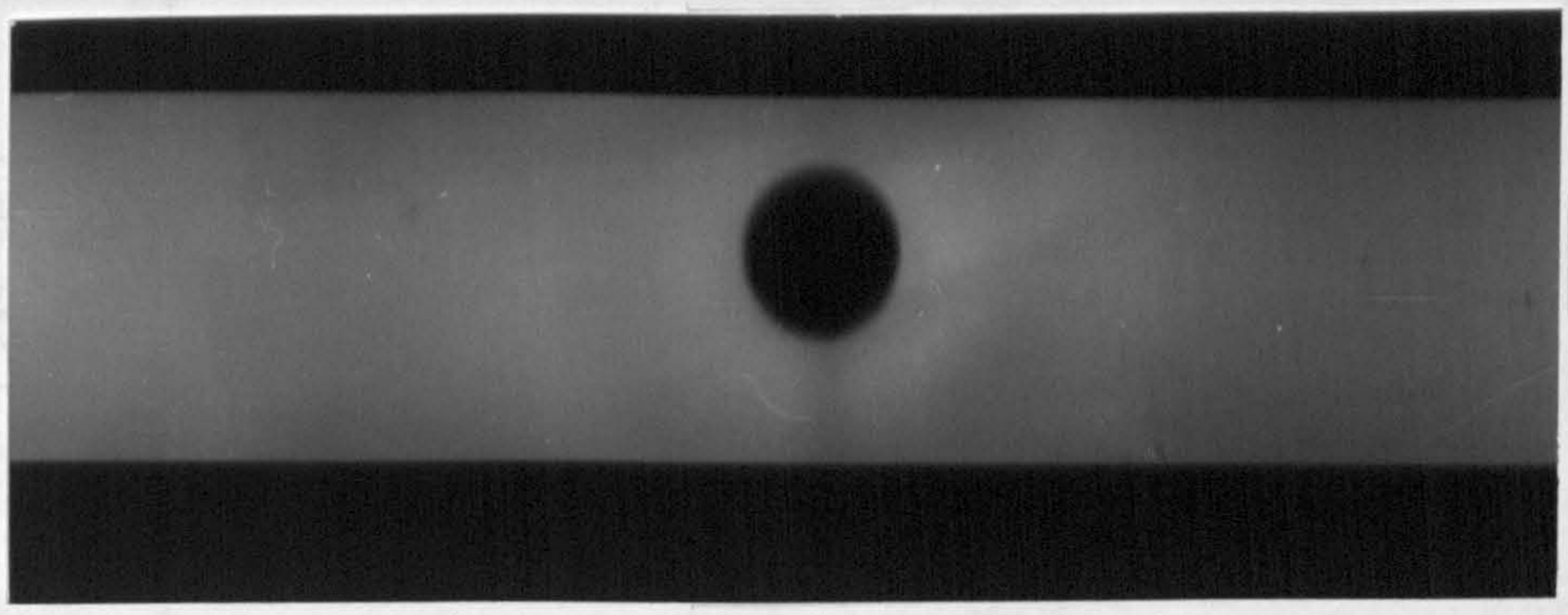

Figure 4.2 X-ray diffraction photograph of
cobalt-phosphate glass (glass 3070)

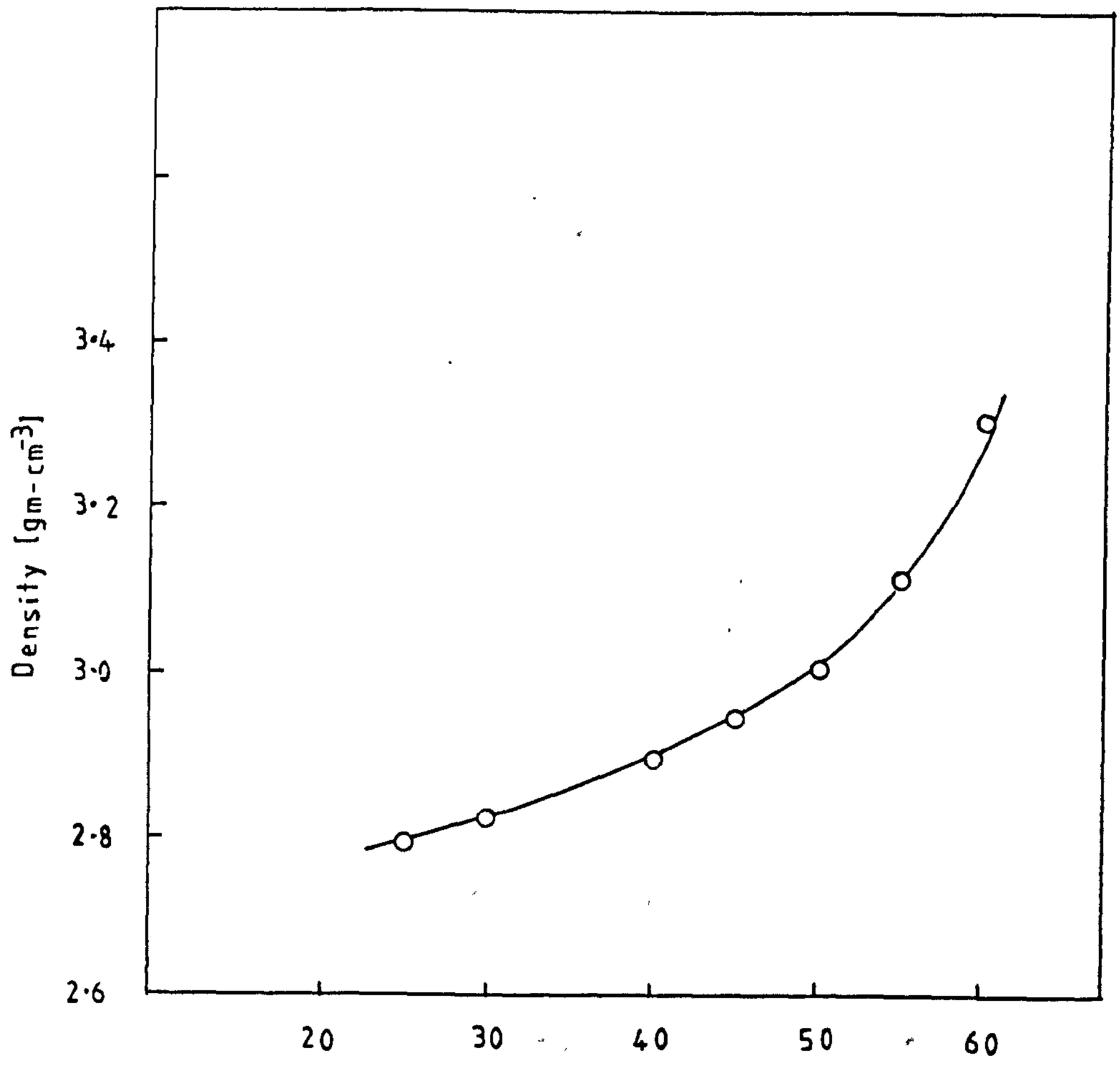

Figure 4.3 Density of CoO-P_2O_5 glasses as a function of CoO content.

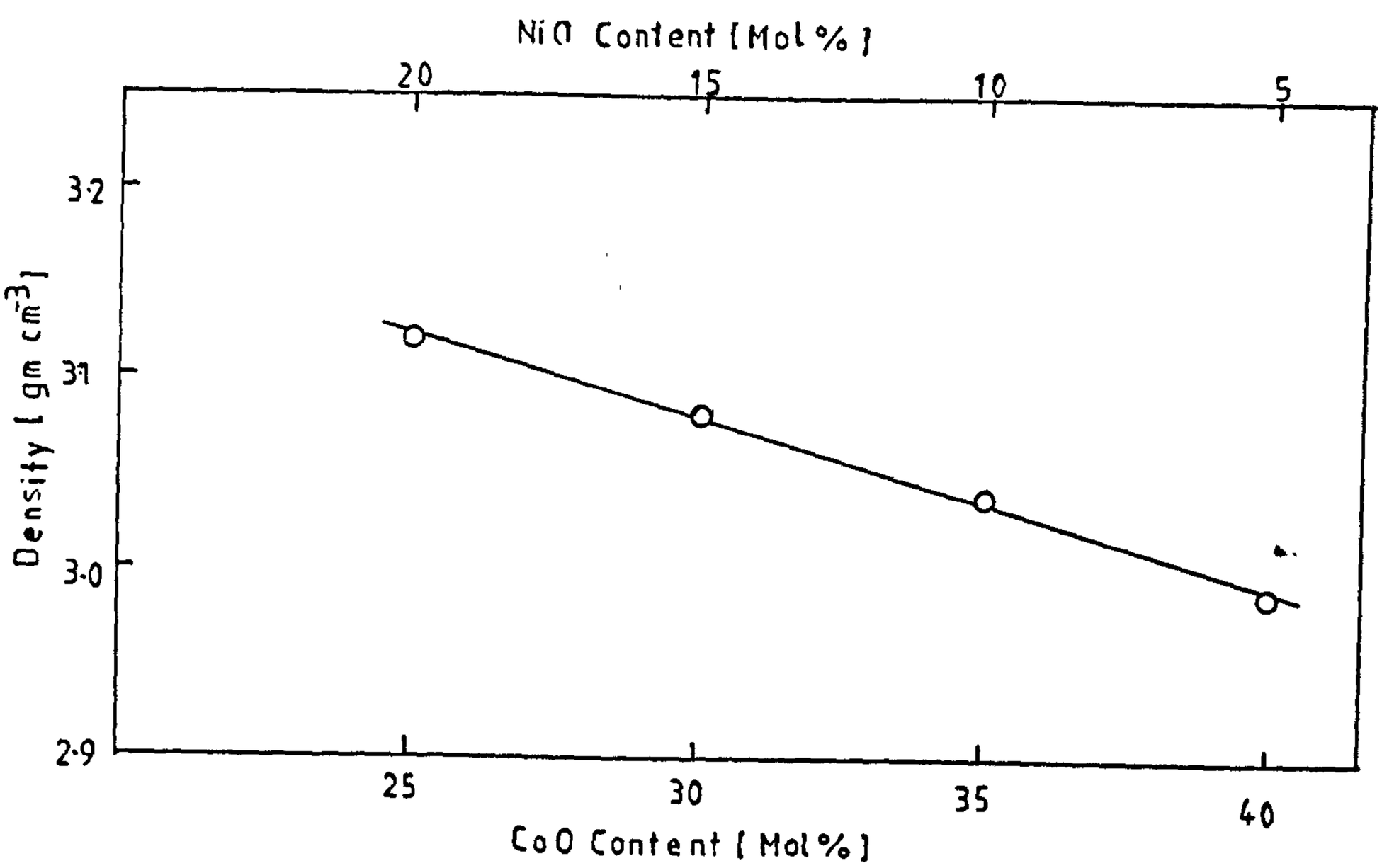

Figure 4.4 Density of CoO-NiO-P_2O_5 glasses as a function of CoO and NiO content.

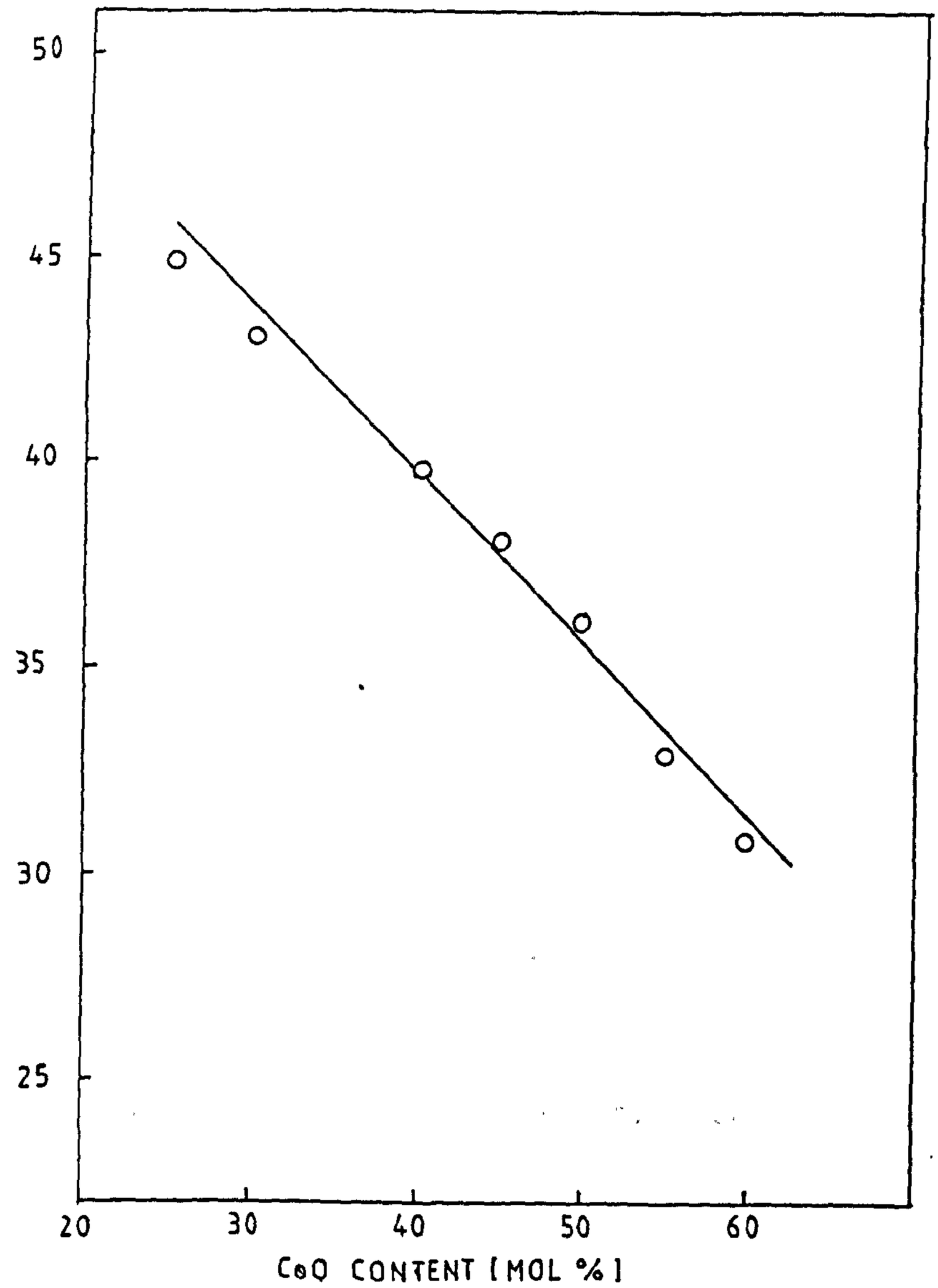

Figure 4.5 Molar volume of CoO-P_2O_5 glasses as a function of CoO content.

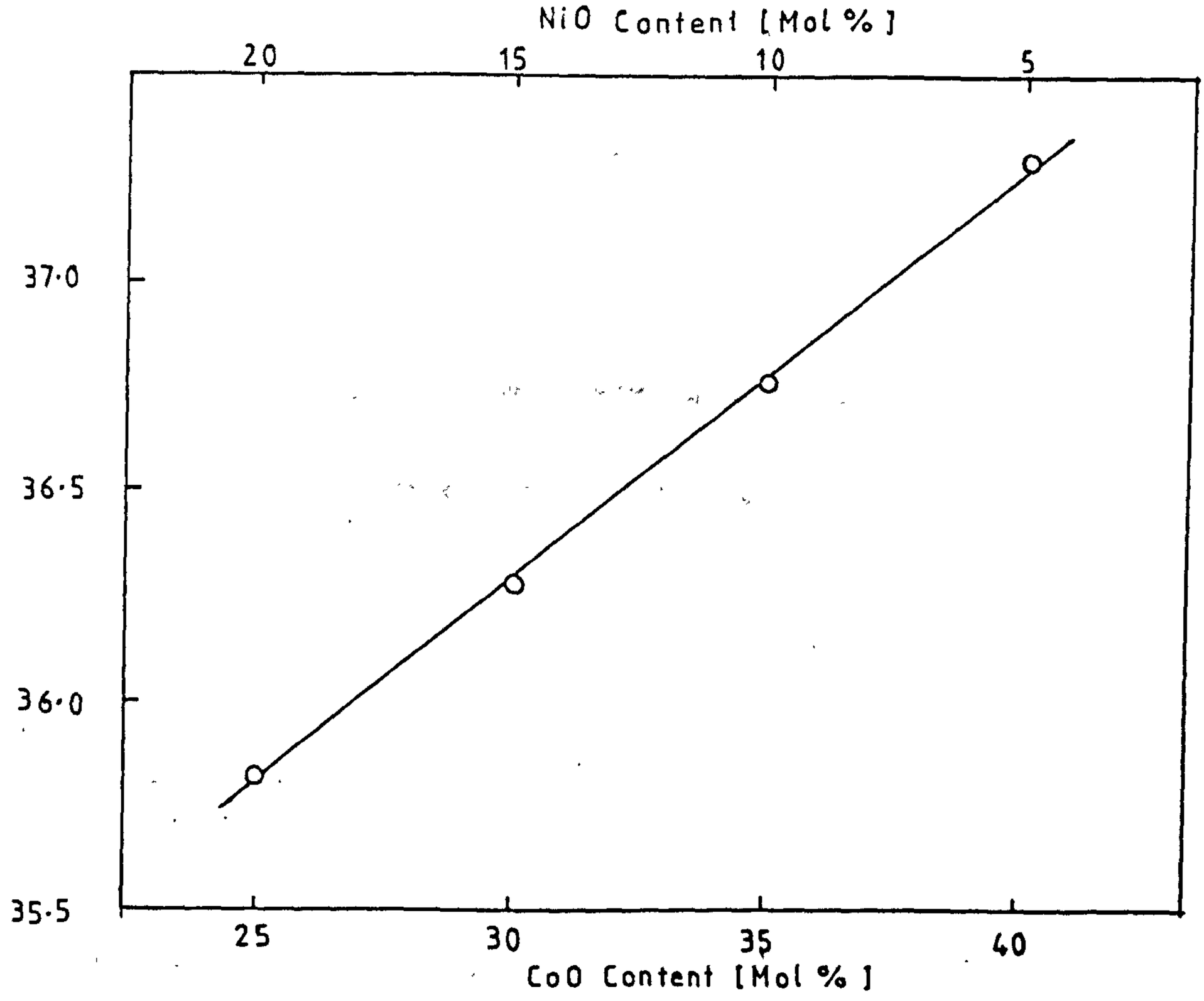

Figure 4.6 Molar volume of CoO-NiO-P_2O_5 glasses as a function of CoO and NiO content.

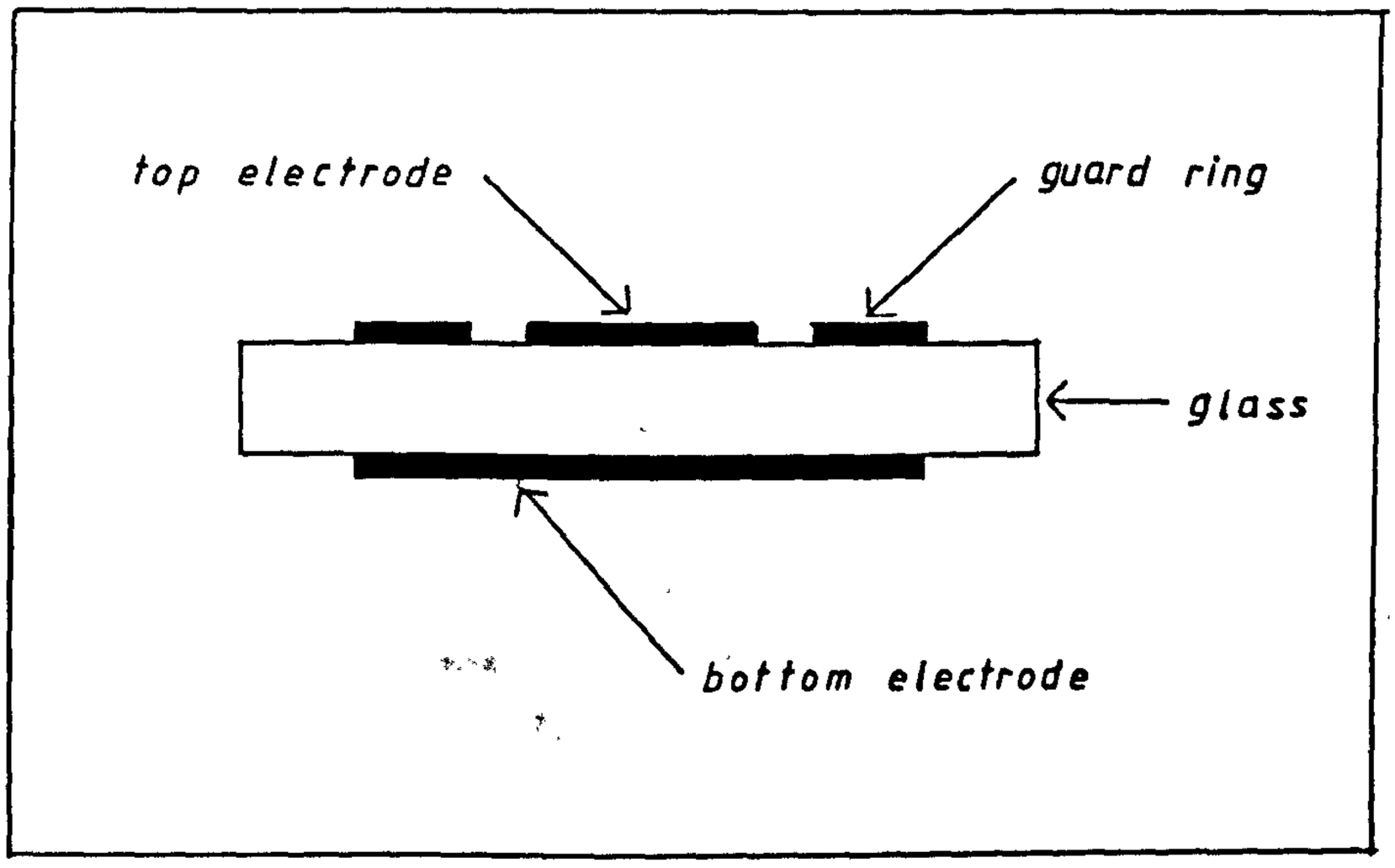

Figure 5.1 Sectioned elevation of the guard ring electrode system.

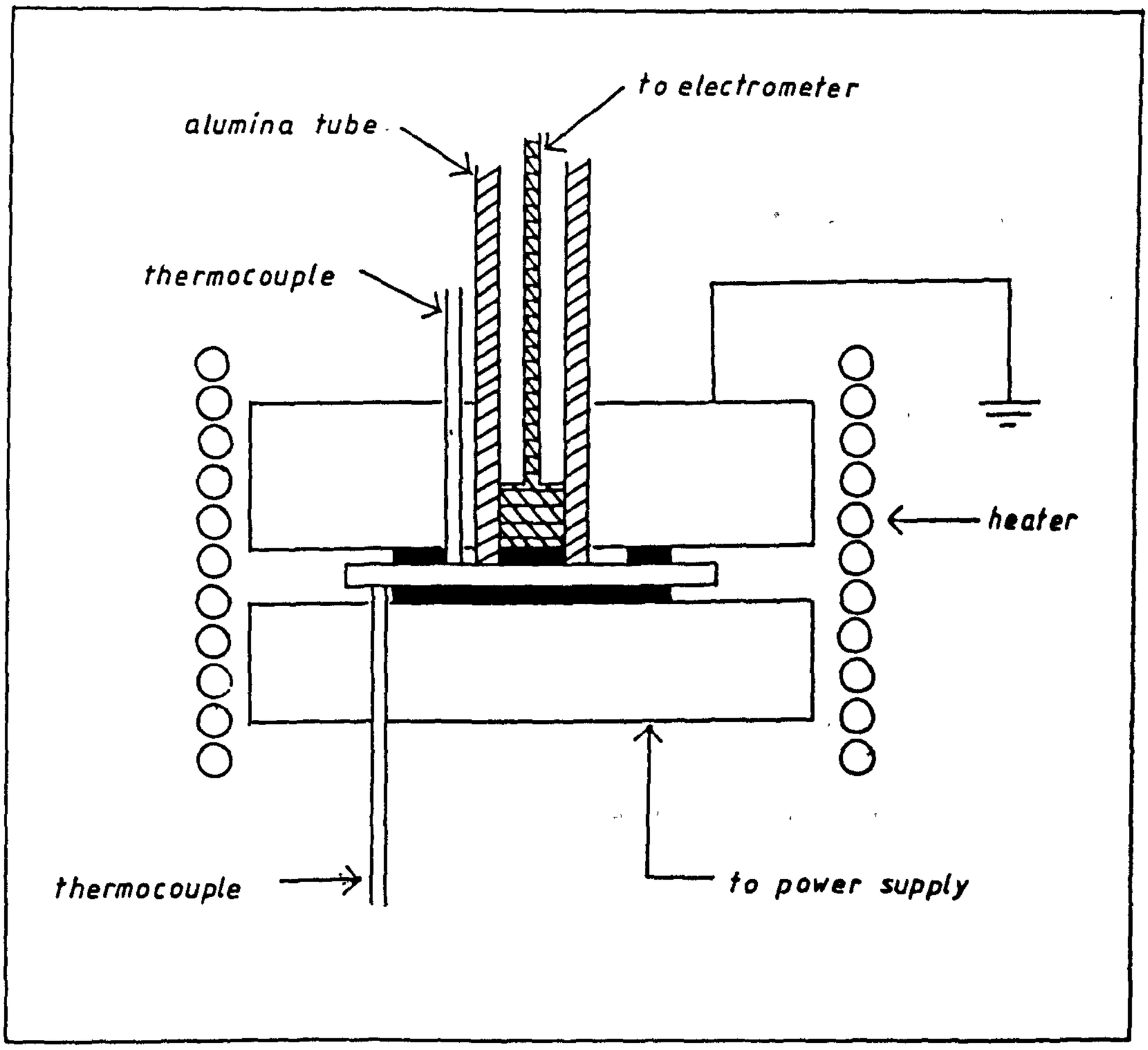

Figure 5.2 Sectioned elevation of the sample holder and heating system.

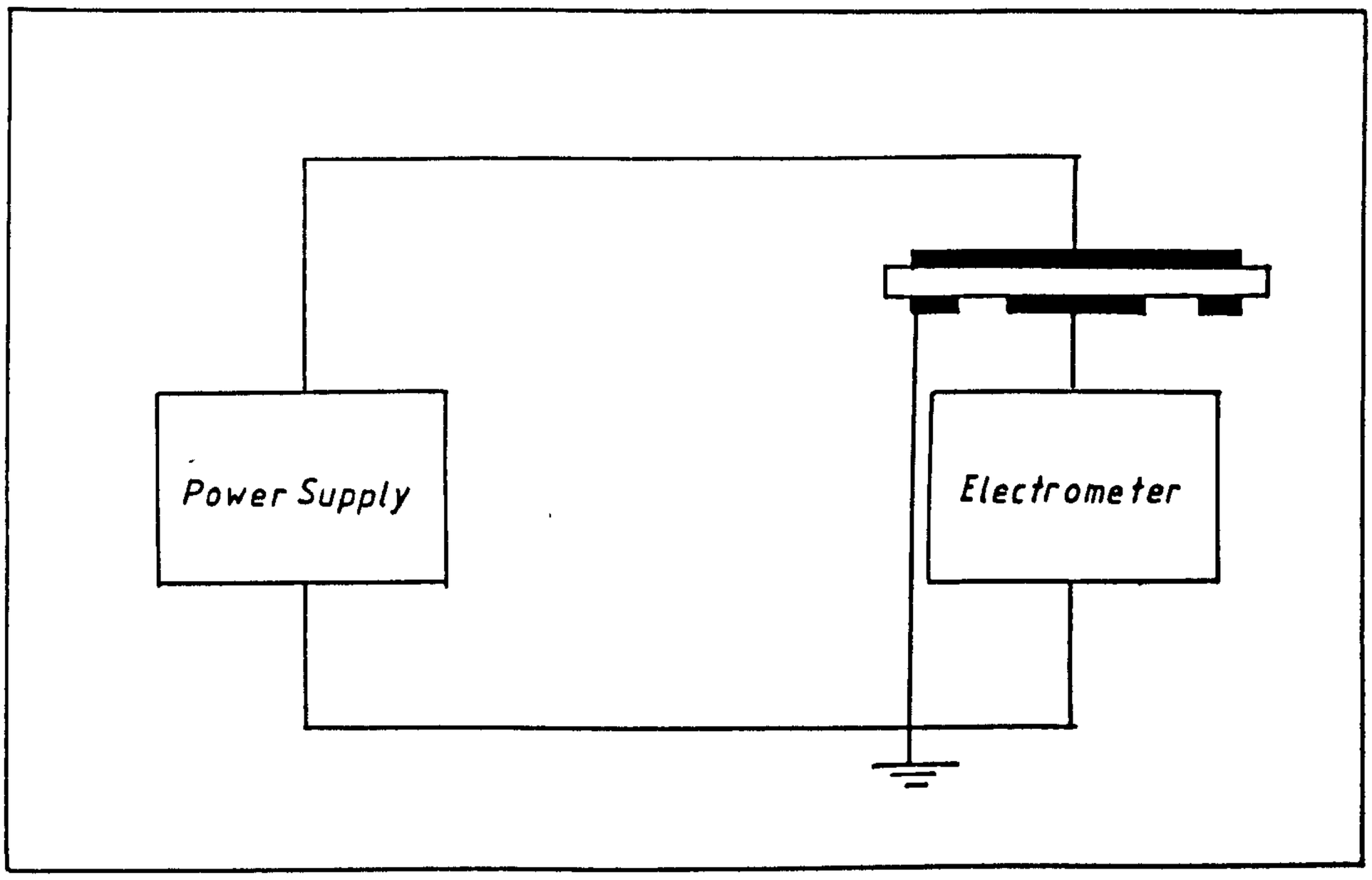

Figure 5.3 Diagram of the circuit used to measure d.c. conductivity.

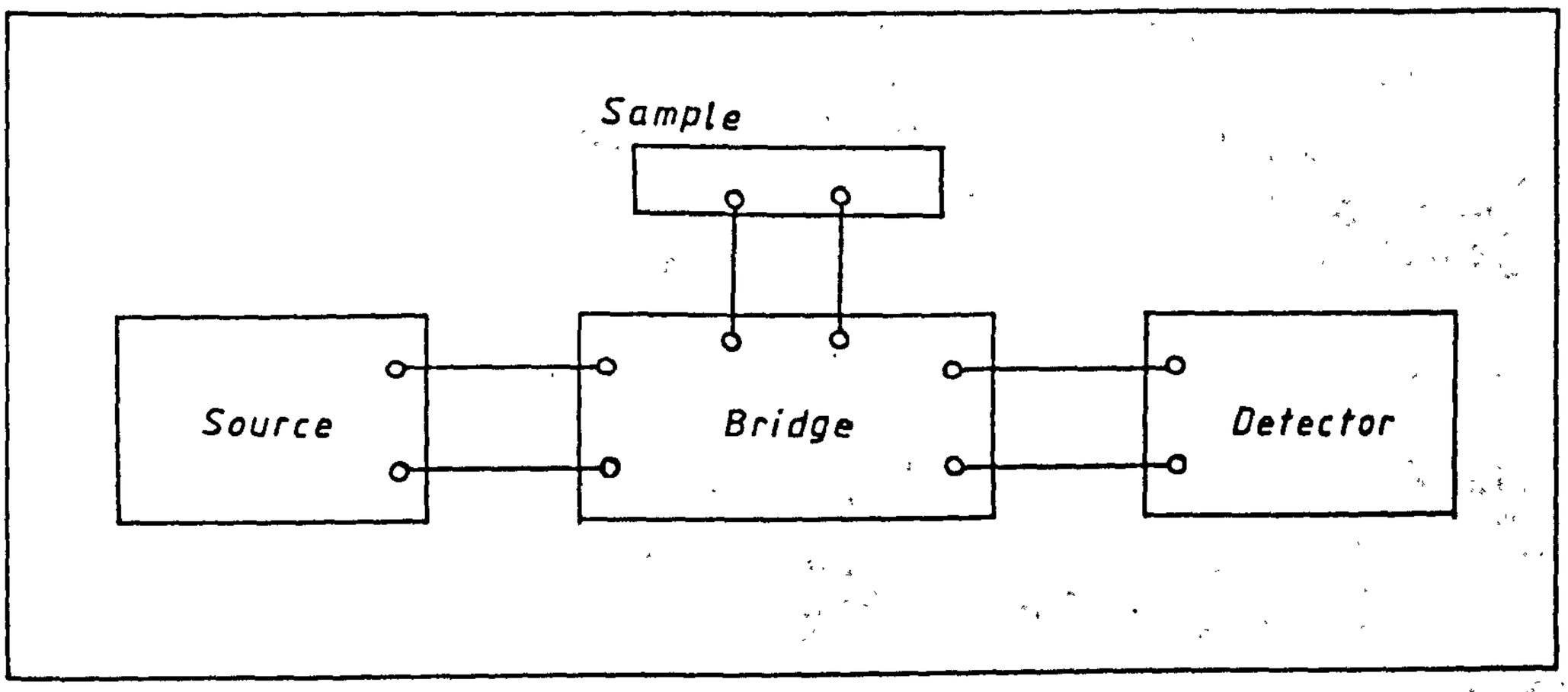

Figure 5.4 Diagram of the circuit used for a.c. measurement.

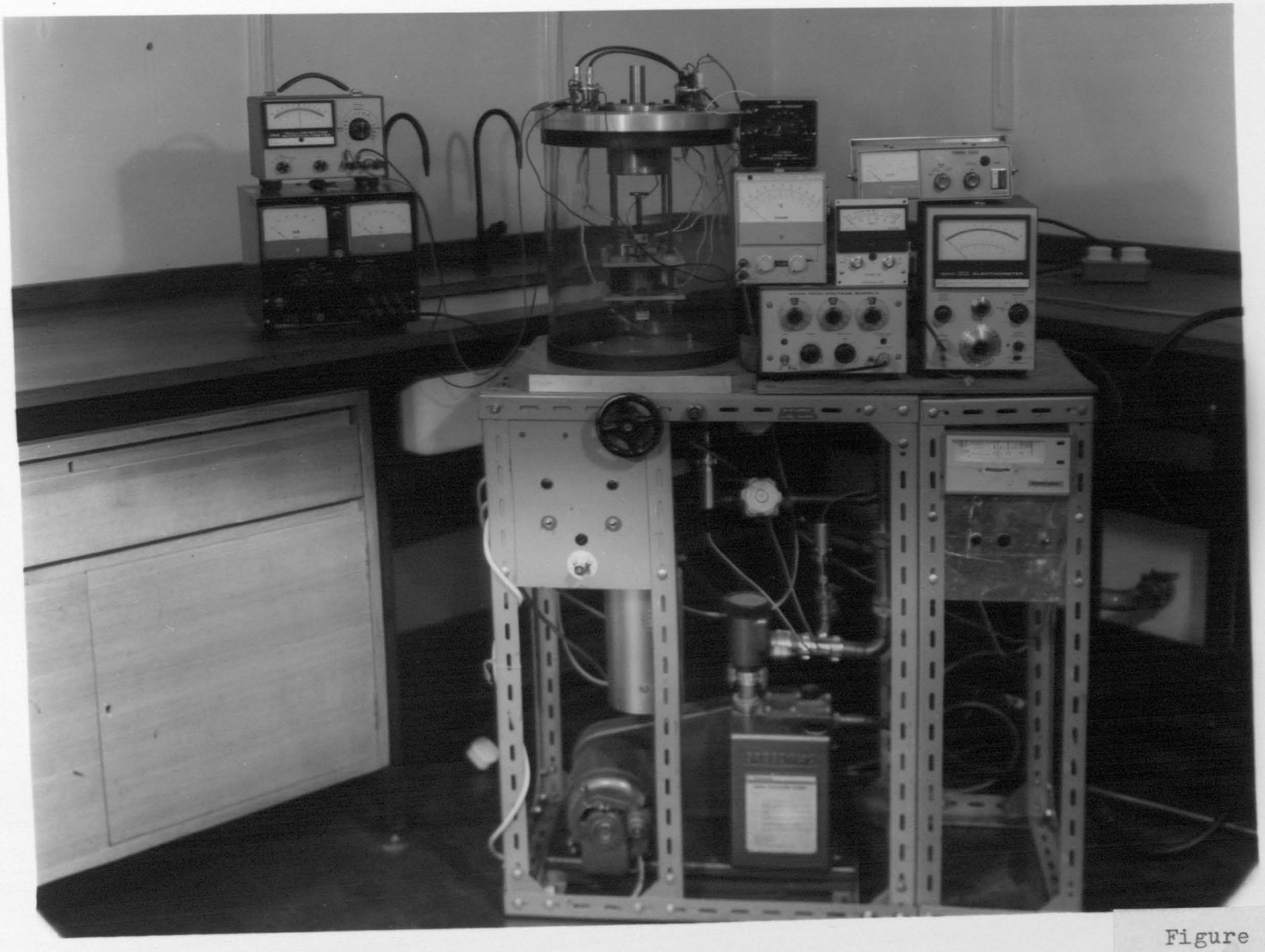

Figure 5.5

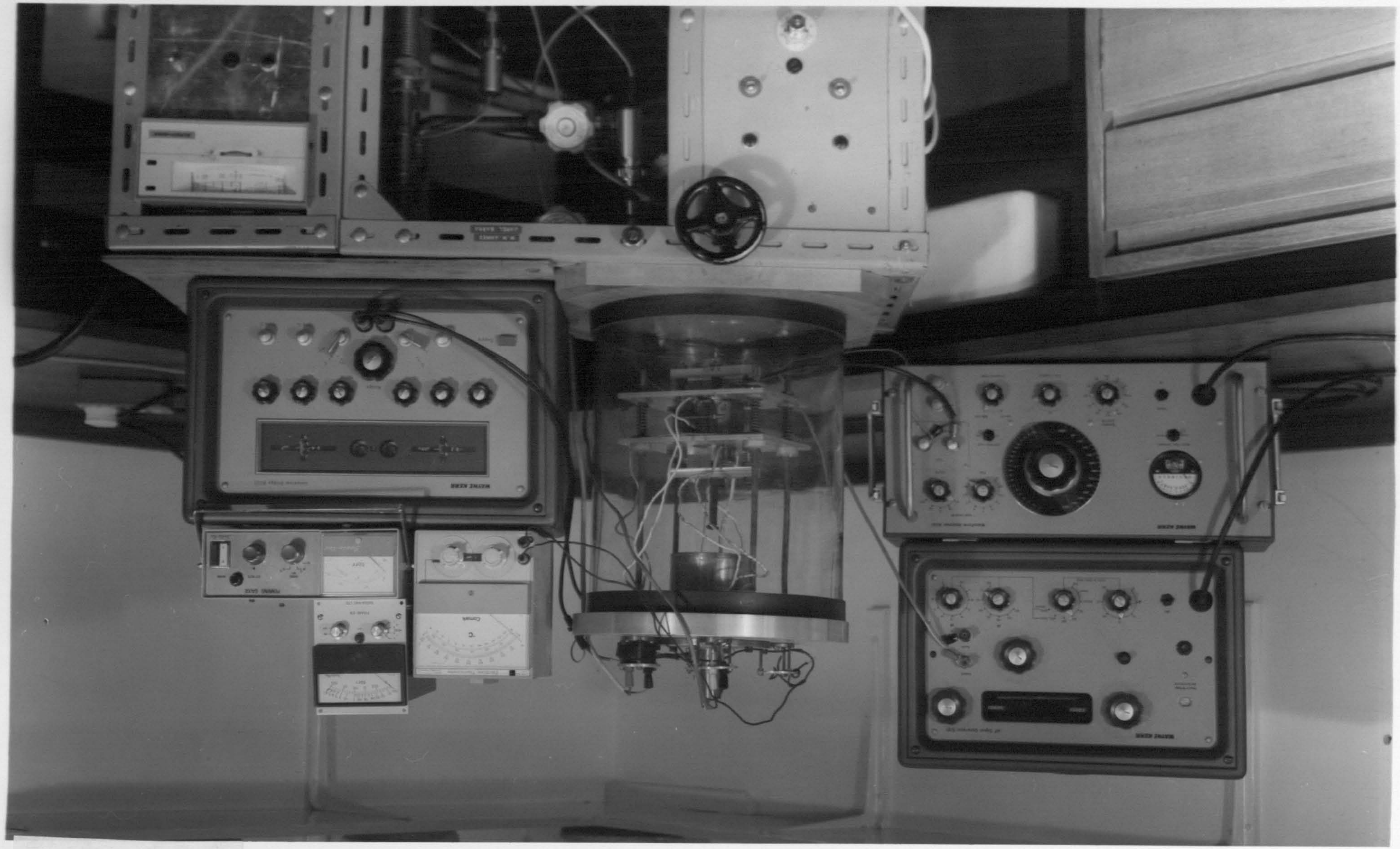

Figure 5.6

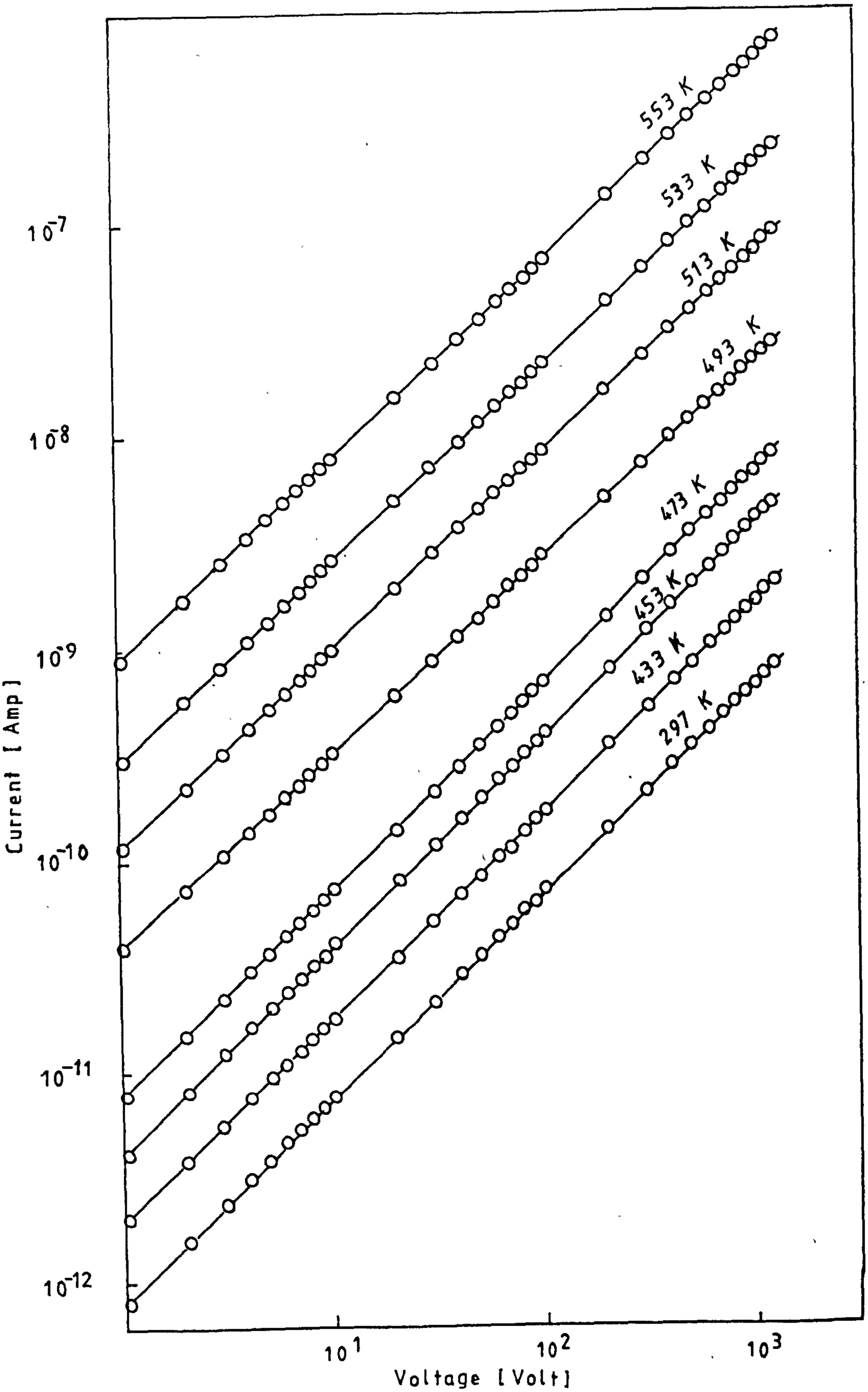

Figure 5.7 V-I characteristics of glass 5050.

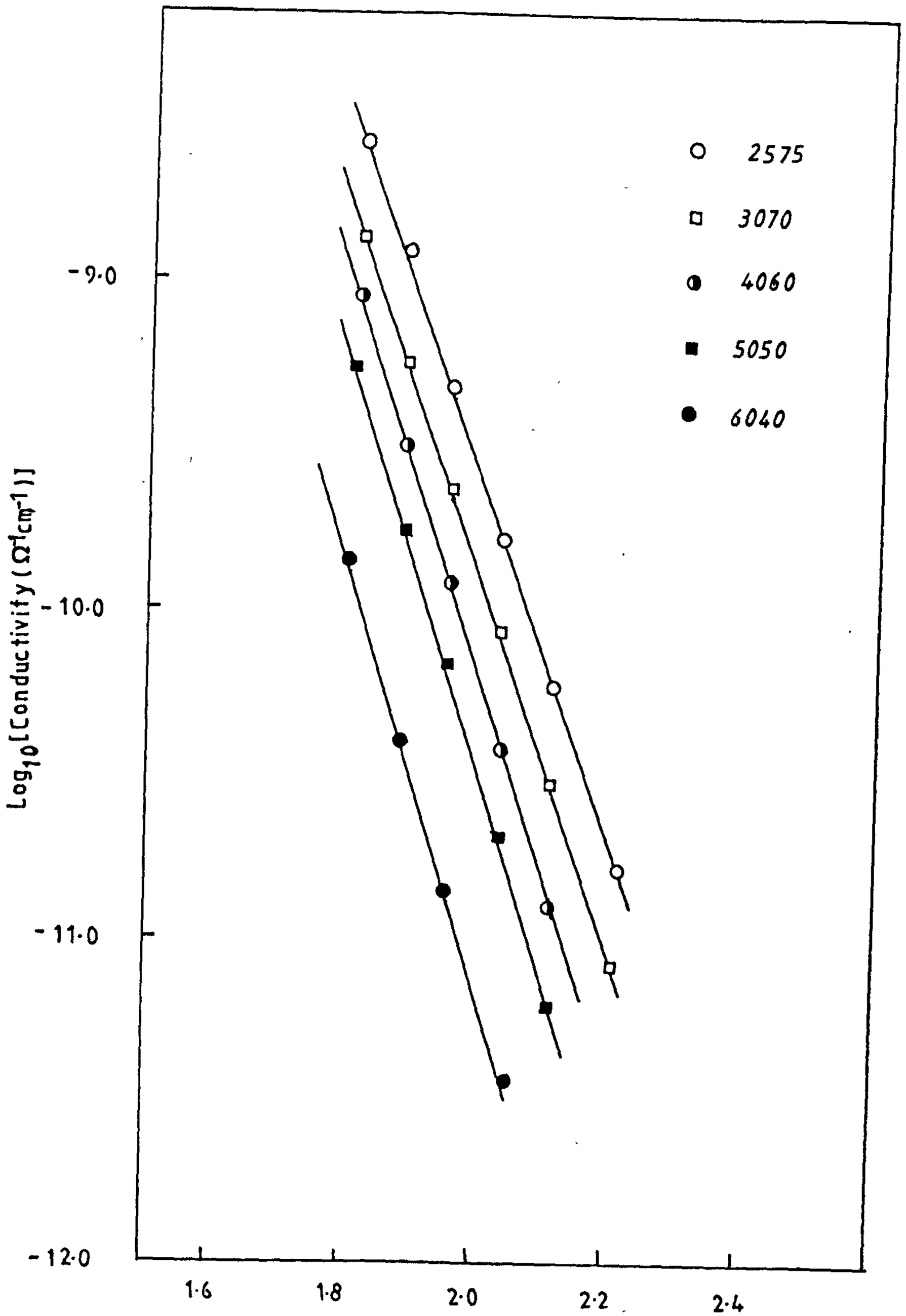

Figure 5.8 Log conductivity versus 1000/T for the binary series.

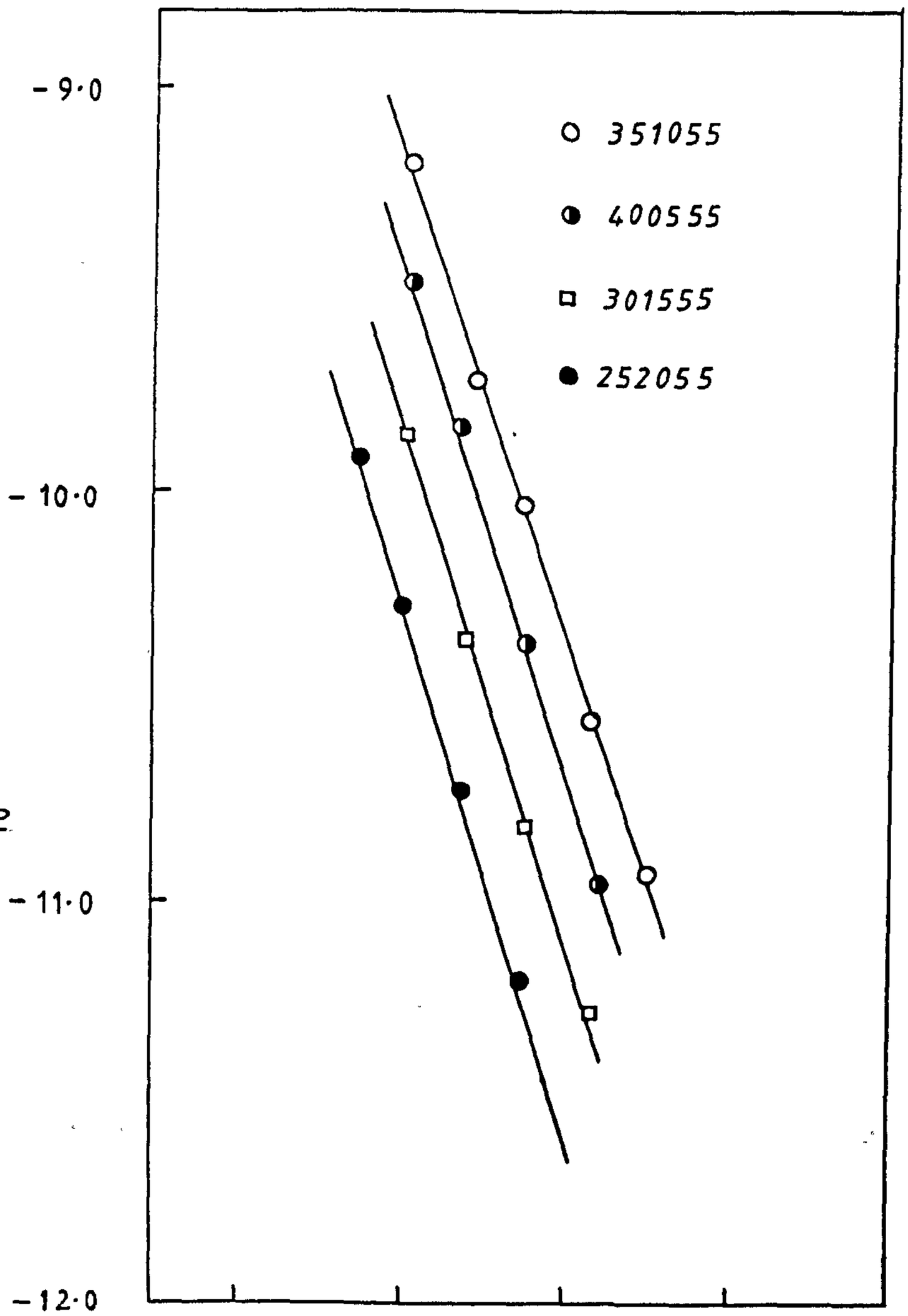

Figure 5.9 Log conductivity versus 1000/T for the ternary series.

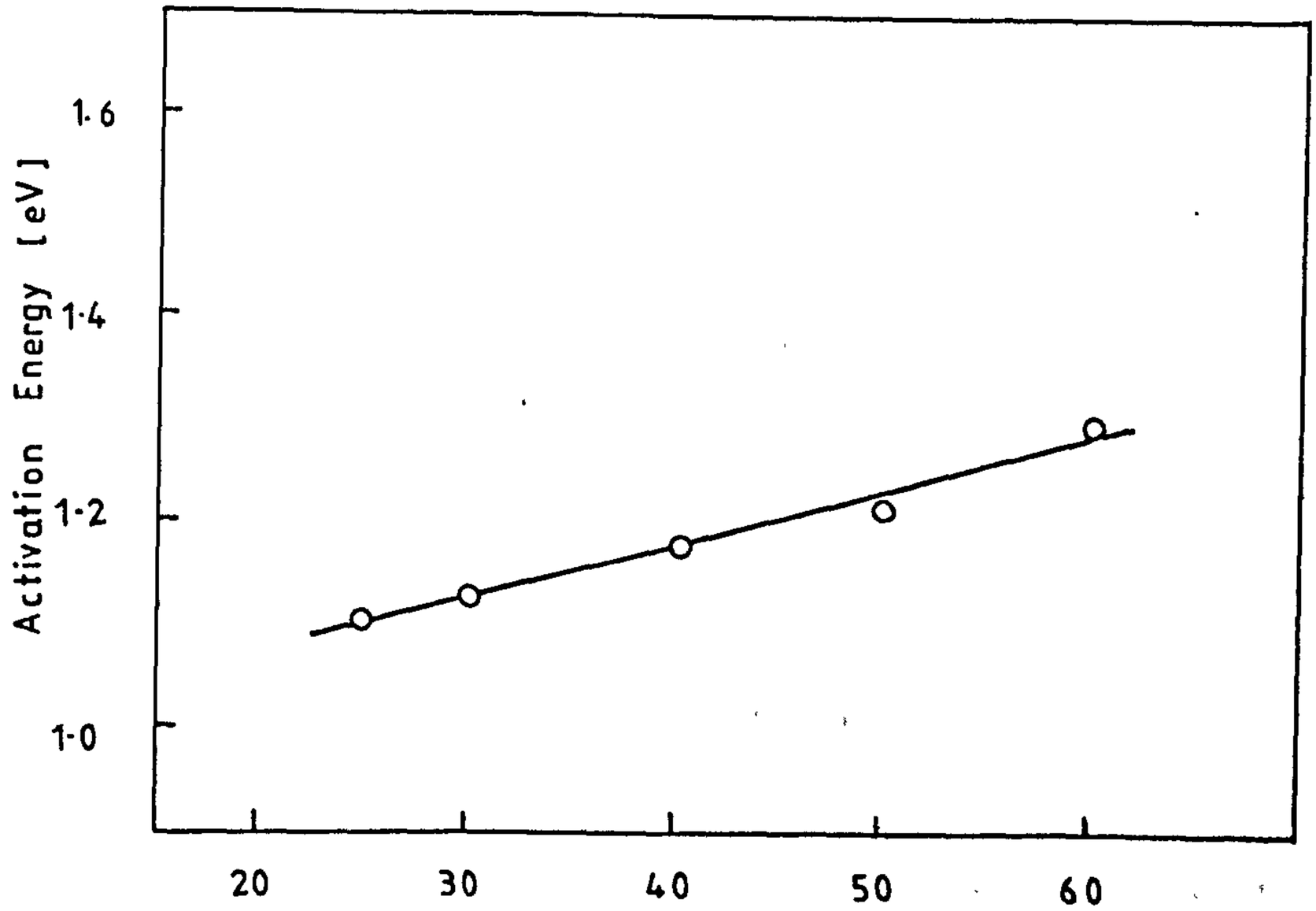

Figure 5.10 Variation of activation energy with CoO content for the binary series.

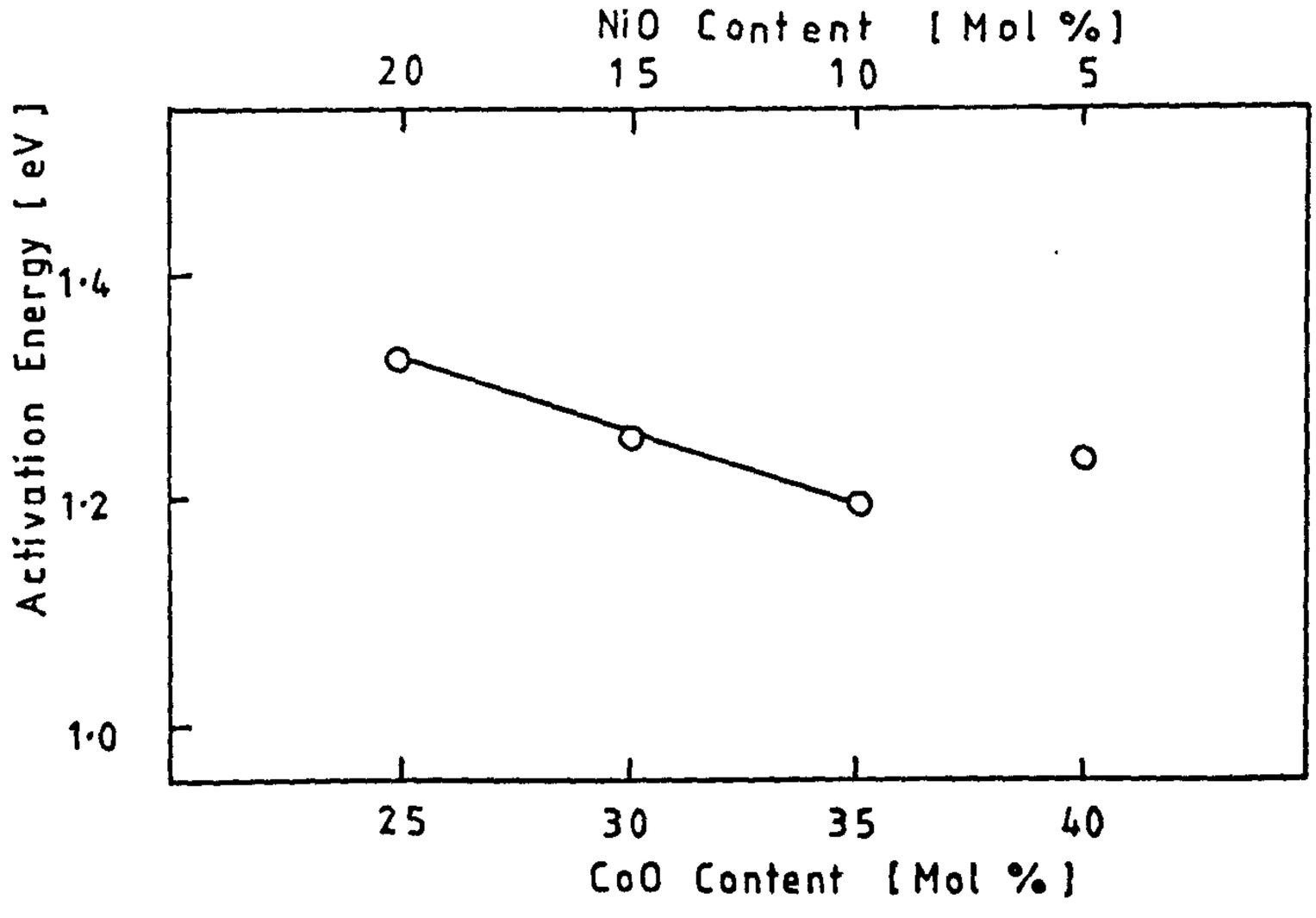

Figure 5.11 Variation of activation energy with CoO content for the ternary series.

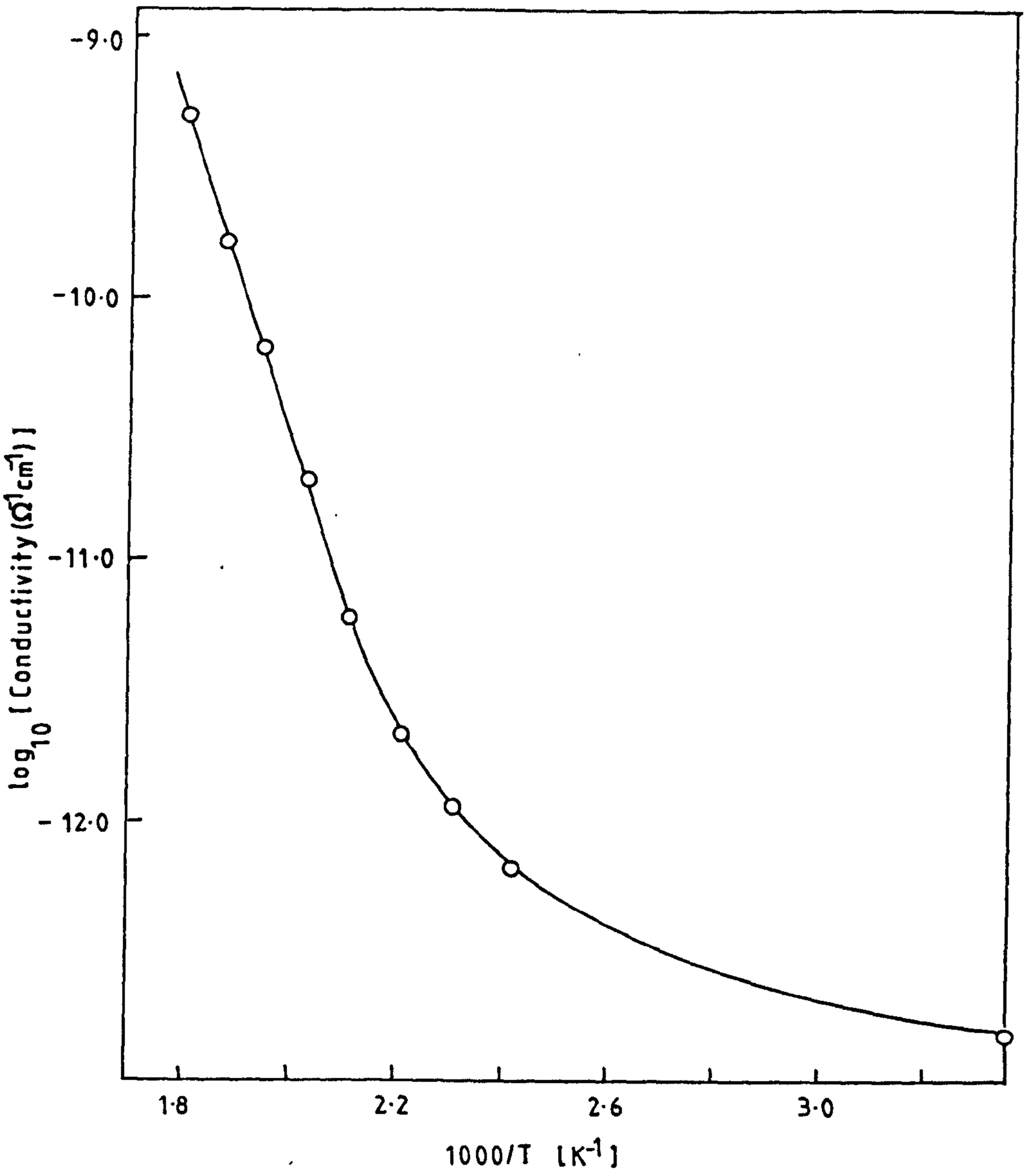

Figure 5.12 Log conductivity versus 1000/T for glass 5050.

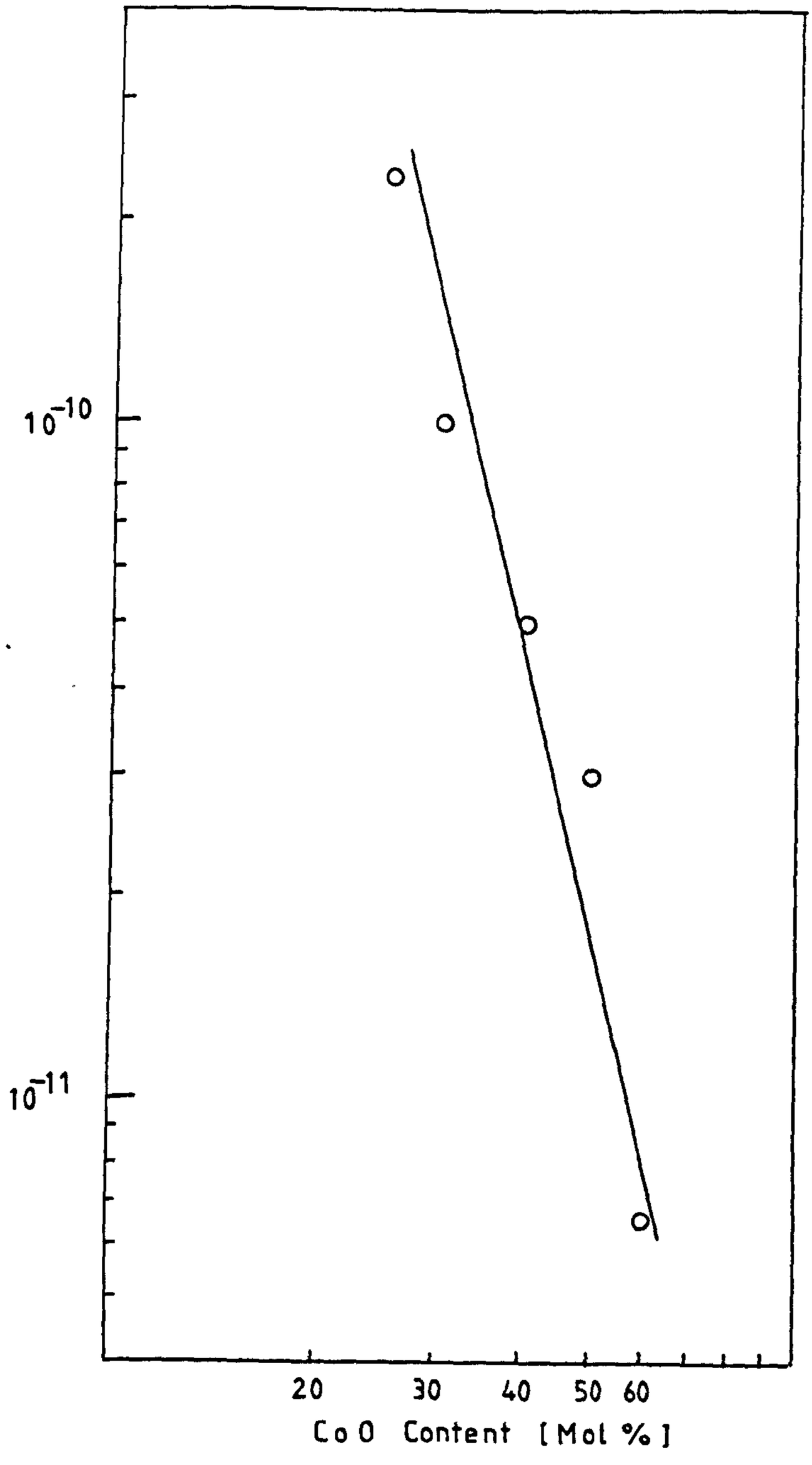

Figure 5.13 Conductivity versus CoO content for the binary system.

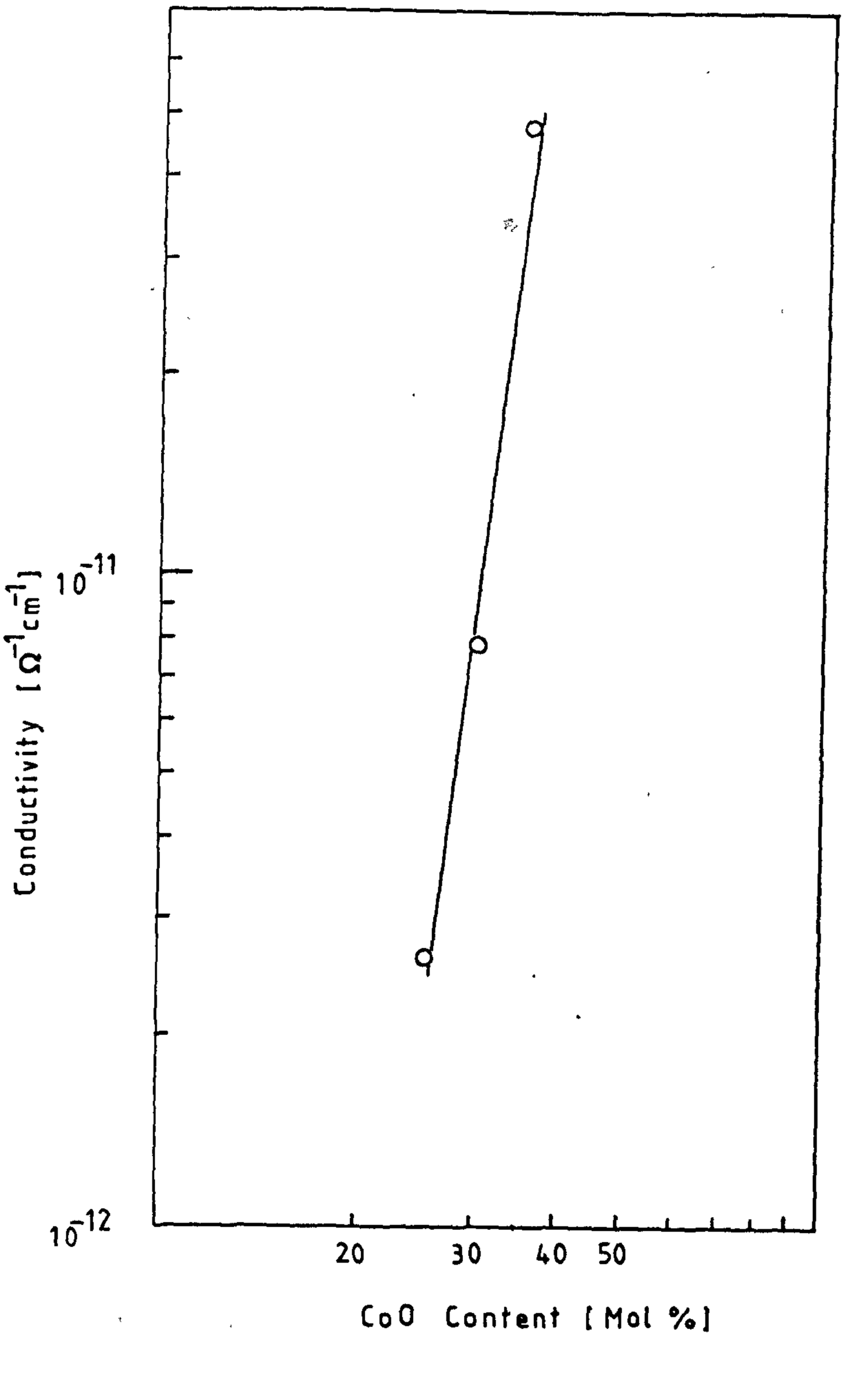

Figure 5.14 Conductivity versus CoO content for the ternary system.

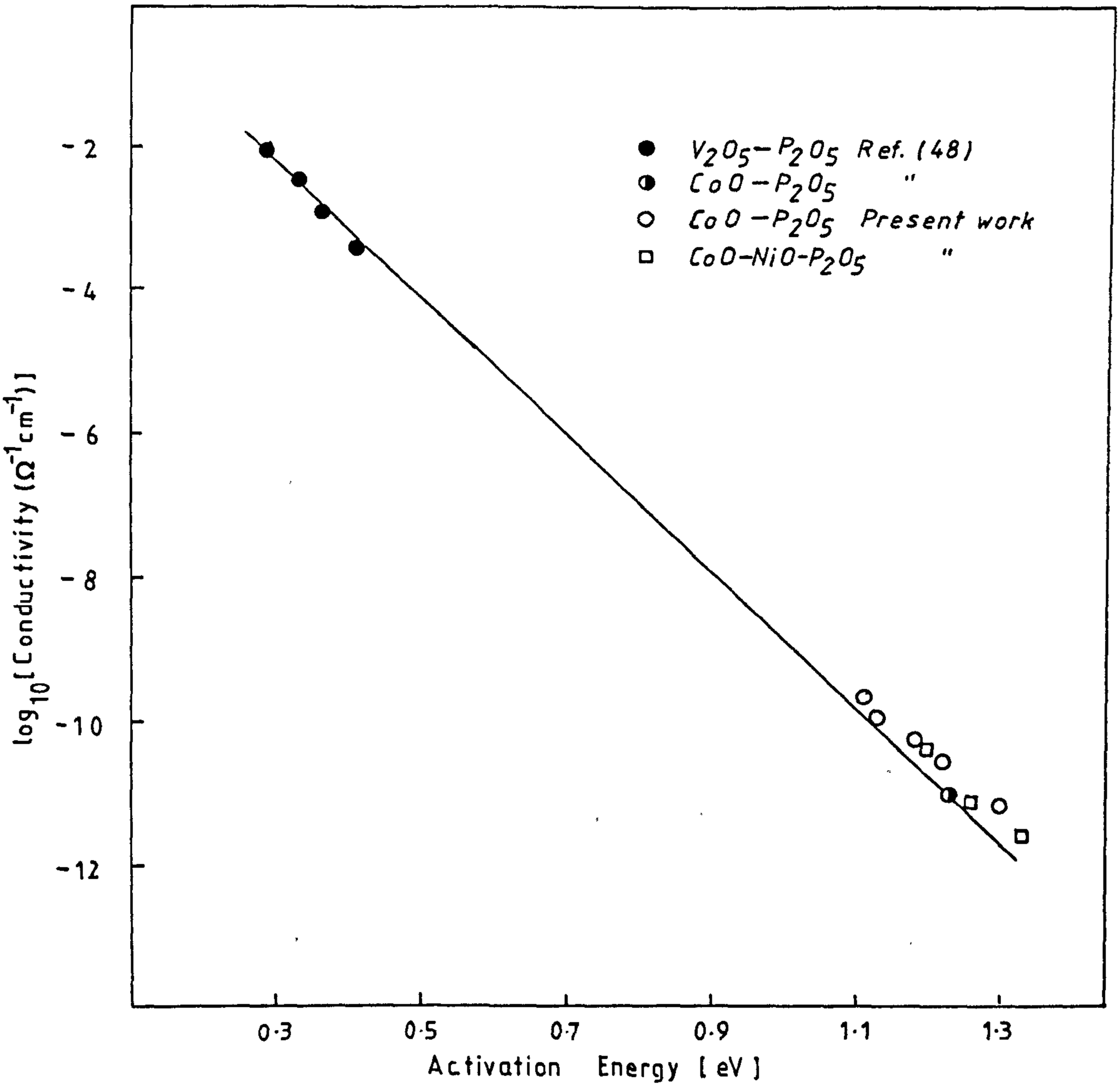

Figure 5.15 Log conductivity versus the high temperature activation energy. Conductivity values measured at 500 K.

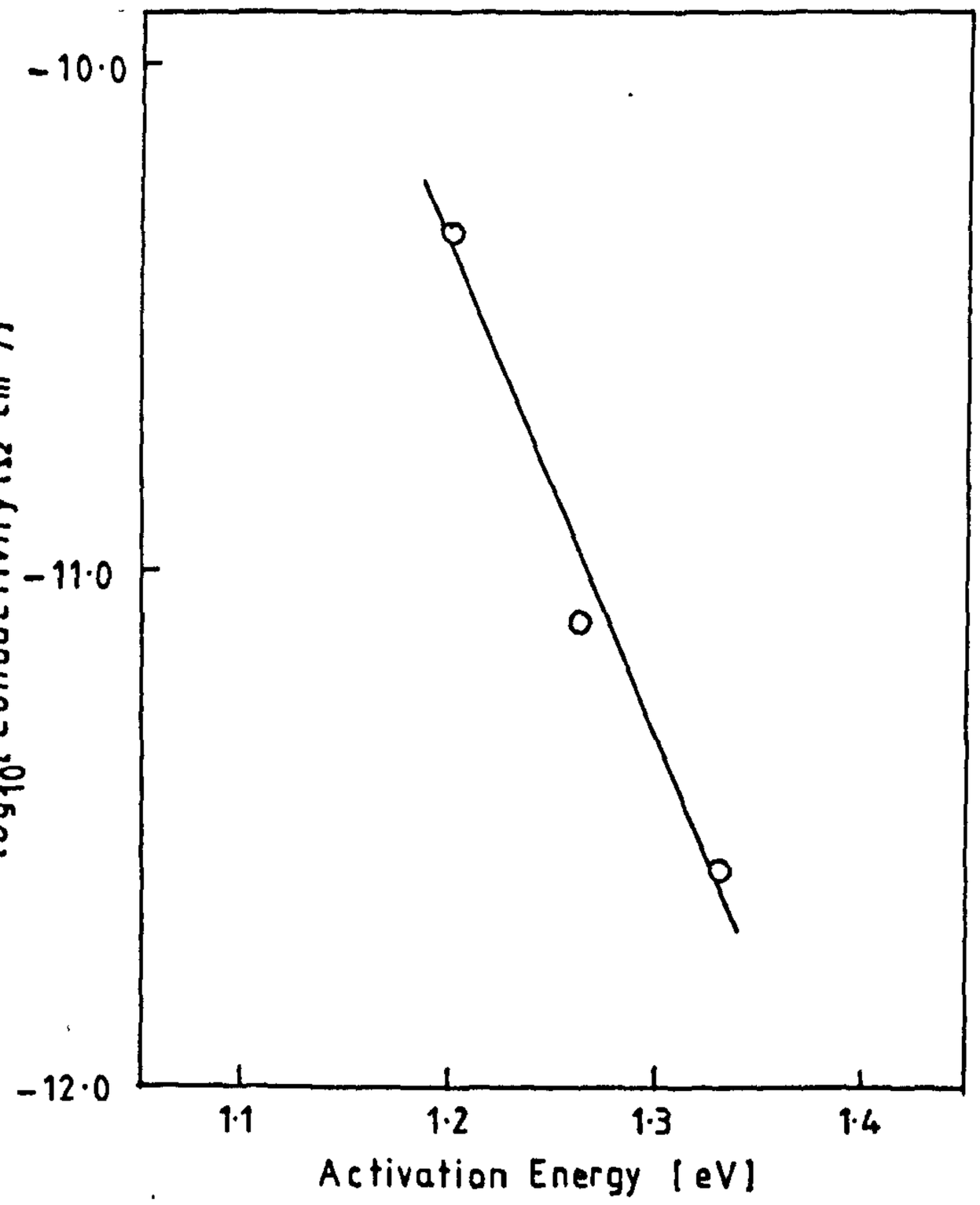

Figure 5.16 Relationship between log conductivity and activation energy for the ternary system. Conductivity values measured at 500 K.

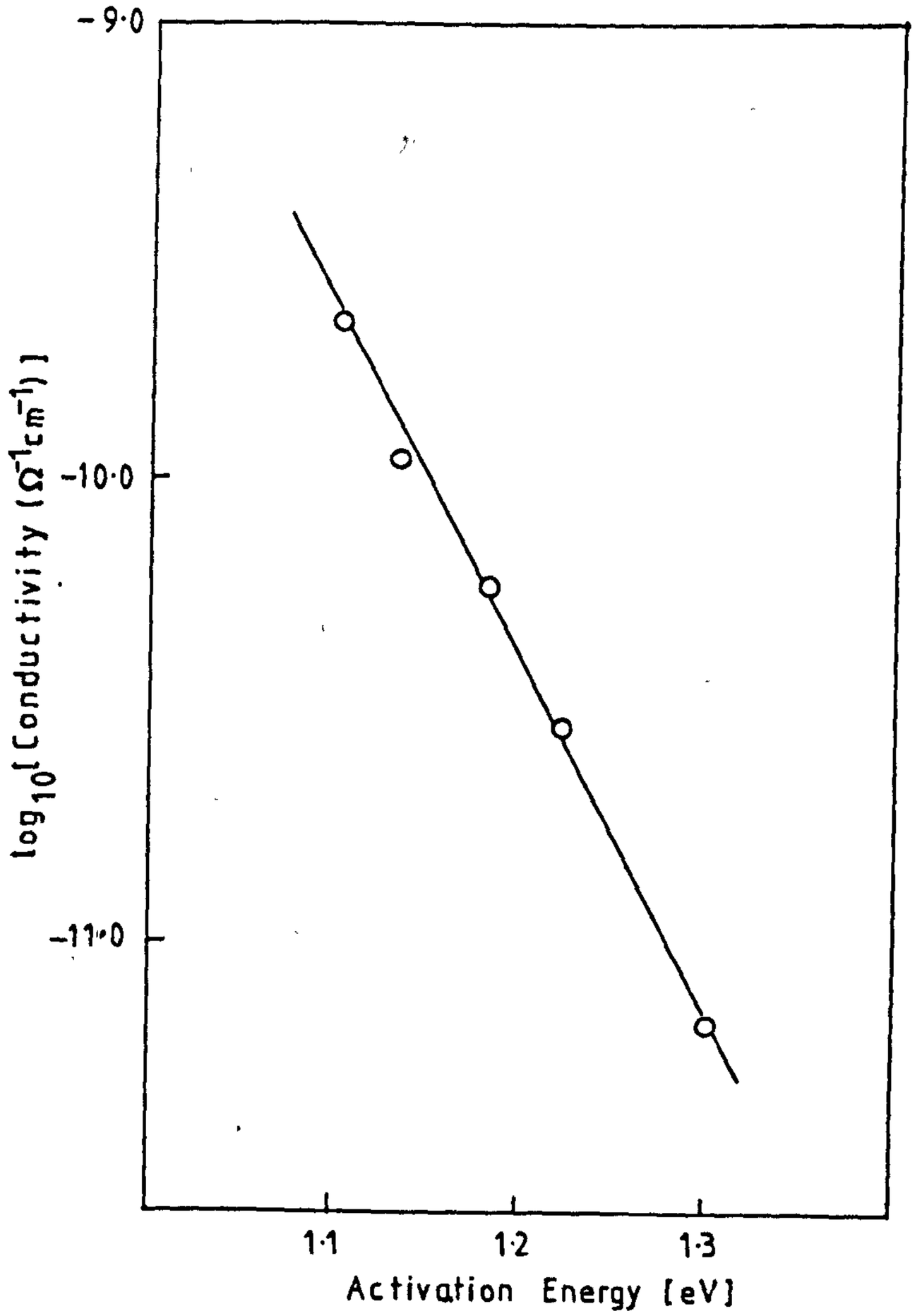

Figure 5.17 Relationship between log conductivity and activation energy for the binary system. Conductivity values measured at 500 K.

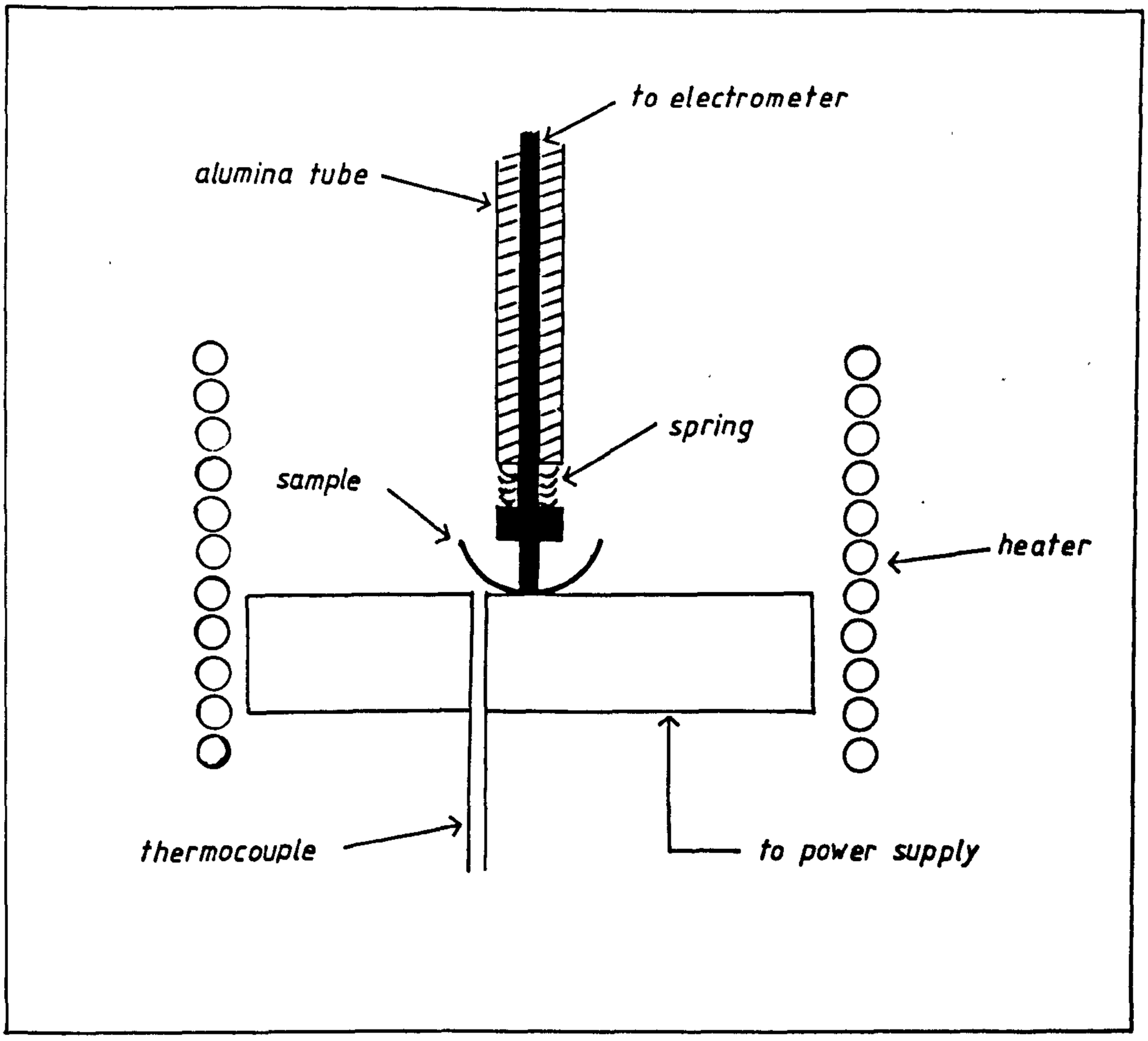

Figure 5.18 Sectioned elevation of the device holder and heating system.

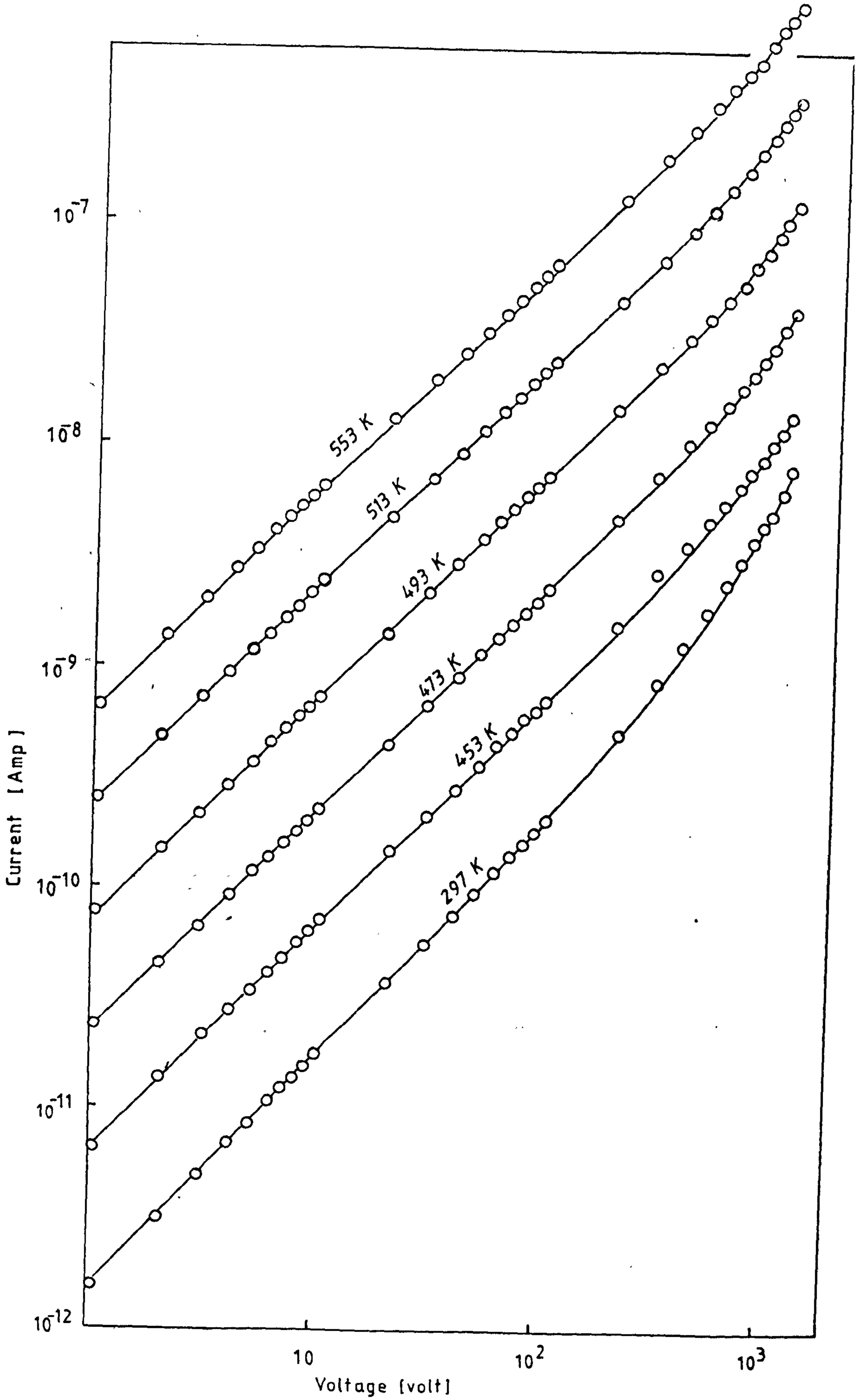

Figure 5.19 I-V characteristics for glass 3070

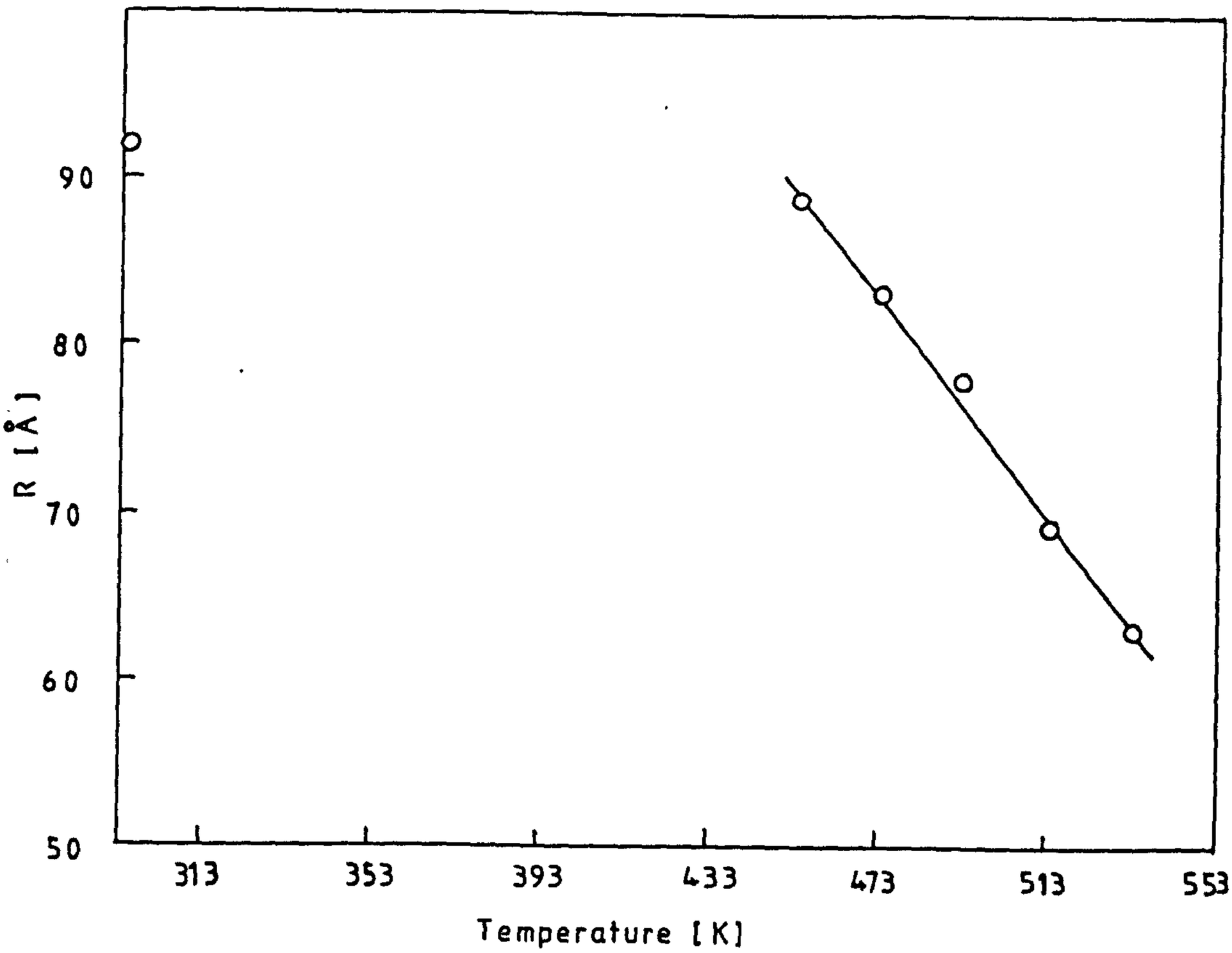

Figure 5.20 Variation of R with temperature for glass 3070.

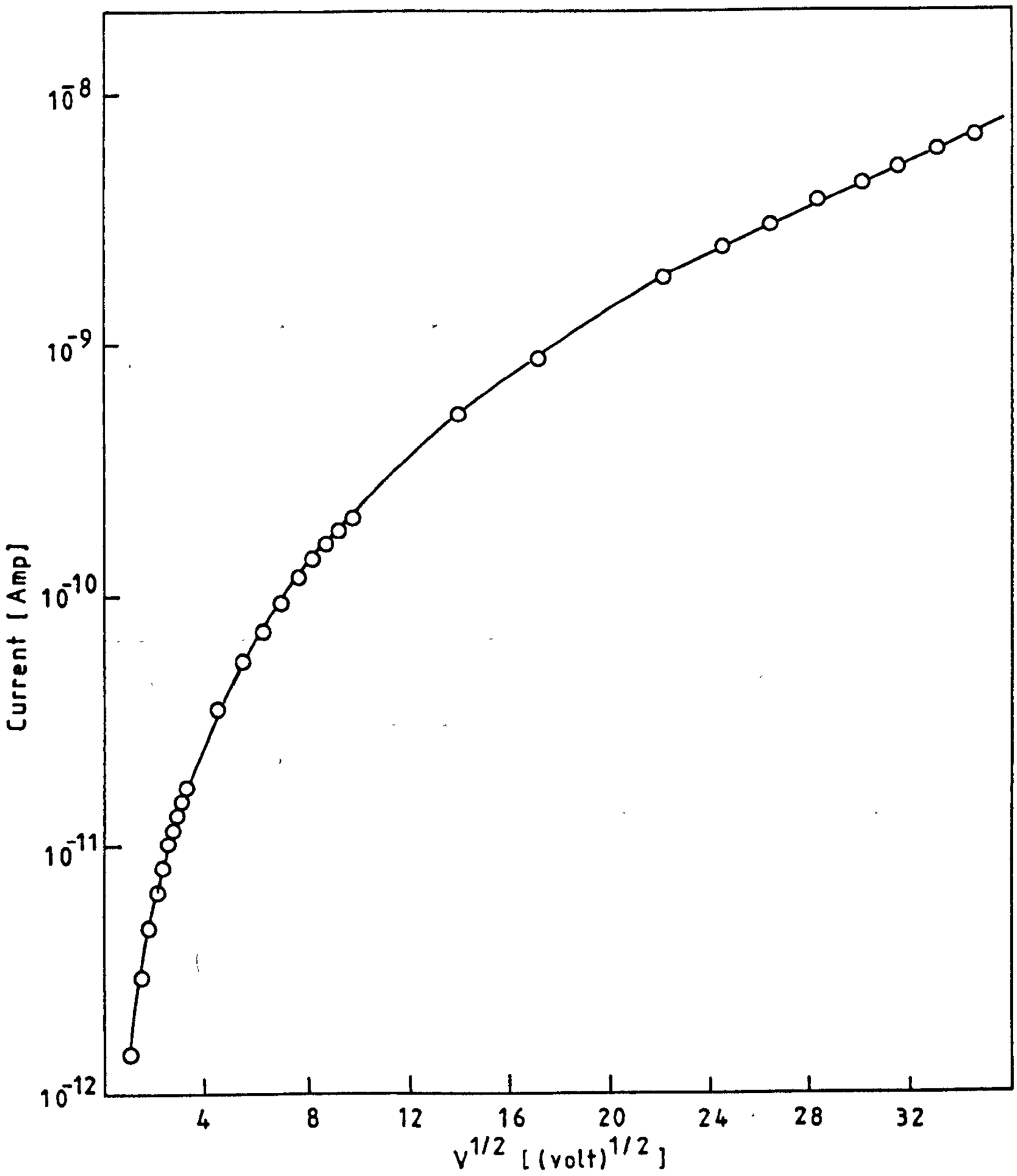

Figure 5.21 A plot of log I versus $V^{\frac{1}{2}}$ for glass 3070.

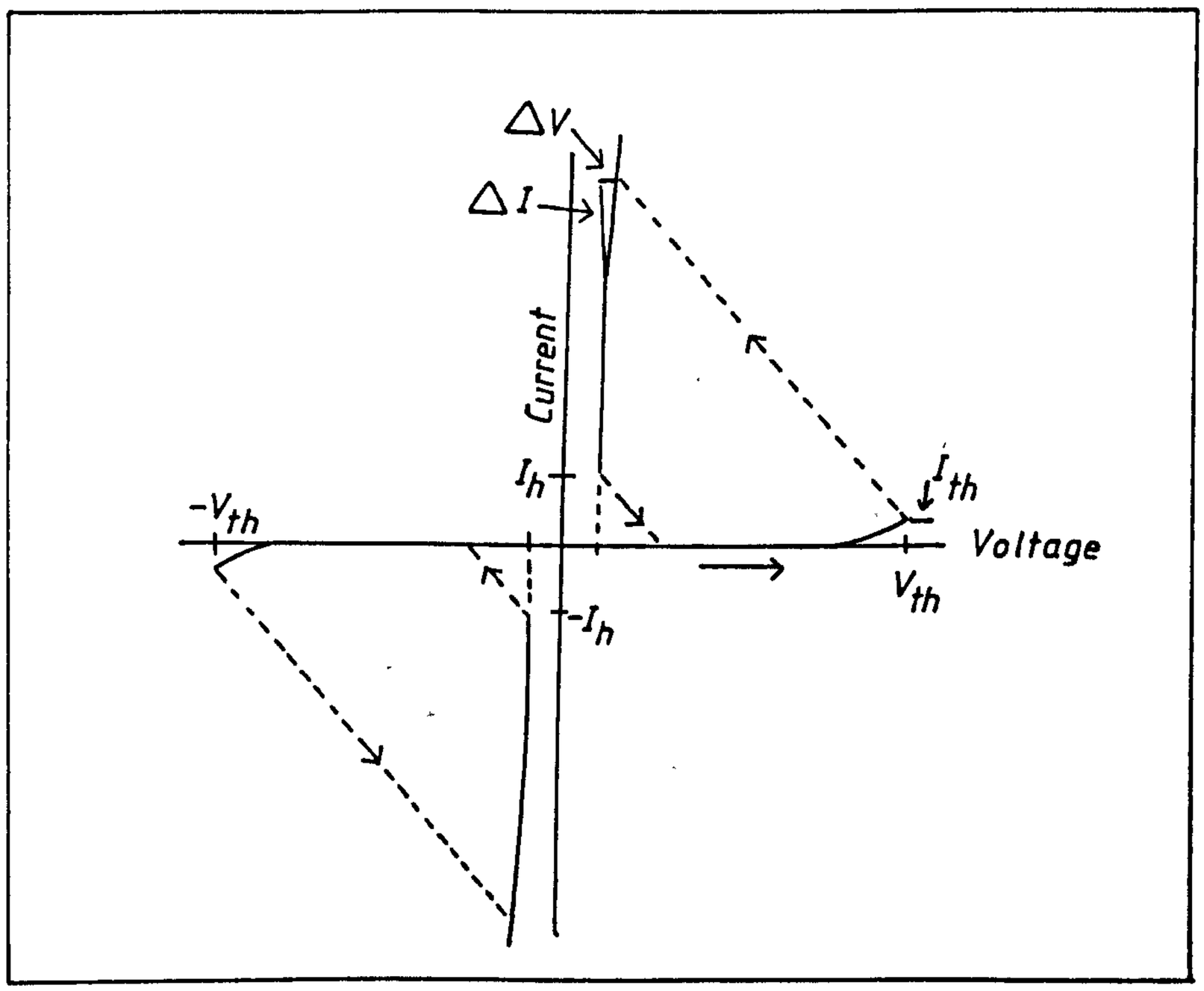

Figure 5.22 I-V characteristics of a threshold switching device.

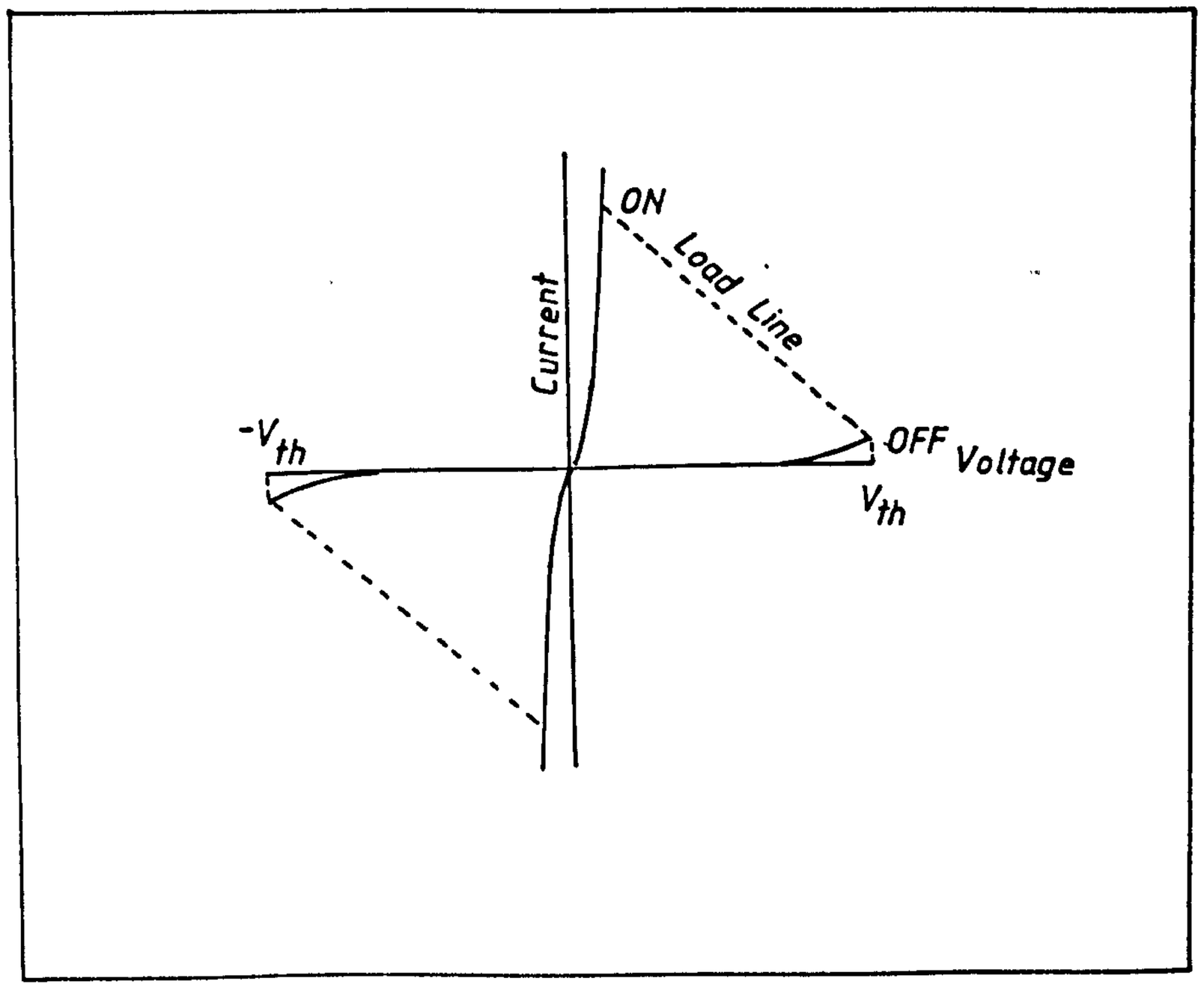

Figure 5.23 I-V characteristics of a memory switching device.

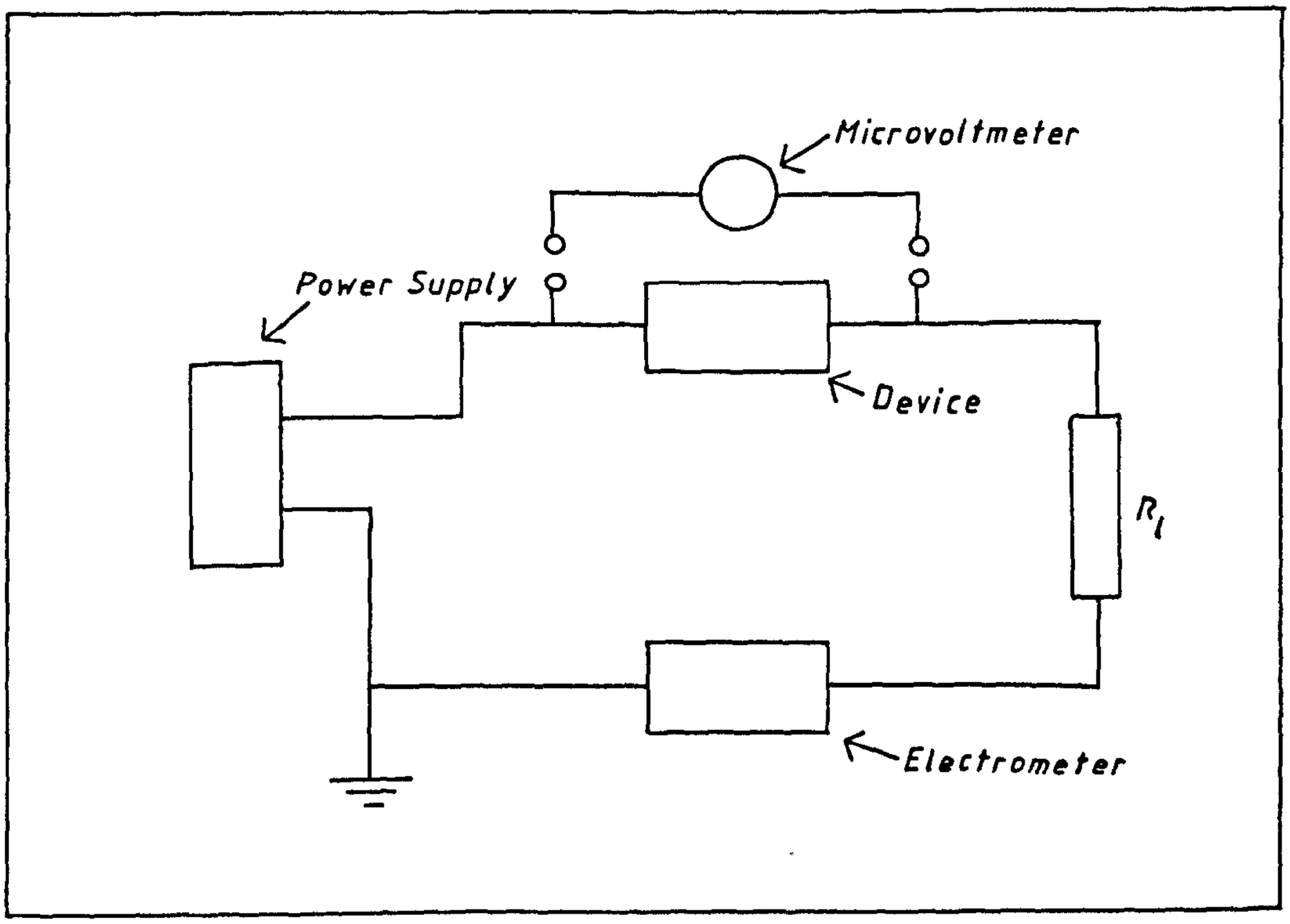

Figure 5.24 Diagram of the circuit used for switching action.

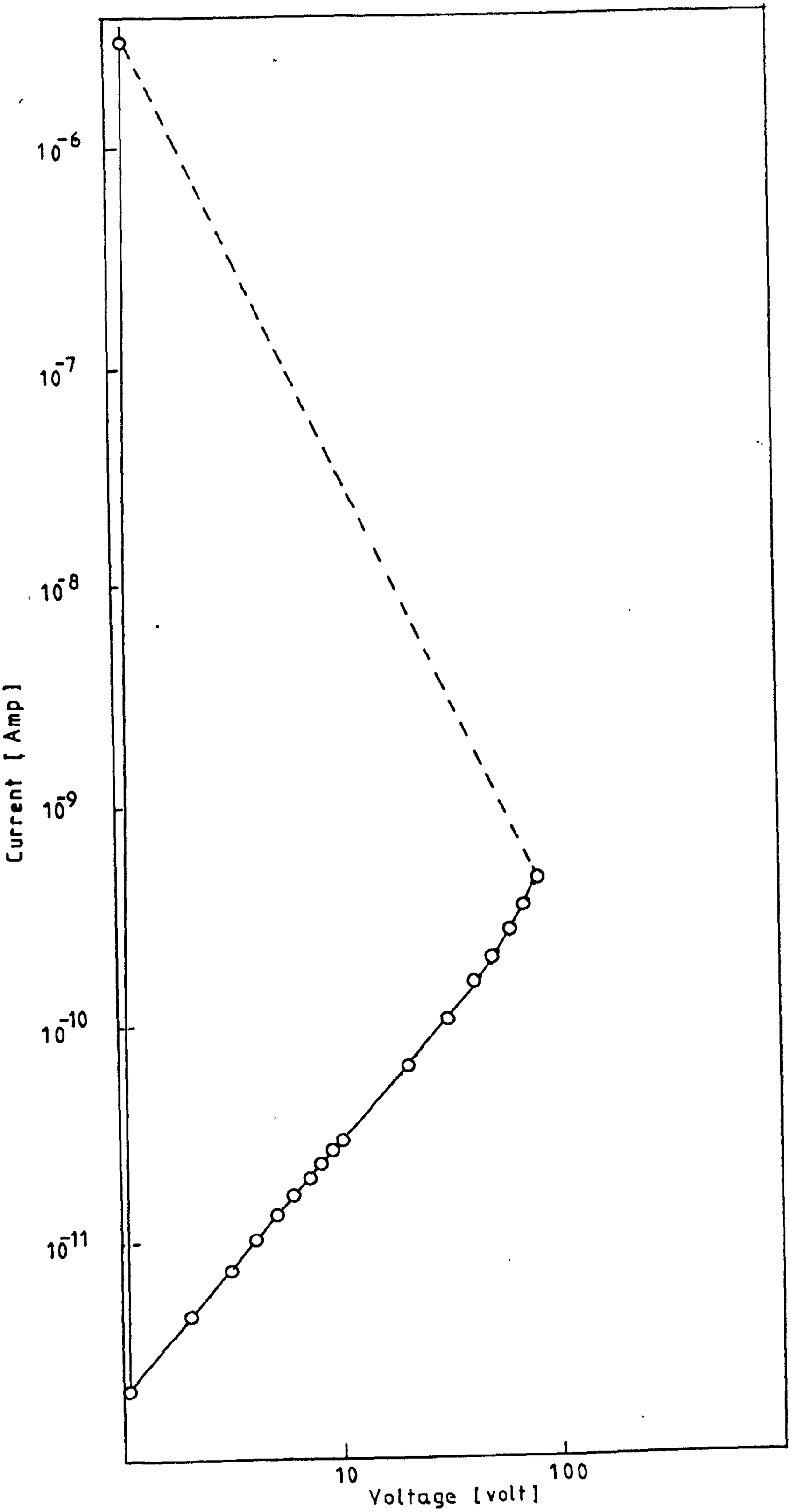

Figure 5.25 I-V characteristics of glass 3070 at room temperature

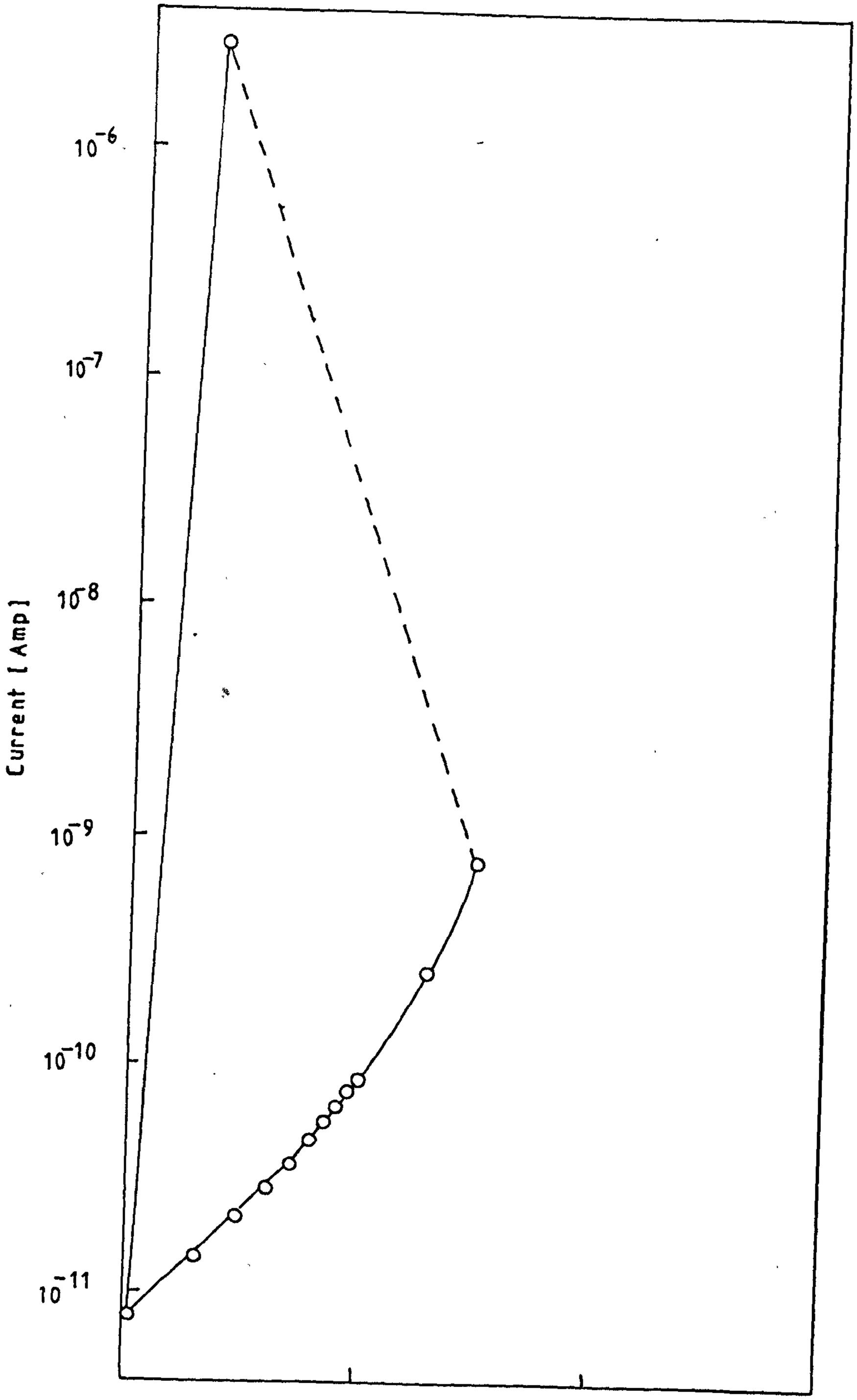

Figure 5.26 I-V characteristics of glass 3070 at 453 K.

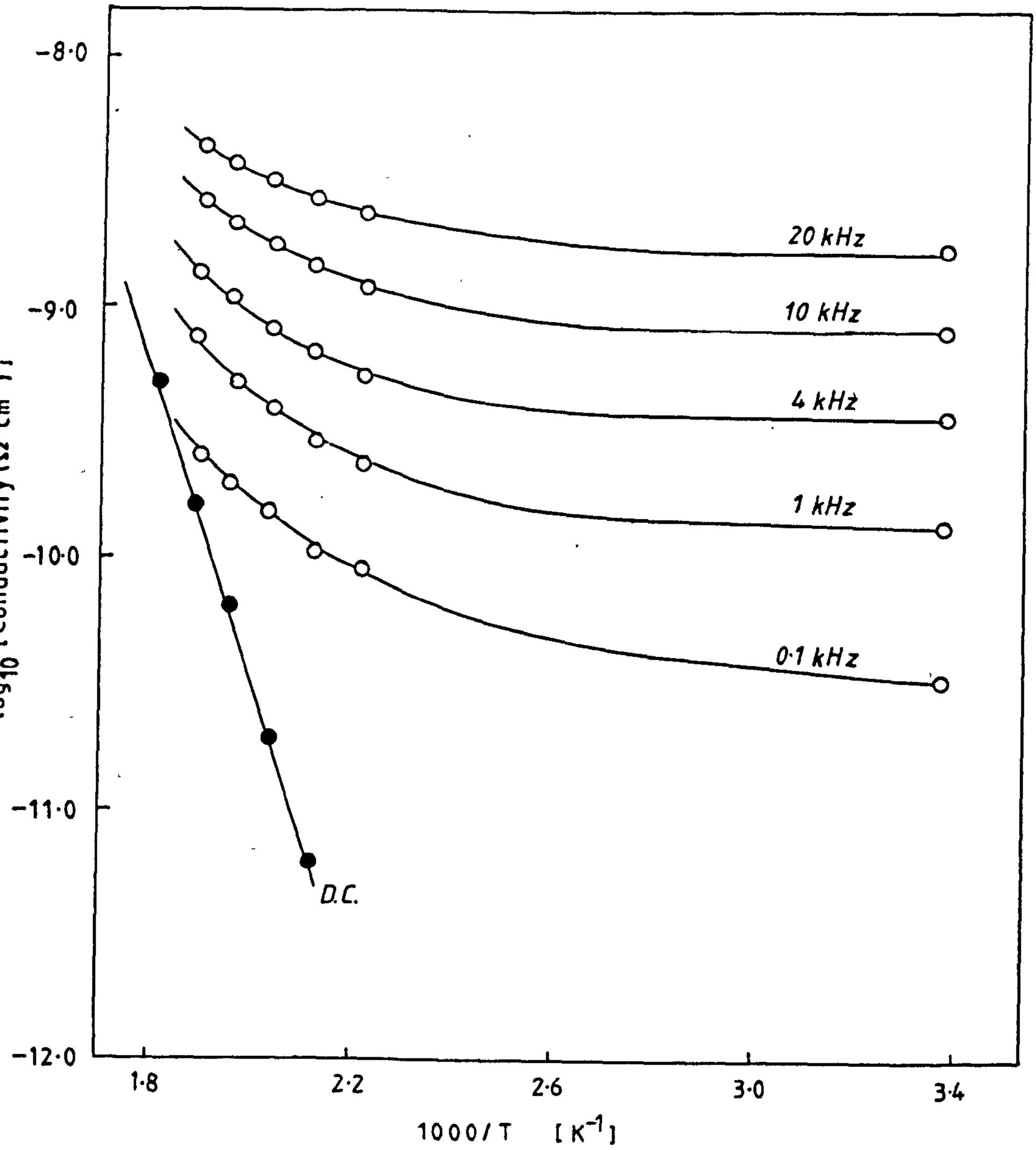

Figure 5.27 The real part of the a.c. conductivity as a function of 1000/T for glass 5050.

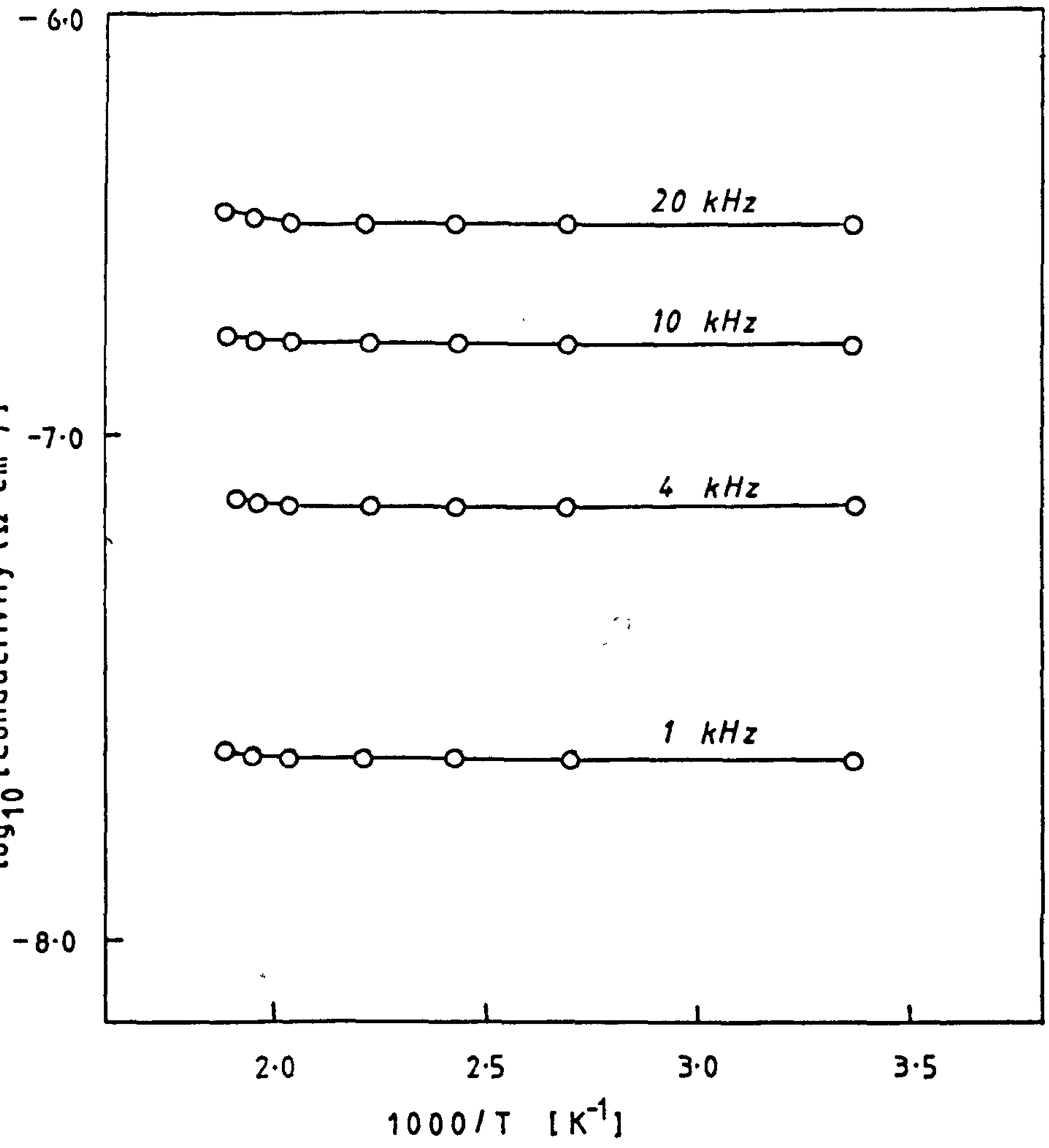

Figure 5.28 The a.c. conductivity as a function of 1000/T (glass 5050).

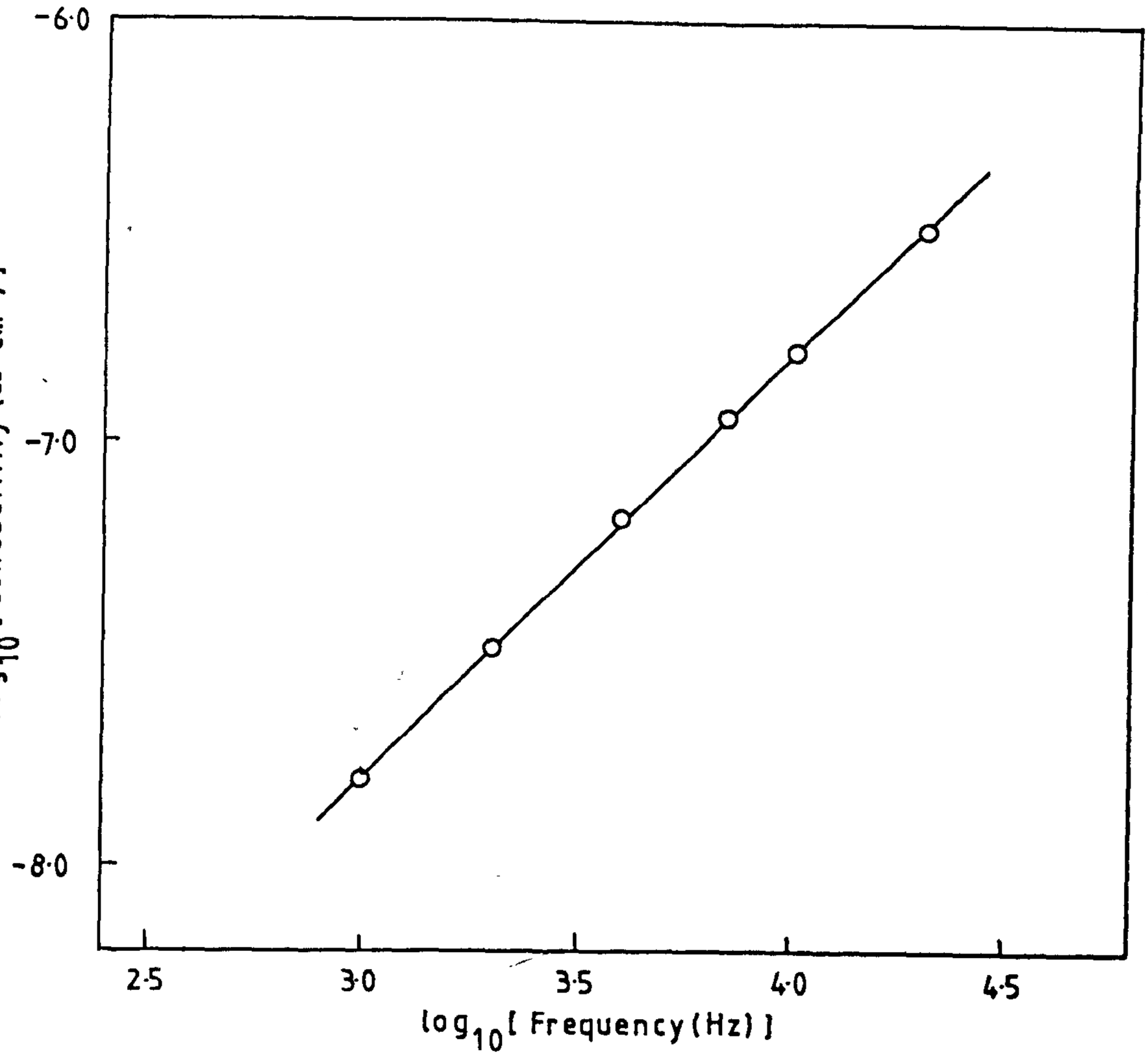

Figure 5.29 The variation of log conductivity with log frequency at room temperature (glass 5050).

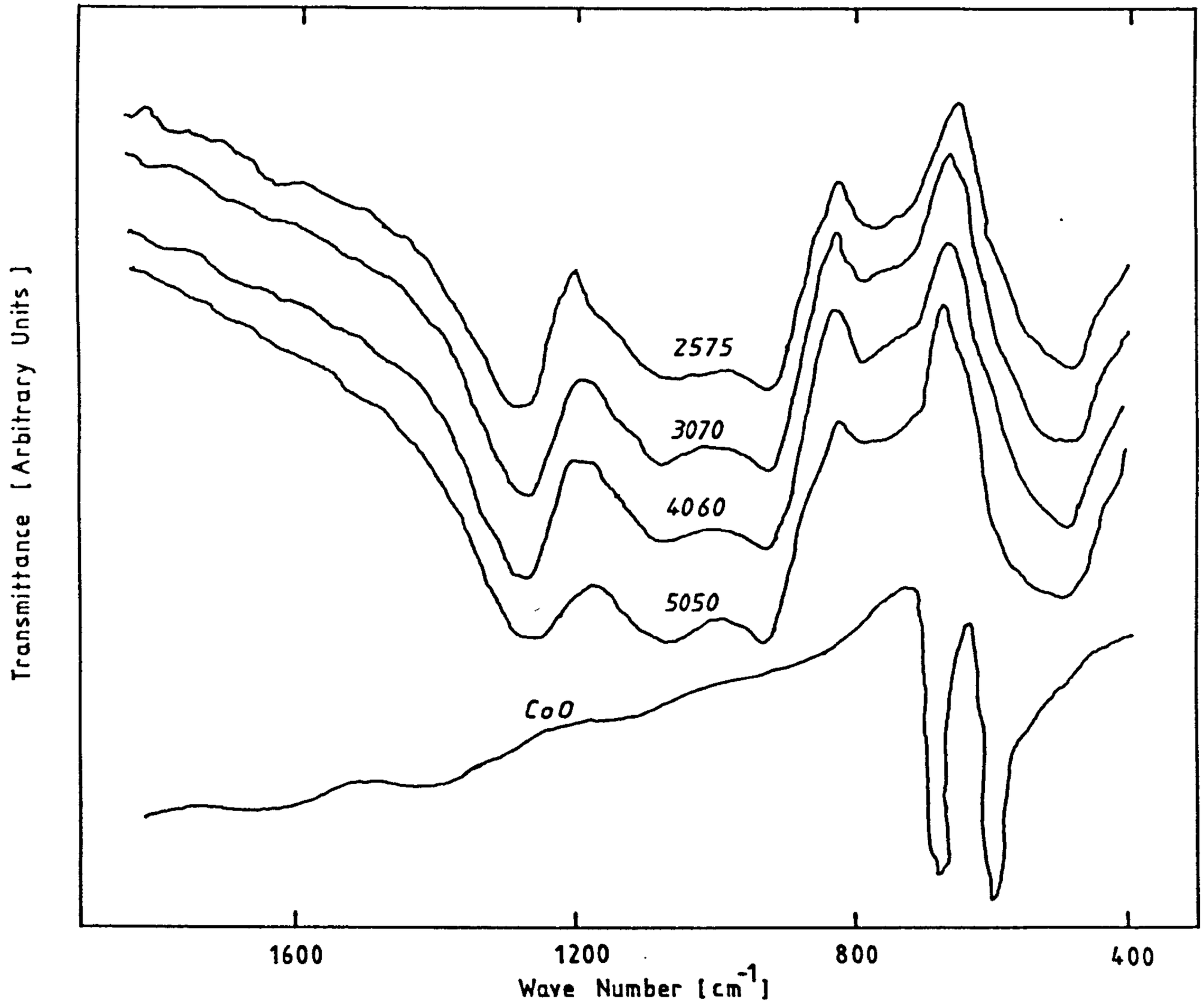

Figure 6.1 The infra-red spectra of $CoO-P_2O_5$ glasses.

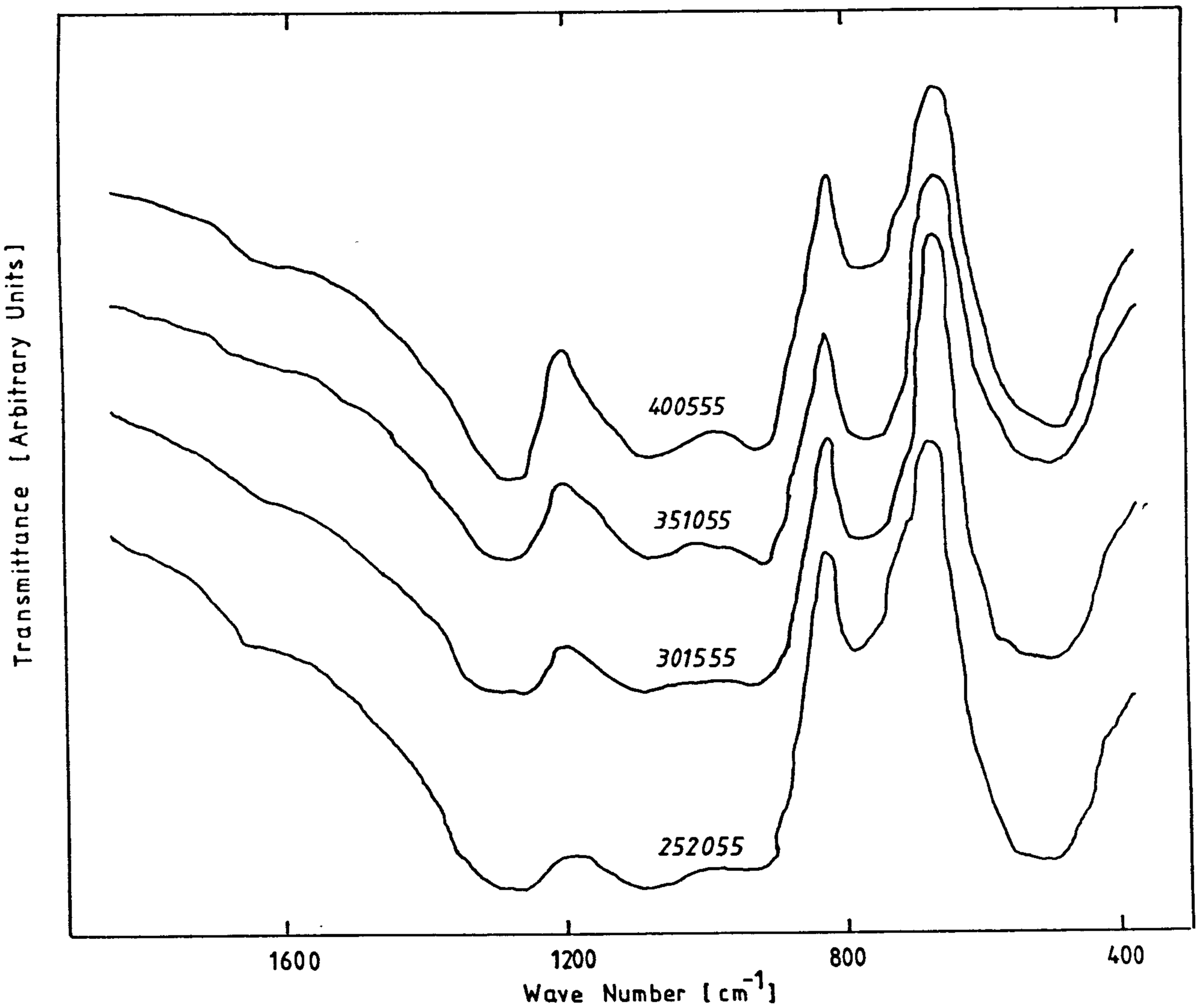

Figure 6.2 The infra-red spectra of CoO-NiO-P_2O_5 glasses.

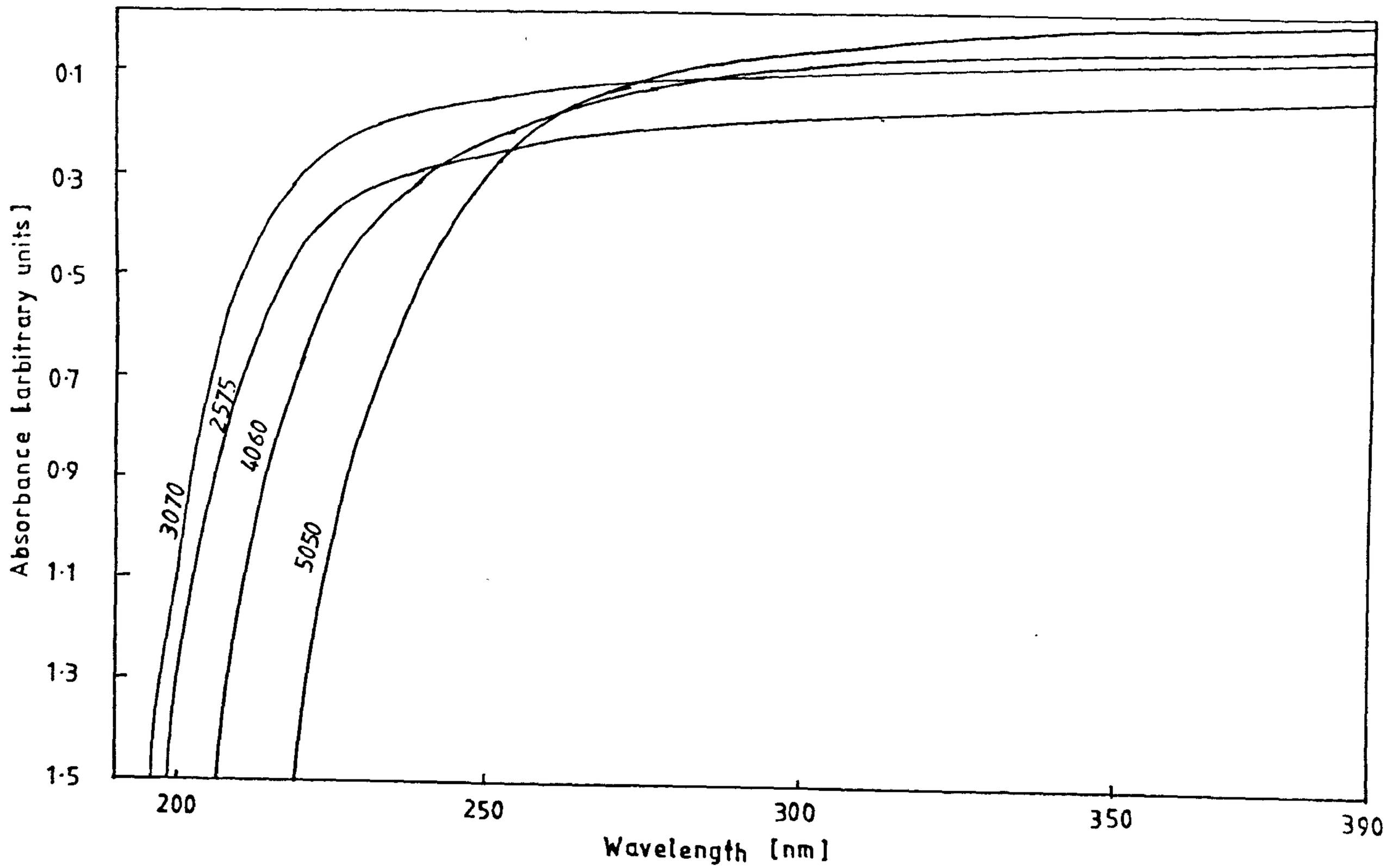

Figure 6.3 The optical absorption spectra for CoO-P_2O_5 glasses as a function of wavelength.

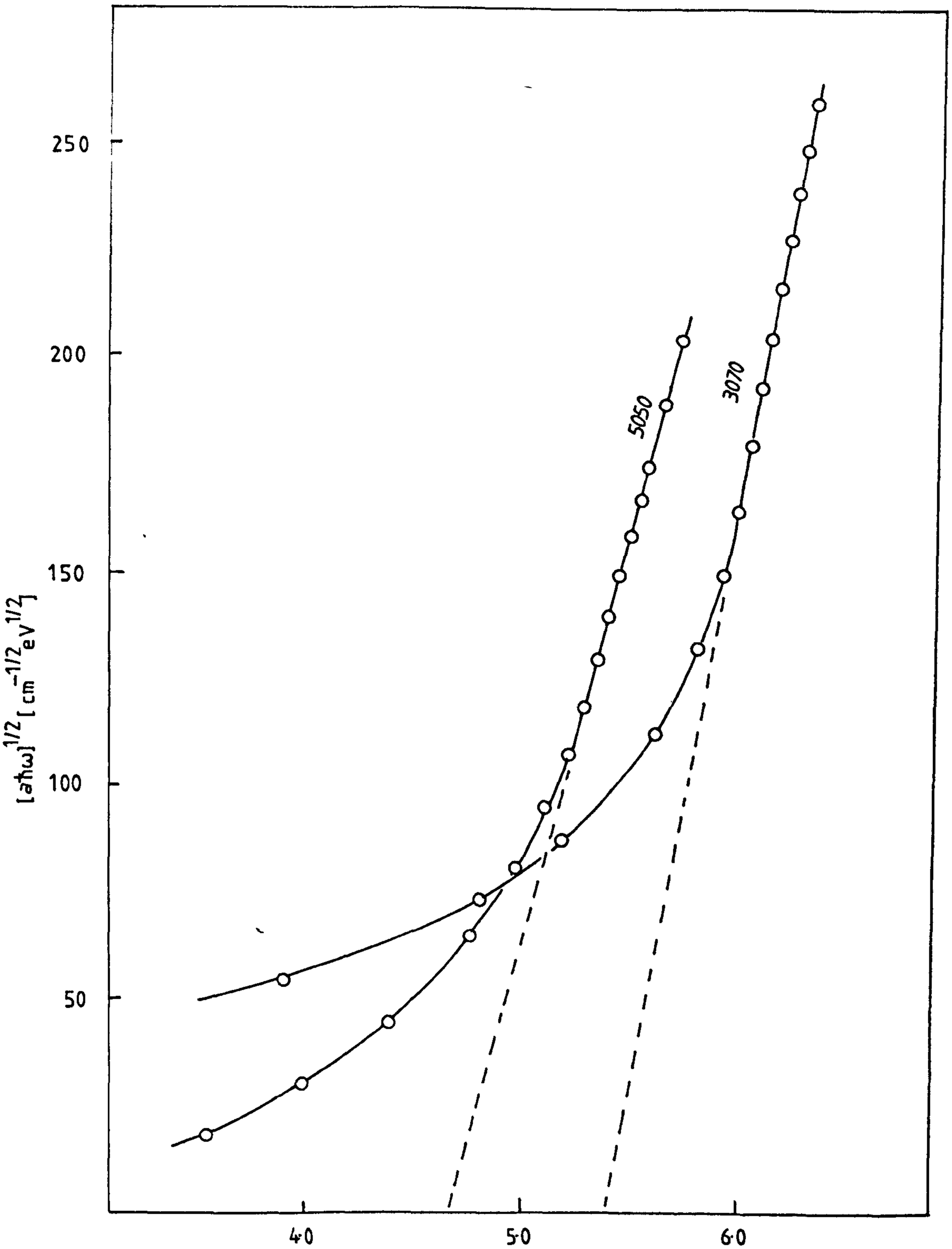

Figure 6.4 The plot of $(a\hbar\omega)^{\frac{1}{2}}$ versus $\hbar\omega$ for glass 3070 and glass 5050.

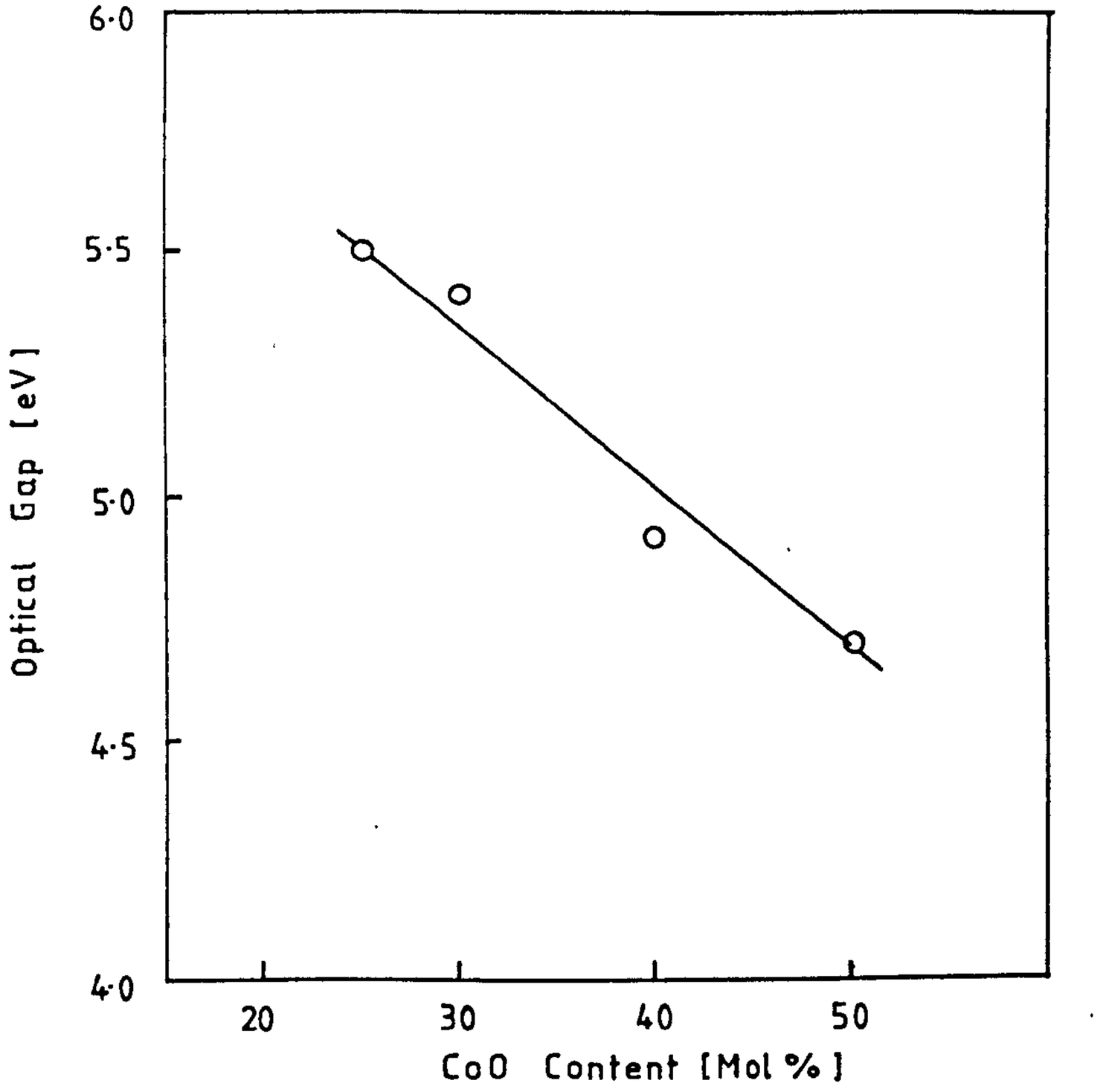

Figure 6.5 Variation of E_g^{opt} as a function of CoO content.

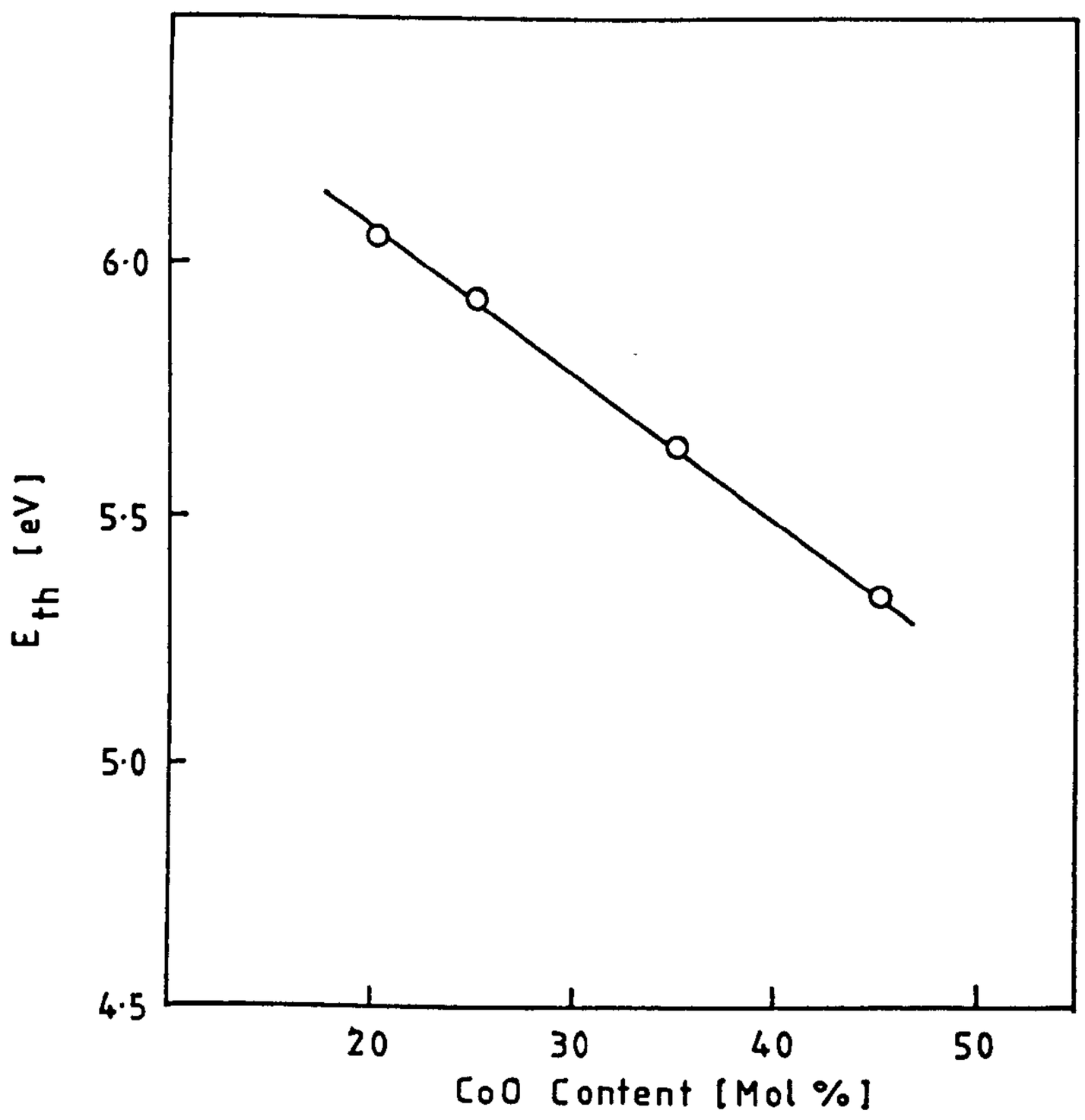

Figure 6.6 Variation of E_{th} versus CoO content.

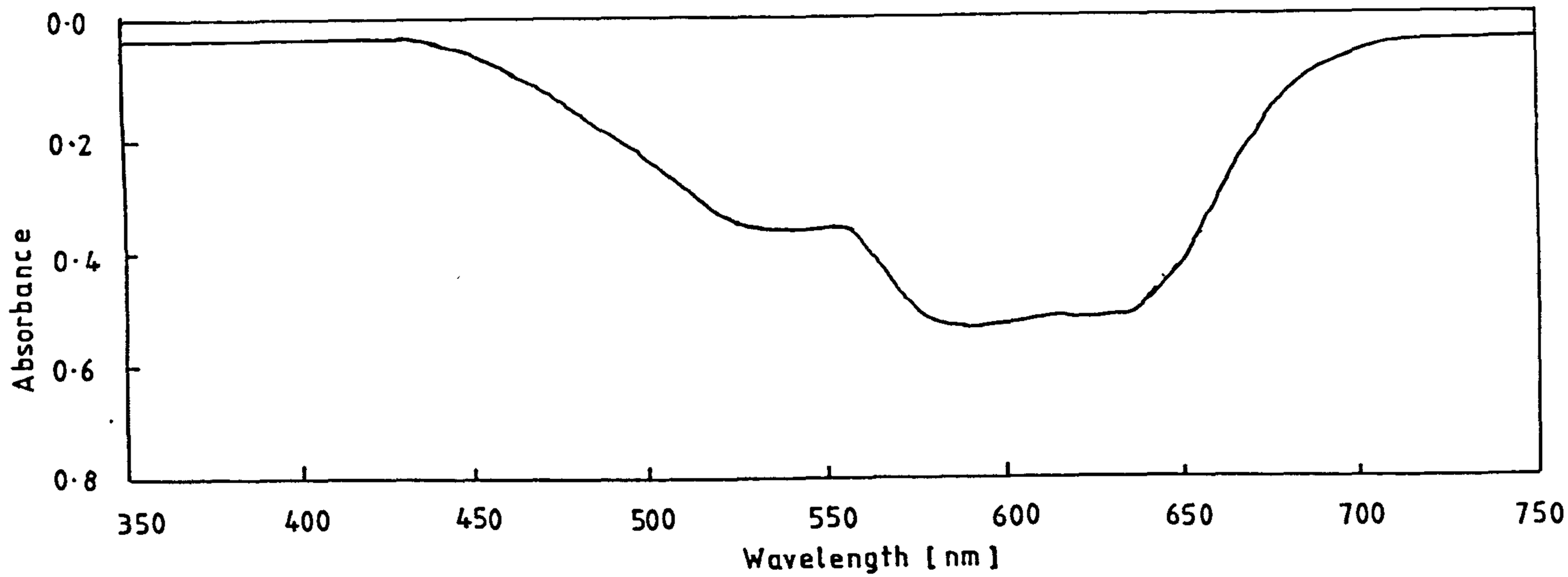

Figure 6.7 The optical absorption spectra of glass 5050 as a function of wavelength.

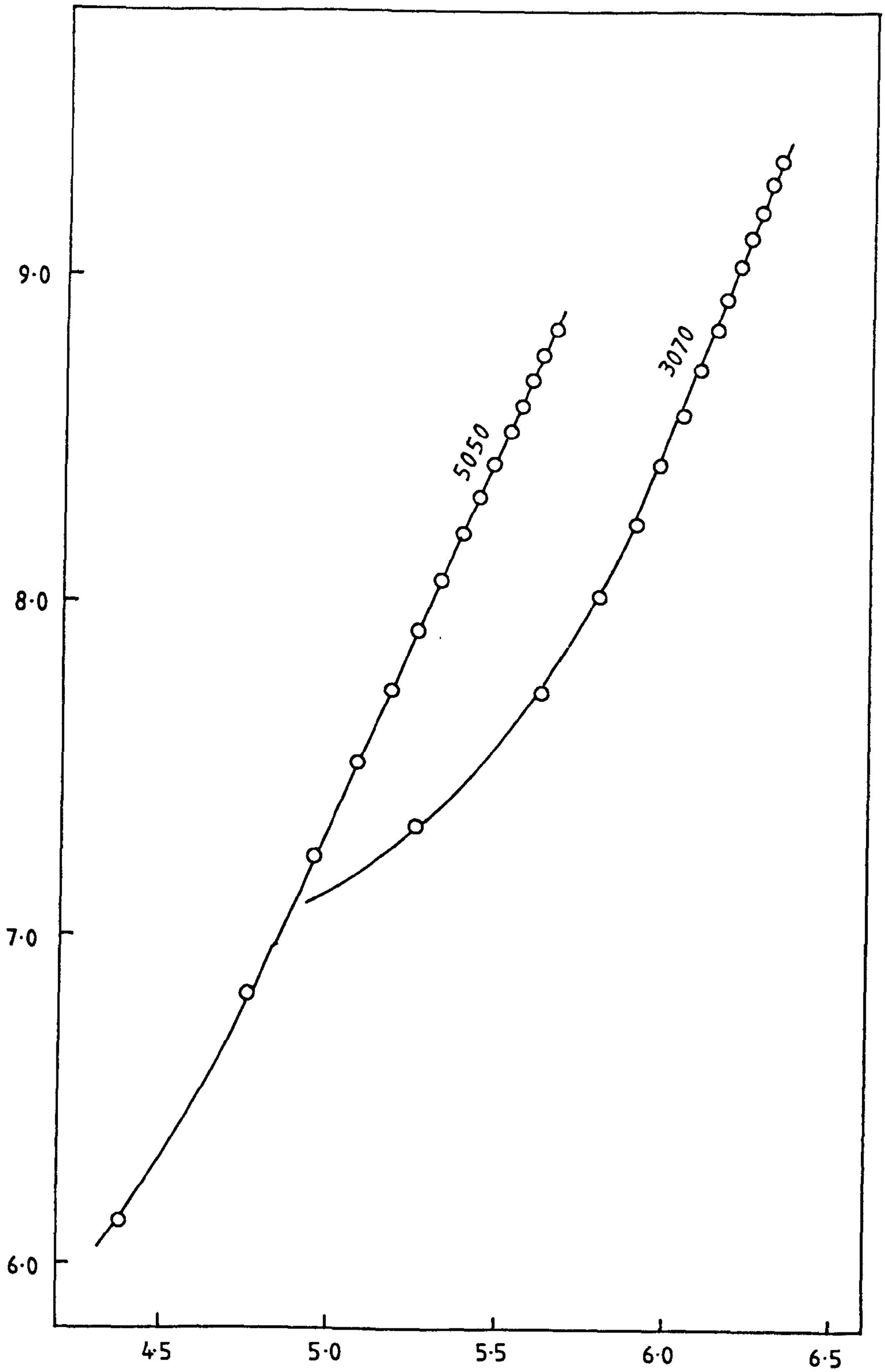

Figure 6.8 Variation of log a versus $\hbar\omega$ for glass 3070 and glass 5050.